

SOFT ERROR RATE & TRACKING

FRANK SORDELLO
CONSULTANT

IIST SHORT COURSE
MARCH 22-24, 1988

SANTA CLARA UNIVERSITY
SANTA CLARA, CALIF.

TYPICAL HIGH PERFORMANCE DISK DRIVE RECORDING CHANNEL

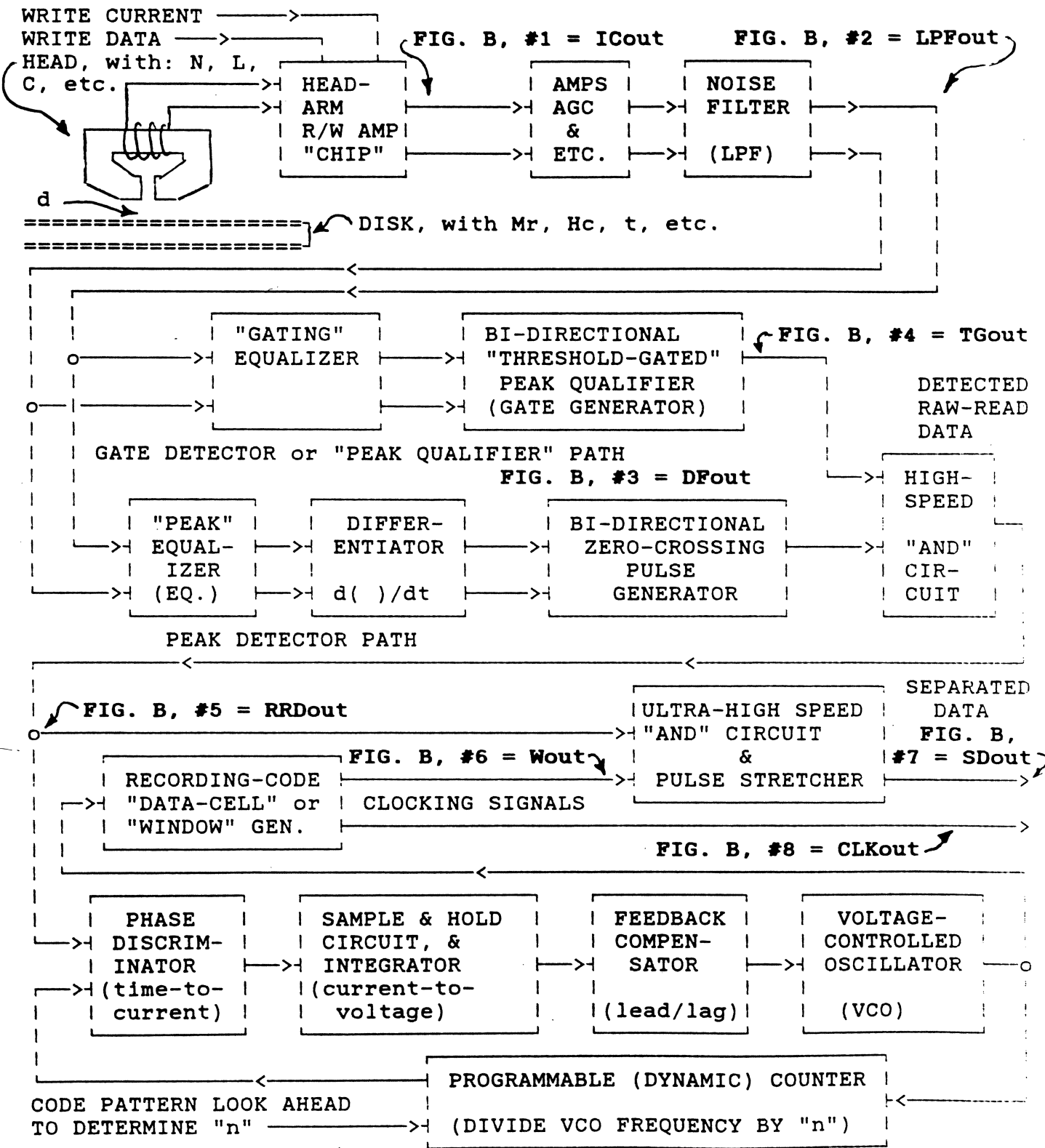
REFER TO FIGURE A ON PAGE 2, AND FIGURE B ON PAGE 3.

THE TYPICAL HIGH PERFORMANCE READ CHANNEL SHOWN EXTRACTS THE INFORMATION CONTAINED IN THE TIME-LOCATION OF THE READBACK PULSES' PEAKS, AND IS SIMILAR TO MANY OTHER DIGITAL MAGNETIC READ CHANNELS IN TERMS OF SIGNAL PROCESSING PATHS. THE READBACK-VOLTAGE SIGNAL SENSED FROM THE HEAD PASSES THROUGH AMPLIFICATION IN THE THE HEAD/(ARM)-IC PREAMP (SEE FIG. B, #1, ICout), AND ON TO OTHER ANALOG AMPLIFICATION INCLUDING AGC, THROUGH THE LINEAR-PHASE (USUALLY) NOISE FILTER. THE OUTPUT OF THE NOISE FILTER (SEE FIG. B, #2, LPFout), IS PASSED THROUGH TWO SPECIALIZED EQUALIZERS, ONE IN THE PATH TO THE THRESHOLD-GATED SIGNAL-PEAK QUALIFIER, AND THE OTHER EQUALIZER IN THE PATH TO THE WIDEBAND DIFFERENTIATOR. IN ORDER TO EXCHANGE READ-BACK "PEAKS" INTO "ZERO-CROSSINGS" (BECAUSE ELECTRONIC CIRCUITS CAN TIME-DECIPHER "ZERO-SIGNAL CROSSINGS" BETTER THAN "PEAK-SIGNALS"), DIFFERENTIATION WITH RESPECT TO TIME IS GENERALLY EMPLOYED (SEE FIG. B, #3, DFout). IN ADDITION, AN AMPLITUDE-THRESHOLD-QUALIFYING "GATING" SIGNAL IS USED TO "UNQUALIFY" ANY FALSE ZERO-CROSSINGS (THE MAJORITY OF WHICH ARE CAUSED BY DIFFERENTIATOR CIRCUITRY "DROOP") FROM READ SIGNAL DETECTION.

THE THRESHOLD-GATED TGout "ANDED" WITH THE HIGHLY-AMPLIFIED DFout ZERO-CROSSING PULSES YIELDS DETECTED RAW-READ DATA PULSES (SEE FIG. B, #5, RRDout), WHOSE AVERAGE TIME LOCATIONS OR "PHASE" ARE USED TO SYNCHRONIZE THE VFO CLOCKING SYSTEM. THE VFO CLOCKING SYSTEM ACTS AS AN ELECTRONIC "FLY-WHEEL" THAT "OPENS AND CLOSES" DATA-CLOCKING WINDOWS (SEE FIG. B, #6, Wout) AS SMALL AS 20.83 nanoseconds-WIDE IN TODAY'S HIGHEST PERFORMANCE DRIVE FAMILIES THAT EMPLOY 2,7 RLL CODES. THE VFO CLOCKING SYSTEM ALLOWS ULTRA-HIGH-SPEED, REAL-TIME, ELECTRONIC CIRCUIT DECISIONS TO BE MADE REGARDING THE EXISTANCE OR NOT OF DETECTED TRANSITIONS WITHIN THE WINDOW TIMES. ANY RRDout PULSE THAT IS COINCIDENT WITH THE "WINDOW" SIGNAL THAT CORRISPONDS TO THE RECORDING CODE'S "DATA CELL", BECOMES A VFO-STANDARDIZED, SEPARATED DATA PULSE (SEE FIG. B, #7, SDout).

THE VFO ALSO PROVIDES A SEPARATED DATA-ORIENTED CLOCKING SIGNAL THAT IS AVAILABLE TO THE DISK DRIVE'S CONTROLLER (CONTROL UNIT) FOR SUCH CONTROLLER FUNCTIONS AS DE-SERIALIZING THE READBACK DATA. SEE FIG. B, #8, CLKout.

THE DIFFERENTIATOR CIRCUIT'S ANALOG OUTPUT SIGNAL'S (DFout's) SHAPE, AS A FUNCTION OF TIME, CAN BE CONSIDERED THE TRANSLATING "MECHANISM" FOR THE GENERATION OF (AND ALSO CALCULATION OF) BIT-SHIFT DUE TO ANY AND ALL ALGEBRAICLY-ADDED-AMPLITUDE, UNWANTED SIGNALS. THE ULTIMATE TIME-LOCATION OF THE DETECTED RAW-READ DATA PULSE OR DETECTED MAGNETIC TRANSITION (OR "DETECTED BIT") OCCURS AT THE ZERO-CROSSING OF THE DFout SIGNAL. ANY "UNWANTED" **ADDITIONAL** SIGNAL WILL CAUSE A TIME-SHIFT OF THE ACTUAL ZERO-CROSSING POINT, IN ONE POLARITY OR THE OTHER, RESULTING IN



"VFO", "PLL", "PLO", or PHASE-LOCKED DATA SEPARATOR CLOCKING SYSTEM

FIGURE A. TYPICAL HIGH-PERFORMANCE DISK DRIVE RECORDING CHANNEL

READBACK TRANSITIONS for 2, 7, RLL

CODE -> 0 0 1 0 0 0 0 0 0 0 1 0 0 1 0 0 0 0 0 0 0 0 1 0 0 1 0 0 1 0 0 0 0 0

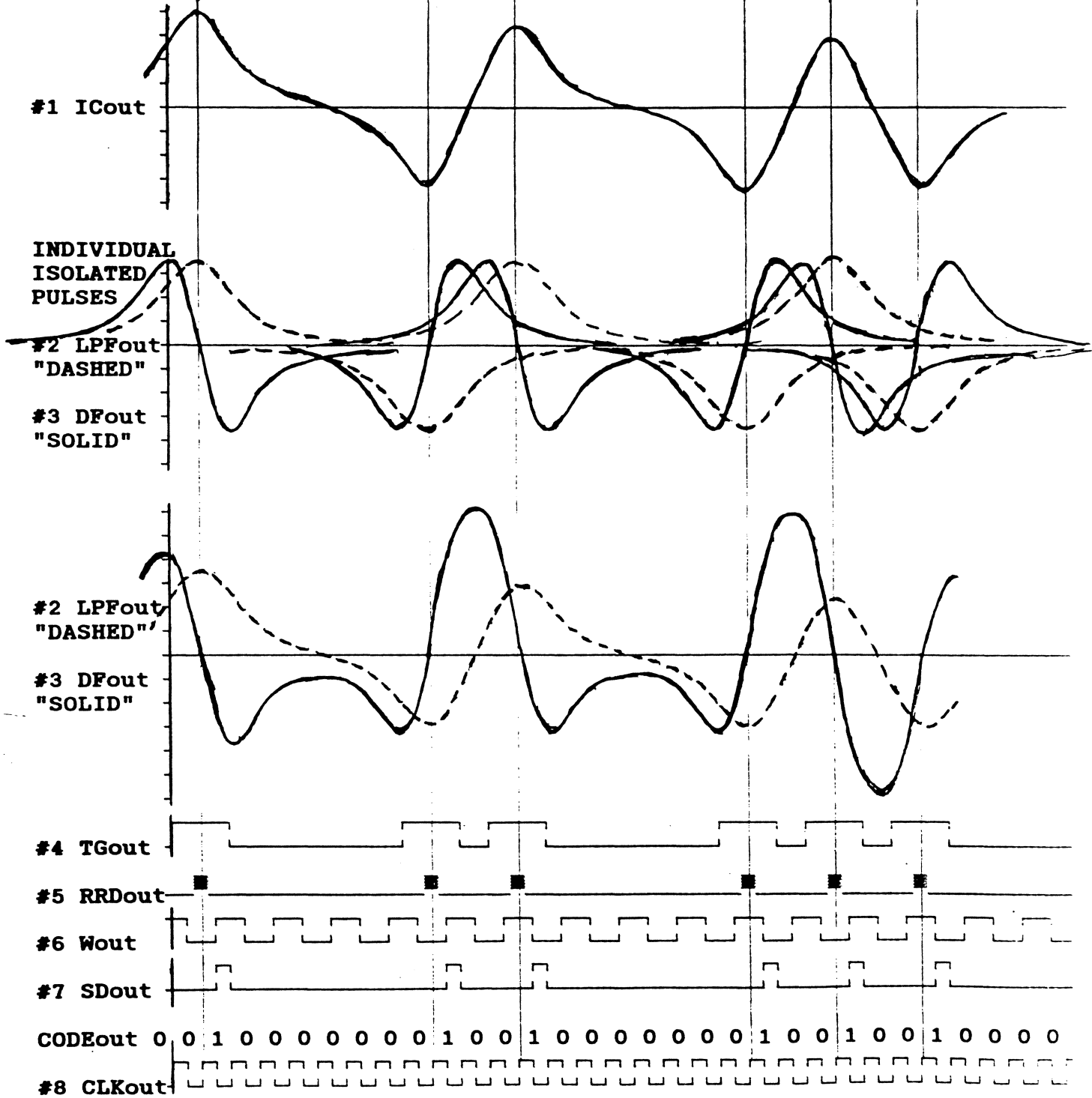
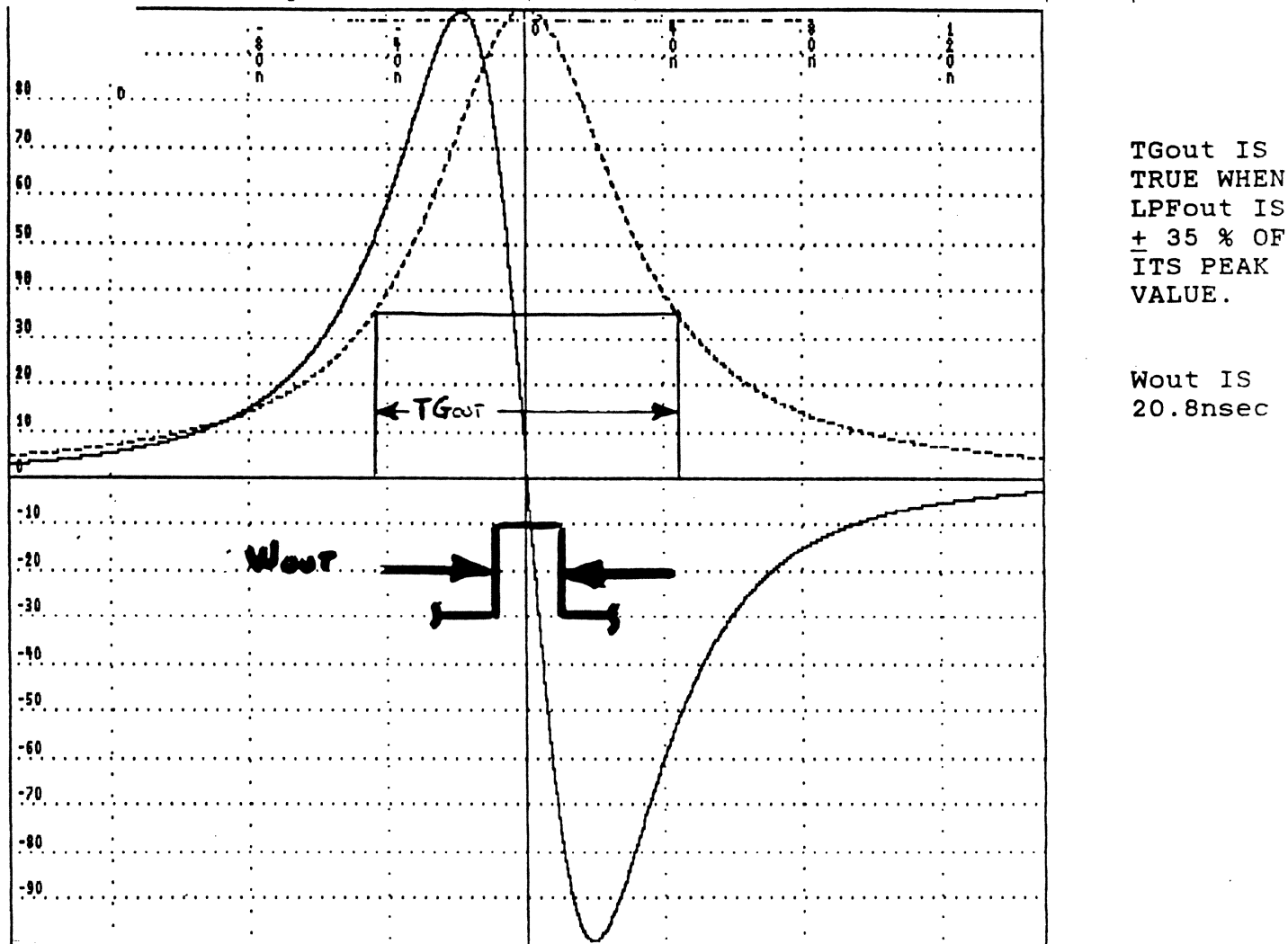


FIGURE B. READBACK SIGNALS AT VARIOUS STAGES WITHIN READ CHANNEL.
 (All intrinsic circuit delays have been eliminated for clarity. For 24 Mbit/sec = 3 Mbyte/sec, one "Wout" cell (1/2 complete cycle of "Wout") = 20.833 nanosecond.)

LORENTZIAN (Pw50=65nS) RESPONSE Frank J. Sordello 3/4/1988 14:07:58
 Left: -150nS, Right: 150nS, Top: 100, Bottom: -100, Time Step:200pS

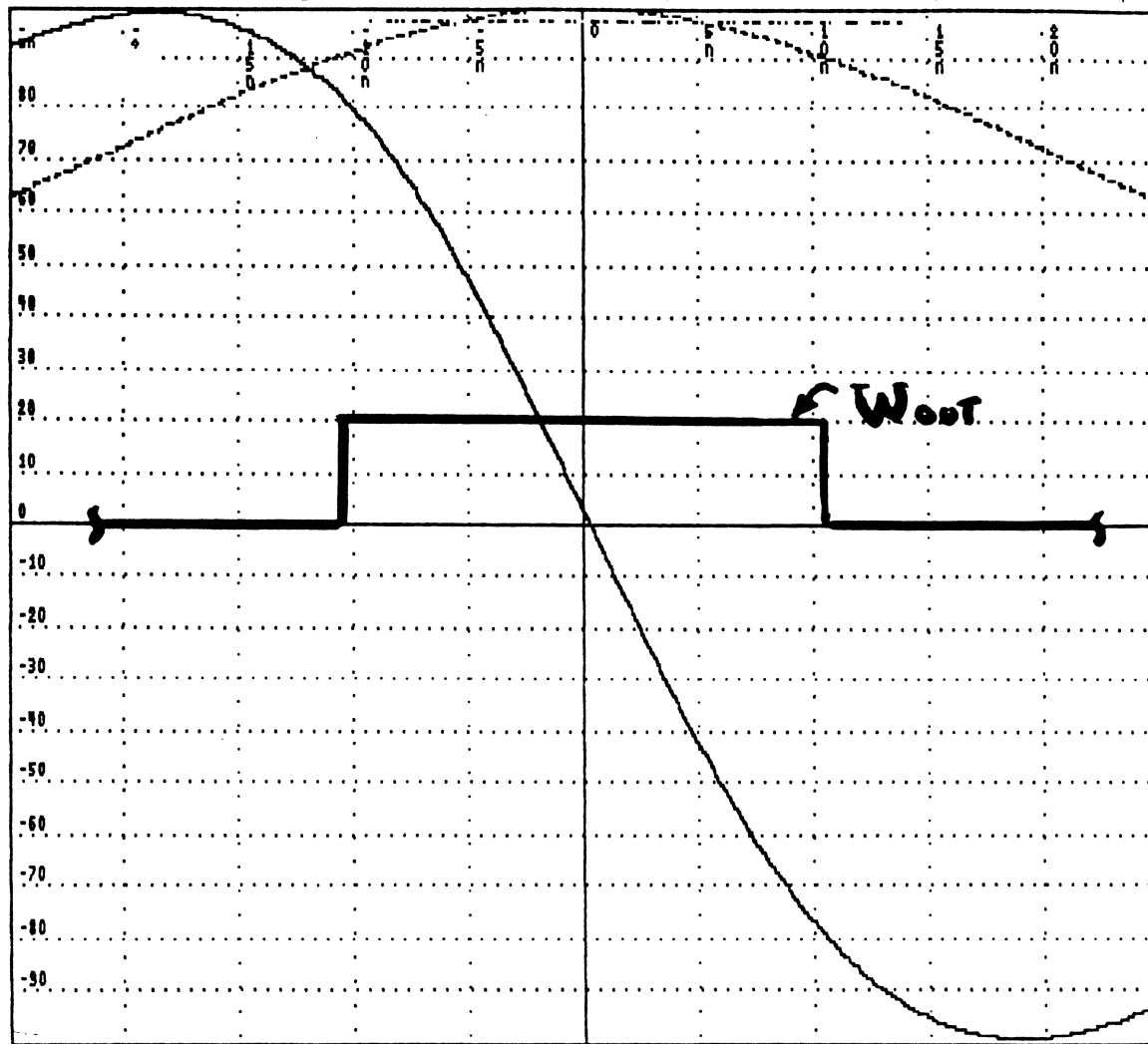


NORMALIZED LPFout (T50 changes from 55 to 65 nsec in LPF) and RESULTING DFout Analysis by Frank J. Sordello. Common Block Zero at: 0Hz; Pole at: 1000MHz; The gain is currently set to -146.089db. This has 0db at 3.333MHz.

FIGURE C:.. NORMALIZED LPFout & DFout, with TGout & Wout TIME-BOUNDARIES MARKED for ISOLATED READBACK PULSE.

A STUDY OF THE CHARACTERISTICS OF THE VARIOUS READ CHANNEL SIGNALS OF FIGURE B, WHEN THE HEAD SHOWN IN FIGURE A READS A SINGLE RECORDED TRANSITION (AN ISOLATED READBACK PULSE) QUICKLY REVEALS A GREAT DEAL. REFER TO FIGURE C. FIGURE C ALLOWS US TO OBSERVE THE SLOPE OF THE DIFFERENTIATED (AND EQUALIZED) NOISE FILTER OUTPUT. THE ZERO CROSSING OF DFout IS INTENDED TO CORRISPOND EXACTLY TO THE TIME OF OCCURANCE OF THE PEAK OUTPUT OF LPFout. IDEALLY, THE PEAK OUTPUT OF LPFout CORRISPONDS TO THE SPATIAL CENTER OF THE MAGNETIC TRANSITION RECORDED IN THE DISK MEDIUM. (AT LEAST WITHIN THE TOLERANCES OF THE PARAMETERS OF THE MANY ENGINEERING DICCIPLINES AND PHENOMENA ASSOCIATED WITH DIGITAL MAGNETIC RECORDING!)

LORENTZIAN (Pw50=65nS) RESPONSE Frank J. Sordello 3/4/1988 14:13:22
 Left: -25nS, Right: 25nS, Top: 100, Bottom: -100, Time Step:200pS



Wout IS
 TRUE FOR
 20.8 nsec,
 AND IS
 CENTERED BY
 THE VFO
 TO THE AVE.
 TIME OCCUR-
 ANCE OF THE
 DFout ZERO-
 CROSSINGS.

NORMALIZED LPFout (T50 changes from 55 to 65 nsec in LPF) and RESULTING DFout Analysis by Frank J. Sordello. Common Block Zero at: 0Hz; Pole at: 1000MHz; The gain is currently set to -146.089db. This has 0db at 3.333MHz.

FIGURE D: EXPANDED TIME-SCALE, NORMALIZED LPFout & DFout, with Wout TIME-BOUNDARY MARKED for ISOLATED READBACK PULSES.

FIGURE D SHOWS THE SLOPE OF DFout TO BE APPROXIMATELY TEN PERCENT PER NANOSECOND IN THE REGION OF "ZERO-CROSSING". ANY UNWANTED SIGNAL, ADDITIONAL TO THE DESIRED INFORMATION-BEARING PORTION OF DFout, SUCH AS MEDIUM NOISE, WILL EITHER ADD OR SUBTRACT DIRECTLY TO OR FROM THE DESIRED PORTION OF DFout AND CAUSE THE ACTUAL TIME OF THE COMPOSITE "ZERO-CROSSING" TO OCCUR LATE OR EARLY RESPECTIVELY! FOR EXAMPLE, IF THE MEDIA NOISE HAS A SIGNAL COMPONENT THAT IS INSTANTANEOUSLY + 20% OF THE DESIRED INFORMATION-CARRYING DFout, THE COMPOSITE DFout SIGNAL WILL BE "LIFTED" BY 20%, AND IF THAT NOISE SIGNAL COMPONENT OCCURS NEAR THE TIME OF THE "ZERO-CROSSING", THE COMPOSITE DFout SIGNAL WILL CROSS ZERO VOLTS APPROXIMATELY 2 NANoseconds LATER THAN SHOWN.

$$\text{BIT SHIFT} = \frac{\% \text{ AMPLITUDE OF UNWANTED ADDITIVE SIGNAL}}{\text{SLOPE OF DFout SIGNAL NEAR "ZERO-CROSSING" POINT}} = \text{nsec}$$

IT IS AS SIMPLE AS THAT! ANY UNWANTED SIGNAL THAT "LIFTS" OR "LOWERS" THE DESIRED RECORDED INFORMATION BEARING DFout SIGNAL WILL CAUSE THE "ZERO-CROSSING" OF THE COMPOSITE DFout SIGNAL TO BE SHIFTED IN TIME FROM THE IDEAL "ZERO-CROSSING" TIME. THE TIME WIDTH OF THE DATA TRANSITION-CLOCKING WINDOW, Wout, DETERMINES THE TOTAL AMOUNT OF "LIFTING" OR "LOWERING" THAT CAN BE TOLERATED BEFORE THE COMPOSITE DFout SIGNAL HAS ITS "ZERO-CROSSING" SHIFTED IN TIME BEYOND A PARTICULAR TRANSITION OR "BIT" CELL. FIGURE D SHOWS THAT THE 24 MEGABIT/SECOND RECORDING SYSTEM DESCRIBED CAN TOLERATE COMPOSITE DFout "ZERO-CROSSING" TIME-SHIFTS ("BIT SHIFTS") UP TO $\pm (20.8 \text{ nsec})/2 = \pm 10.4 \text{ nsec}$ BEFORE OCCURRING OUTSIDE OF THE TIME BOUNDARIES OF Wout. FIGURE D ALSO SHOWS THAT THE $\pm 10.4 \text{ nsec}$ BIT SHIFT WILL BE CAUSED BY THE ADDITION OF UNWANTED SIGNALS EQUAL TO APPROXIMATELY $\pm 80 \%$ OF THE BASE-TO-PEAK VALUE OF THE INFORMATION BEARING DFout SIGNAL.

THE ABOVE NUMBERS ARE ASSOCIATED WITH A SINGLE ISOLATED READBACK TRANSITION. THE AMPLITUDE OF THE BASE-TO-PEAK VALUE OF DFout CONTROLS THE ABSOLUTE AMOUNT OF "BIT SHIFT" THAT OCCURS FOR A GIVEN AMOUNT OF UNWANTED ADDITIVE SIGNAL. WHEN PORTIONS OF ISOLATED DFout PULSES COMBINE DUE TO THEIR PROXIMITY, THE BASE-TO-PEAK VALUE OF THE NET RESULTING DFout SIGNAL MAY INCREASE BY AS MUCH AS 50%, YIELDING LESS "BIT SHIFT" FOR A GIVEN AMOUNT OF UNWANTED ADDITIVE SIGNAL. SEE FIGURE B, ON PAGE 3, AND ESTIMATE THE POSITIVE PORTIONS OF THE DFout SIGNAL CORRESPONDING TO THE SECOND, THIRD, FOURTH, AND FIFTH TRANSITIONS; AND THE NEGATIVE PORTIONS OF THE FIFTH AND SIXTH TRANSITIONS. THEN, COMPARE THE ESTIMATED PORTIONS STATED ABOVE WITH THE NEGATIVE PORTIONS OF THE DFout SIGNAL CORRESPONDING TO THE FIRST, SECOND, THIRD, AND FOURTH TRANSITIONS, AS WELL AS THE POSITIVE PORTIONS OF THE FIRST AND SIXTH TRANSITIONS.

THERE ARE OTHER WAYS THAT THE "ZERO CROSSING" CAN OCCUR SHIFTED. MOST PROMINENT IS BY WRITING THE ZERO MAGNETIZATION POINT IN THE MEDIUM IN AN UNWANTED, SHIFTED LOCATION. HEAD/MEDIUM COMBINATIONS WITH POOR OVERWRITE CAPABILITIES, COMBINED WITH FINITE WRITE CURRENT AND/OR HEAD GENERATED WRITE FLUX RISETIMES AND PREVIOUS RECORDED HISTORY IN THE MEDIUM MAY CAUSE TWO OR THREE NANoseconds BIT SHIFT.

THE MAJOR CAUSES OF DIGITAL MAGNETIC RECORDING CHANNEL BIT-SHIFT ARE THE FOLLOWING:

1. NOISE INDUCED BIT-SHIFT (NIB).
2. PATTERN INDUCED BIT-SHIFT (PIB).
3. OVERWRITE INDUCED BIT-SHIFT (OWIB).

4. ASYMMETRY INDUCED BIT-SHIFT (ASIB).
5. SYSTEM NOISE INDUCED BIT-SHIFT (SNIB).
6. MINOR MEDIA DEFECTS THAT PASS DEFECT SCANNING TESTING BECAUSE THE MINOR DEFECTS ARE WITHIN SPECIFICATIONS. (MMD)
7. ADJACENT TRACK INDUCED BIT-SHIFT (ATIB).

NIB IS CAUSED BY MEDIA, HEAD, AND ELECTRONIC CIRCUIT NOISE SOURCES. THE INSTANTANEOUS AMPLITUDE OF THIS NOISE IS COMMONLY ASSUMED TO BE DEPENDENT UPON THE NOISE SOURCE'S RMS VALUE, MAGNIFIED BY THE SIGMAS ASSOCIATED WITH THE PROBABILITIES OF GAUSSIAN DISTRIBUTION OF CHANCE. IF THE NOISE IS ASSUMED TO BE GAUSSIAN, IT LENDS ITSELF TO THE FOLLOWING PROBABILITIES:

RMS VALUE = SIGMA

SIZE OF NOISE "SPIKE" IN TERMS OF NOISE RMS VALUE	PROBABILITY OF OCCURRENCE OF THAT NOISE "SPIKE"
0	1/1
1	1/3.2
2	1/21.74
3	1/370.4
4	1/15,625
5	1/1,724,137.9
6	1/500,000,000
6.47 ~ 6.5	1/10,000,000,000
7	1/400,000,000,000
8	1/80,000,000,000,000,000

FIGURE D SHOWS THAT IF THE 24 MEGABIT/SECOND EXAMPLE SYSTEM HAD SNR EQUAL TO 26db (BASE-TO-PEAK SIGNAL DIVIDED BY RMS NOISE) AT THE OUTPUT OF THE DIFFERENTIATOR, THE COMPOSITE "ZERO CROSSING" WOULD SHIFT IN TIME WITH AN RMS JITTER EQUAL TO:

26db = 20:1; THE RMS NOISE IS 5% OF THE BASE-TO-PEAK DF_{out}.

HENCE, THE "ZERO-CROSSING" WILL SHIFT: (5%)/(10%/nsec) = 0.5 nsec.(RMS)

* NORMALLY, SNR IS SPECIFIED AT THE HEAD'S OUTPUT OR THE HEAD'S IC PREAMP'S OUTPUT. IN ORDER TO OBTAIN THE SNR AT THE DIFFERENTIATOR'S OUTPUT, THE RMS NOISE OR THE SPECIFIED NOISE SPECTRA CHARACTERISTICS ARE OBTAINED FROM THE SPECIFIED SNR TEST CONDITIONS, THEN POWER SPECTRA MODIFIED BY THE INVOLVED READ CHANNEL BLOCKS SUCH AS AGC AMPLIFIER, NOISE FILTER, "PEAK" EQUALIZER, AND, OF COURSE, THE DIFFERENTIATOR. THE RMS NOISE PRESENT AT THE OUTPUT OF THE DIFFERENTIATOR OBTAINED CAN BE USED EITHER TO CALCULATE SNR OR DIRECTLY TO PREDICT NIB.

IF THE NOISE IS GAUSSIAN, AND SUCH PROBABILITIES HOLD, EVERY 10^{10} EVENTS (TRANSITIONS, ON THE AVERAGE), THE INSTANTANEOUS VALUE OF NOISE WILL "SPIKE" TO APPROXIMATELY 6.5 TIMES THE RMS VALUE OF NOISE. WHEN THIS OCCURS, THE INSTANTANEOUS SNR OF THE ABOVE EXAMPLE SYSTEM CAN BE CONSIDERED TO FALL TO:

$(20/6.5) : 1$; THE INSTANTANEOUS NOISE "SPIKE" IS 32.5% OF DF_{out} !

HENCE, THE "ZERO-CROSSING" WILL SHIFT: $(32.5\%)/(10\%/nsec) = 3.25$ nsec.

OR, ONE CAN READ THE BIT-SHIFT DIRECTLY FROM THE DF_{out} PLOT OF FIGURE D, AUTOMATICALLY TAKING INTO ACCOUNT THE CURVING SHAPE OF DF_{out} VERSUS TIME. A POSITIVE NOISE "SPIKE" EQUAL TO 32.5% OF THE BASE-TO-PEAK VALUE OF DF_{out} WILL "LIFT" THE DF_{out} SIGNAL BY 32.5% CAUSING THE "ZERO-CROSSING" TO BE LATE BY APPROXIMATELY 3.3 nsec.

PIB IS CAUSED BY THE NON-ZERO AMPLITUDE OF THE "TAILS" OF THE DF_{out} SIGNAL OF OTHER TRANSITIONS, ADJACENT TO THE SPECIFIC READBACK TRANSITION UNDER DETECTION, ALGEBRAICALLY ADDING TO THE IDEAL ZERO-CROSSING OF THE DF_{out} SIGNAL BEING DETECTED. FIGURE C SHOWS THAT IF ONE NEIGHBORING TRANSITION IS AT THE CLOSEST PROXIMITY THAT THE 2, 7, RLL CODE ALLOWS, (62.5 NANoseconds AWAY IN THE EXAMPLE SYSTEM), IN EITHER DIRECTION, THEN A TAIL OF THAT NEIGHBORING TRANSITION WILL ADD APPROXIMATELY 24% TO THE DF_{out} SIGNAL CAUSING THE COMPOSITE DF_{out} "ZERO-CROSSING" TO BE SHIFTED BY:

$(24\%)/(10\%/nsec) = 2.4$ nSEC.

THE PHYSICS OF OVERWRITING CAUSES BIT-SHIFT (OWIB) IN TWO COMPONENTS:

1. BY INCOMPLETE ERASURE LEAVING UNWANTED RESIDUAL SIGNALS FROM PREVIOUSLY RECORDED DATA, AND,
2. BY WRITING THE NEWLY MAGNETIZED TRANSITION IN A SPATIAL LOCATION ALONG THE MEDIUM'S RECORDED TRACK PATH THAT CORRESPONDS TO A PLACE THAT IS EITHER EARLIER OR LATER THAN THE PLACE THAT WRITE CURRENT TRANSITION TIME AND MEDIUM ROTATIONAL SPEED CALCULATIONS PREDICT. THIS CAUSES BIT-SHIFT THAT IS PERMANENTLY LOCKED IN THE TIME LOCATION OF THE TRANSITION IN THE MEDIA DURING WRITING.

THE FIRST COMPONENT OF OWIB CAN BE CALCULATED CONSERVATIVELY BY ASSUMING THAT THE WORST CASE RESIDUAL SIGNAL "LEFT-OVER" FROM A PREVIOUS RECORDING IS THE BIT-SHIFTING UNWANTED SIGNAL THAT APPEARS AT THE OUTPUT OF THE DIFFERENTIATOR. THE BIT SHIFT CAUSED BY THE UNWANTED RESIDUAL'S AMPLITUDE CAN BE FOUND IN THE SAME MANNER THAT NIB WAS DETERMINED. MAGNIFICATION BY SIGMA DOES NOT APPLY, HOWEVER, BECAUSE THE RESIDUAL

SIGNALS ALWAYS APPEAR AT THE SAME TIME (SAME RECORD LOCATION) AND ARE ALWAYS THE SAME AMPLITUDE. HENCE IF THE OVERWRITE SPECIFICATION WERE ONLY DUE TO RESIDUAL SIGNALS, THEN 24db OF "OVERWRITE" (MEASURED AT THE OUTPUT OF THE DIFFERENTIATOR) WOULD ASSERT THAT THE UNWANTED RESIDUAL SIGNAL IS APPROXIMATELY 8% OF THE OF THE DESIRED READBACK SIGNAL. THE BIT SHIFT CAUSED BY THE UNWANTED RESIDUAL SIGNALS WOULD BE:

$$(8\%)/(10\%/nsec) = 0.8 \text{ nsec.}$$

THE SECOND COMPONENT OF OWIB IS THE LARGER OF THE TWO, AND IS CAUSED BY THE HEAD'S MAGNETIC FIELD INTENSITY'S CAPABILITY TO RE-MAGNETIZE PREVIOUSLY WRITTEN DATA IN A TIMELY MANNER. THE FACTORS INVOLVED ARE:

HEAD EFFICIENCY
GAP SIZE
FLYING HEIGHT
MEDIA THICKNESS
MEDIA COERCIVITY
WRITE CURRENT RISE TIME
GAP'S MAGNETIC FLUX RISE TIME (EDDY CURRENT-CAUSED DELAYS)
MAGNETIC STATE OF MEDIA TO BE WRITTEN (HISTORY)

LET US IGNORE HEAD CORE AND EDDY-CURRENT LOSSES, AND ASSUME THAT THE ONLY PARAMETER THAT CAUSES THE FIELD INTENSITY IN THE GAP (H_g) TO BE TIME DEPENDENT IS WRITE CURRENT RISE TIME. THEN, IN THE SIMPLEST MODEL, THE MAGNETICALLY COERCING FIELD INTENSITY AT THE MID-POINT IN THE MEDIUM (H_x) MUST AT LEAST EQUAL HALF THE VALUE OF THE COERCIVITY (H_c) OF THE MEDIUM, IN THE POLARITY OPPOSITE TO THE PREVIOUSLY RECORDED MAGNETIC STATE IN ORDER TO MAGNETICALLY "SWITCH". (HALF THE VALUE OF H_c IS USED ARBITRARILY BECAUSE THE SWITCH-INDUCING FIELD IS DISTRIBUTED SPATIALLY ALONG THE MEDIUM'S THICKNESS (t) AND IN ADDITION, THERE IS A CONTRIBUTION HELPING TO START THE SWITCHING DUE TO SELF-DEMAGNETIZATION FIELDS.)

IF THE RISE TIME OF I_{write} IS ZERO, THEN THE TRANSITION POINT ALONG THE RECORDED TRACK IS PROPERLY, AND EXACTLY IN THE CORRECT LOCATION. IF THE RISE TIME OF I_{write} IS NON-ZERO, THEN THE RECORDED TRANSITION UNDERGOES A "POSITION-SHIFT" ALONG THE DIRECTION OF THE RECORDED TRACK, HENCE A TIME-SHIFT OCCURS.

CASE I. THE MEDIUM WAS PREVIOUSLY MAGNETIZED BY A NEGATIVE I_{write} . THE HEAD HAS BEEN RE-MAGNETIZING (OVERWRITING) THE MEDIUM WITH NEW INFORMATION CONSISTING OF POSITIVE I_{write} . AT A SPECIFIC POINT IN TIME, THE WRITE DRIVER RECEIVES A TRANSITION COMMAND TO REVERSE THE POLARITY OF I_{write} TO NEGATIVE I_{write} . I_{write} COMMENCES TO EXPONENTIALLY CHANGE FROM POSITIVE I_{write} TOWARDS NEGATIVE I_{write} . THE VALUE OF H_x ALSO COMMENCES TO EXPONENTIALLY CHANGE FROM A POSITIVE VALUE IN OERSTEADS (A FIELD INTENSITY THAT HAS BEEN "COERCING" THE PREVIOUSLY MAG-

NETIZED MEDIUM TO RE-MAGNETIZE FROM NEGATIVELY WRITTEN TO POSITIVELY WRITTEN) TO A NEGATIVE VALUE IN OERSTEADS.

CASE II. THE MEDIUM WAS PREVIOUSLY MAGNETIZED BY A POSITIVE I_{write} . THE HEAD HAS BEEN ATTEMPTING TO RE-MAGNETIZE (OVERWRITE) THE MEDIUM WITH NEW INFORMATION CONSISTING ALSO OF POSITIVE I_{write} , WHICH MERELY DRIVES THE MEDIUM TOWARDS THE MAGNETIC STATE THAT IT IS ALREADY AT, SO ESSENTIALLY NO "RE-MAGNETIZATION" ACTUALLY OCCURS. AT A SPECIFIC POINT IN TIME, THE WRITE DRIVER RECEIVES A TRANSITION COMMAND TO REVERSE THE POLARITY OF I_{write} TO NEGATIVE I_{write} . I_{write} COMMENCES TO EXPONENTIALLY CHANGE FROM POSITIVE I_{write} TO NEGATIVE I_{write} . THE VALUE OF H_x ALSO COMMENCES TO EXPONENTIALLY CHANGE FROM A POSITIVE VALUE IN OERSTEADS (A FIELD INTENSITY THAT WAS NOT REALLY REQUIRED TO MAGNETIZE THE ALREADY POSITIVELY MAGNETIZED MEDIUM), TO A NEGATIVE VALUE IN OERSTEADS TO COMMENCE RE-MAGNETIZING THE MEDIUM.

THREE QUANTITATIVE ENGINEERING QUESTIONS NEED TO BE ASKED AND ANSWERED:

1. "AT WHAT TIME DURING THE HEAD'S WRITE CURRENT RISE TIME DOES THE MEDIUM IN CASE I **STOP** BEING RE-MAGNETIZED?"
2. "AT WHAT TIME DURING THE HEAD'S WRITE CURRENT RISE TIME DOES THE MEDIUM IN CASE II **START** BEING RE-MAGNETIZED?"
3. "ARE TIMES IN QUESTION FOR CASES I AND II THE SAME?"

IT CAN BE SHOWN BY CALCULATIONS THAT TIME LOCATION OF THE NEWLY RECORDED TRANSITION WILL OCCUR **EARLIER IN CASE I THAN IN CASE II.**

A SUITABLE TESTING PROCEDURE TO OBSERVE THE SECOND COMPONENT OF OWIB IS TO DC ERASE THE MEDIUM WITH A SPECIFIC POLARITY HEAD CURRENT, WRITE THE LOWEST FREQUENCY, THEN MEASURE THE "PULSE PAIRING", FROM TRANSITION TO TRANSITION. FROM 1 TO 3 NANoseconds OF "PULSE PAIRING" (DIFFERENCES IN CASE I AND CASE II TIMES) CAN USUALLY BE OBSERVED.

ASIB IS CAUSED DIRECTLY IN TIME BY ASYMMETRY IN THE WRITING CIRCUITS AND IN ANY OF THE "DIGITAL" WRITE AND/OR READBACK TRANSITION DETECTION LOGIC CIRCUITS. (THE BI-DIRECTIONAL ZERO-CROSSING PULSE GENERATOR THAT RECEIVES D_{fout} FROM THE DIFFERENTIATOR IN FIGURE A, IS AN EXAMPLE OF SUCH.) IN ADDITION, THE ADDED-AMPLITUDE AT THE D_{fout} 'S "ZERO-CROSSING" POINT OF "NEW" UNWANTED SIGNAL COMPONENTS GENERATED BY ANY SECOND AND/OR EVEN HARMONIC DISTORTION IN THE HEAD AND/OR ANALOG READING CIRCUITS ALSO CONTRIBUTES TO ASIB.

SNIB IS CAUSED BY THE INSTANTANEOUS AMPLITUDE OF "SYSTEM NOISE" SIGNALS FROM OTHER PHYSICALLY ADJACENT CIRCUITS THAT SHARE THE SAME CIRCUIT BOARDS, POWER SUPPLIES, BACK PANELS, ETC. THE UNWANTED SIGNALS MAY ENTER THROUGH THE HEAD, OR READ CHANNEL CIRCUIT TRACES BY CAPACITIVE, OR INDUCTIVE OR RF COUPLING MECHANISMS (SOMETIMES ALL THREE SIMULTANEOUSLY). THE BIT SHIFT CAUSED BY THE UNWANTED SYSTEM NOISE'S AMPLITUDE CAN BE FOUND IN THE SAME MANNER THAT NIB WAS DETERMINED. MAGNIFICATION BY SIGMA DOES NOT APPLY, HOWEVER, BECAUSE THE "SYSTEM NOISE" SIGNALS TEND TO BE SYNCHRONIZED TO SOME OTHER DRIVE FUNCTION (SUCH AS PLO CLOCK, OR SERVO AND/OR SPINDLE POWER AMPLIFIERS). ALTHOUGH THE OPERATION AND HENCE THE SYSTEM NOISE OF THE CAUSING DRIVE FUNCTIONS MAY BE INDEPENDENT, THE MAXIMUM AMPLITUDE TO BE GENERATED IS USUALLY QUICKLY OBSERVED.

BIT-SHIFT THAT IS CAUSED BY MINOR MEDIA DEFECTS THAT PASS DEFECT SCANNING AND TESTING BY BEING WITHIN SPECIFICATIONS, CAN BE CONSIDERED SIMILAR TO THE COMBINATION OF NIB AND SNIB. LIKE NIB THERE ARE MILLIONS OF MINOR DEFECT NOISE AMPLITUDES AND SHAPES THAT MAY APPEAR RANDOMLY AROUND THE MEDIUM'S TRACK. AND, LIKE SNIB THE NOISE AMPLITUDES AND OCCURRENCES ARE SYNCHRONIZED (TO THE TRACK). THE BIT-SHIFT CAUSED BY ANY SINGLE MINOR MEDIA DEFECT WHOSE CHARACTERISTICS ARE DEFINED CAN BE CALCULATED BY USING THE D_{fout} OF FIGURE D. THE NUMBER OF DIFFERENT MINOR DEFECTS THAT ARE POSSIBLE TEND TO FORCE BIT-SHIFT ANALYSIS TO BE LIMITED TO THE EFFECTS OF POSSIBLE AMPLITUDE VARIATIONS IN THE READBACK SIGNAL THAT ARE AT THE SCANNING REJECTION THRESHOLDS. AS EXPECTED, ANY REDUCTION IN THE AMPLITUDE OF THE D_{fout} SIGNAL (AS CAN BE CAUSED BY A MINOR DEFECT'S PARTIAL "DROP-OUT", TYPICALLY <70%) WILL REDUCE THE ABSOLUTE VALUE OF THE SLOPE AND INCREASE THE AMOUNT OF BIT-SHIFT FOR A GIVEN AMOUNT OF UNWANTED ADDITIVE SIGNAL THAT CAUSE NIB, PIB, AND ETC.

ATIB IS CAUSED BY THE INSTANTANEOUS AMPLITUDE OF CROSS-TALK DUE TO THE HEAD PICKING-UP SIGNALS FROM THE ADJACENT TRACK DUE TO HEAD FRINGING AND/OR HEAD-TO-TRACK MISALIGNMENT. WHEN ATIB IS PRIMARILY DUE TO HEAD-TO-TRACK MISALIGNMENT, THE BIT-SHIFT GENERATED IS COMPOUNDED. NOT ONLY IS AN UNWANTED SIGNAL ADDING TO THE DESIRED D_{fout} SIGNAL CAUSING "LIFTING" OR "LOWERING" OF THE COMPOSITE D_{fout} SIGNAL, BUT THE AMPLITUDE OF THE DESIRED D_{fout} SIGNAL IS SIMULTANEOUSLY DECREASING. THIS ALLOWS MORE BIT-SHIFT TO OCCUR FOR A GIVEN AMOUNT OF ANY UNWANTED ADDITIVE SIGNAL. IF THE HEAD WERE TO BE MIS-POSITIONED SUCH THAT THE DESIRED DATA TRACK READBACK AMPLITUDE WAS REDUCED BY 25%, WHILE THE ADJACENT TRACK WAS UNDESIRABLY BEING SENSED AT A 15% LEVEL, THE BIT-SHIFT FOR THE EXAMPLE SYSTEM WOULD BE:

$$(15\%) / \{ [(10\%) * (.75)] \} / \{ \text{nsec} \} = 2 \text{nsec}$$

BECAUSE THE D_{fout} SLOPE HAS DECREASED TO 7.5 % PER NANOSECOND BY THE 25% REDUCTION IN DESIRED TRACK READBACK SIGNAL, ANY OF THE ADDITIVE-AMPLITUDE CAUSES OF BIT-SHIFT SUCH AS NIB AND SNIB, WILL GENERATE A THIRD MORE BIT-SHIFT FOR A GIVEN AMOUNT OF NOISE.

THE OVERALL RAW-READ DATA ERROR RATE FOR THE 24 MEGABIT/SEC EXAMPLE SYSTEM CAN BE NOW ESTIMATED:

**BIT-SHIFT
ON TRACK**

	(@ ANY TIME	@ $\times 10^{10}$ (6.5*sigma)
NIB	0.71	3.25
PIB	2.4	2.4
OWIB I	0.8	0.8
OWIB II	1 -> 3	1 -> 3
ASIB	0.5 -> 2	0.5 -> 2
SNIB	0.1 -> ?	0.1 -> ?
ATIB	~0	~0
	<hr/> 5.51	<hr/> 8.05
ERROR RATE	10^{10}	10^{10}
MARGIN	4.91	2.37

**BIT-SHIFT
ON TRACK and DURING MINOR DEFECT**
(DFout slope divided by 0.7)

	(@ ANY TIME	@ $\times 10^{10}$ (6.5*sigma)
	1.01	4.64
	3.43	3.43
	0.8	0.8
	1 -> 3	1 -> 3
	0.5 -> 2	0.5 -> 2
	0.14 -> ?	0.14 -> ?
	~0	~0
	<hr/> 6.88	<hr/> 9.71
ERROR RATE	10^{10}	10^{10}
MARGIN	3.54	0.71

**BIT-SHIFT
OFF TRACK**

(DFout slope divided by 0.75)

	(@ ANY TIME	@ $\times 10^{10}$ (6.5*sigma)
NIB	0.95	4.33
PIB	2.4	2.4
OWIB I	0.8	0.8
OWIB II	1 -> 3	1 -> 3
ASIB	0.5 -> 2	0.5 -> 2
SNIB	0.13 -> ?	0.13 -> ?
ATIB	1.5	1.5
	<hr/> 7.28	<hr/> 10.66
ERROR RATE	10^{10}	10^9
MARGIN	3.14	0

**BIT-SHIFT
OFF TRACK and DURING MINOR DEFECT**
(DFout slope divided by 0.7*0.75)

	(@ ANY TIME	@ $\times 10^{10}$ (6.5*sigma)
	1.35	6.19
	3.43	3.43
	0.8	0.8
	1 -> 3	1 -> 3
	0.5 -> 2	0.5 -> 2
	0.19 -> ?	0.19 -> ?
	2.14	2.14
	<hr/> 9.41	<hr/> 14.25
ERROR RATE	10^{10}	10
MARGIN	1.01	0.

HIGH PERFORMANCE HEAD POSITIONING SERVO SYSTEM (HPHPSS) BLOCK DIAGRAM

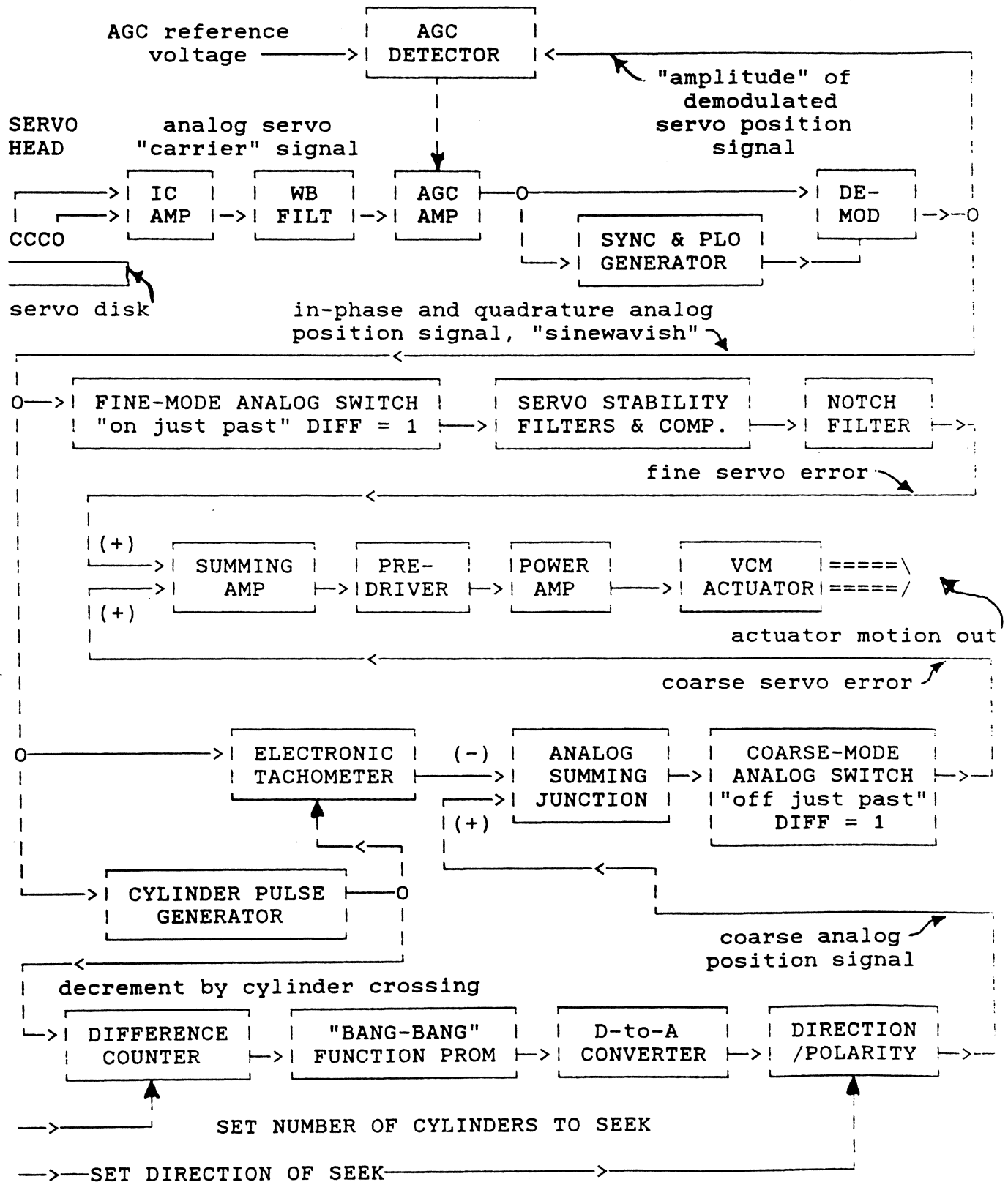


FIGURE E

HPHPSS DESCRIPTION:

Refer to figure E on page 13. A two-terminal, single or multi-layered voice-coil actuator (VCM) is electrically driven by a linear, class B, or switching, class D, T-bridge (push-pull) power amplifier requiring two actuator power supply voltages, or H-bridge, needing only one actuator power supply.

The servo error signal is medium-level analog, and is gated to the SUMMING AMP and on to the power amplifier PRE-DRIVER through either the FINE-MODE ANALOG SWITCH or the COARSE-MODE ANALOG SWITCH. Current mode operation of the POWER AMP is accomplished through sensing voltage across a resistor (<0.5 ohm) placed in series with the motor's coil (not shown), and subtracting this signal (negative feedback) from the total servo error signal at the output of the SUMMING AMP. By utilizing current mode operation, the effects of motor inductance can be ignored, for small servo-error signal levels, as is the case in fine mode when track-following a track/cylinder. Hence the actuator transfer function appears second order. When large servo-error signals exist, such as the case during coarse mode, any practical power amplifier saturates and the operation becomes voltage mode. During power amplifier saturation times, the effects of motor coil inductance become significant and adversely affect the access time to the order of five to ten percent.

The fine mode servo loop obtains position information by demodulating amplified and wideband-filtered servo head output voltage that the SERVO HEAD generates when sensing magnetic field patterns written on the servo surface of the SERVO DISK by a "servo writer" during manufacture of the HDA¹. HPHPSS utilize di-pulse-like multiple servo patterns to produce both IN-PHASE and QUADRATURE sinewave-like analog position signals out of the demodulator. If the IN-PHASE position signal has its zero value at the centerline of a given data cylinder as measured by the SERVO HEAD and associated electronics mentioned above, then the quadrature position signal is used to more accurately determine the entering of the linear zone of the addressed cylinder near the end of a multiple cylinder seek. Switching from coarse-mode to fine-mode after the previous peak of the IN-PHASE position signal assures the smoothest (and usually the fastest) servo settling time. The output of the DE-MOD consists of position signals that are sinewave-like ("SINEWAVISH") with zero values at spatial distances that correspond to cylinder centerline distances along the radius of the disk. Having both in-phase and quadrature position signals helps the ELECTRONIC TACHOMETER circuit to generate fairly-linear (undistorted) velocity signals (by differentiating smaller segments of the more straight-line portion of each "SINEWAVISH" position signal), in addition to extracting all-important, direction information.

¹ HDA: Abbreviation for "Head-Disk-Assembly".

The analog position signals are also processed by the CYLINDER PULSE GENERATOR to generate cylinder crossing, "digital pulses" that are used by the coarse-mode system. During the coarse-mode part of a multiple cylinder seek, the total servo error signal consists of the ELECTRONIC TACHOMETER output signal subtracted from the output of the DIRECTION/POLARITY controlled D-to-A CONVERTER whose input digital values are the output of a "look-up" function-generating prom, the 'BANG-BANG' FUNCTION PROM. The input to the PROM is the output of the DIFFERENCE COUNTER, whose instantaneous digital value is the difference between the desired cylinder seek length at the beginning of the seek, and the number of cylinders crossed during the seek as decremented by cylinder crossing pulses as they occur. The PROM performs "squareroot-like" operations on the difference counter's value as required per "optimal-switching", or "Bang-Bang" servo theory.

Most HPPSS employ microprocessors to attend to various chores such as monitoring safety circuits such as "PLO locked", for proper servo pattern demodulation, guardband detection to assure the "home position" during initialization and recovery from a fault, emergency retraction detection to assure actuator retreat to the recording heads' landing zone on the disks after loss of power source(s) or normal servo-controlled action. Microprocessors can also make the HPPSS more "intelligent" and perform "self adaptive" control and optimization adjustments as a function of its operating conditions.

QUADRATURE POSITION TRANSDUCTION

In the past, HPPSS used linear potentiometers, magnetic differential transformers, Inductosyns®, and optical gratings with light emitting solid state semiconductors to generate the classical "sinewavish" or "sawtooth-like" track position-indicating signals, with zero position error signal level corresponding to the center of the data track and/or cylinder to be read or written on. Today nearly all utilize the specially recorded "servo surface" band of one of the surfaces of disk(s) in the spindle's stack. Figure E on page 13 shows a servo-head sensing the special indelible servo pattern on the servo disk. The servo pattern is written at the factory, and is intended to never to be erased **DELIBERATELY** by any function or action initiated by the disk product-using customer. The sensed electrical signals correspond to magnetized medium polarity reversals or transitions that are shown in cross-hatched patterns in figure F on page 18. As the head senses each magnetic transition, the electrical output voltage is a single pulse, either positive or negative in electrical polarity, depending on the magnetic polarity change (north to south, or south to north) of the transition. Figure F shows the recorded servo patterns and the corresponding sensed output signals of the head for one "servo-byte" of the pattern for "QUADRATURE DI-PULSE" that is commonly used by today's HPPSS. The pattern includes two sets of synchronizing di-pulses ("sync-bits") located in time by phase-locked oscillator clocking signals (PLO) to be "cell" 0 and "cell" 3 of 32 total "cells" (0 to 31) in each servo byte.

Several thousands of servo bytes are recorded around the total circumference of the disk.

The PLO is synchronized to the disk by these first synchronizing sets, with transitions occurring at the beginning of "cells" 0, 1, 3, and 4. After these synchronizing sets, a total of four, different, repeating, radial position information-bearing recorded-"cell" patterns are shown:

"ONE/THREE"	=	OT	=	TRANSITIONS AT BEGINNING OF "CELLS"	8, 10, 20, 22.
"ONE/FOUR"	=	OF	=	" " " " " "	8, 10, 26, 28.
"TWO/FOUR"	=	TF	=	" " " " " "	14, 16, 26, 28.
"TWO/THREE"	=	TT	=	" " " " " "	14, 16, 20, 22.
"ONE/THREE"	=	OT	=	" " " " " "	8, 10, 20, 22.

The individual servo tracks are recorded at the track density that the disk product will use for customer data tracks (here = 1400 TPI) at the factory by an expensive, instrument-quality, servo writer. The servo-head in the disk drive product has **TWICE** the core width of the data head such that it reads **TWO** servo tracks simultaneously! The servo head, being twice the recorded servo pattern's track width, assures smoother and more continuous increases and decreases of the sensed amplitude of di-pulses as the servo head moves across the disk's radius. Servo pattern di-pulses are amplified and linear-phase, low-pass filtered to maximize signal-to-noise ratio while maintaining di-pulse waveform fidelity. The demodulator can be nothing more than a set of four (or eight) gated diode, peak-rectifying, sample-and-hold (S&H) circuits, with controlled held-voltage sag, that obtain and store the di-pulse amplitudes read by the servo head. For the pattern of figure F, a minimum of four S&H circuits are needed, one to be gated-on by timed signals from the synchronized PLO for each dipulse time location within the servo byte. Careful study of the complex servo surface patterns and associated electrical signals of figure F yields the method of generation of the IN-PHASE, and QUADRATURE servo transduction signals for locating data track/cylinder centerlines.

Refer once again to figure F. Assume that the servo head is centered along data cylinder 002. (The terms "Tracks" and "Cylinders" are interchangeable for this analysis: "Cylinders" referring to a plurality of "Tracks" due to a plurality of disks and hence data-surfaces at a servo position null.) At the top of figure F is shown two of the four demodulating gates logically generated by the syncbit-pattern-locked PLO system. Gate "TWO's" turns-on the diode demodulator (see figure G on page 20) that S&H's the radial position-sensitive readback amplitude of di-pulses written at the beginning of PLO count 14. The demodulated servo-head position signal,

consisting of the S&H'ed algebraic sum of the servo-head sensed di-pulse zero-to-positive-peak amplitudes of servo tracks "TWO/FOUR" and "TWO/THREE", is shown as "2's" varying radially at the right-hand side in figure F. Note its maximum value occurs at the centerline of data cylinder 002.

At the same radial location, the demodulating circuit that is gated by gate "THREE's" will S&H'ed a signal value that is half of the possible peak value, since the servo-head senses a dipulse contribution from only servo pattern track "TWO/THREE" at that time. The S&H'ed output of the demodulator controlled by gate "FOUR's" (not shown) will also be half of the maximum possible amplitude value since the servo-head senses only the contribution from servo track "TWO/FOUR" at gate "FOUR's" time (not shown). Following the same analysis, the output of the demodulator controlled by gate "ONE's" (not shown) is zero volts at the stated servo-head radial position.

Hence the four demodulator outputs ("1's", "3's", "2's", and "4's") vary as a function of servo-surface disk-radius as shown at the right-hand side in figure F.

Refer to figure H on page 21. The IN-PHASE servo position signal is formed by demodulated signals "3's" minus "4's". The QUADRATURE servo position signal is formed by demodulated signals "1's" minus "2's". The reason for the above algebraic combinations is due to the fact that each demodulated di-pulse signal or any magnetically recorded, read-back and demodulated signal tends to have sharper "pointed" maximum values and quite "sloppy" or "rounded" near-zero voltage values. When "locking-on" to cylinder 002, the Fine Mode servo uses IN-PHASE position signal by which a positive voltage causes VCM current to force the VCM towards a lower-numbered cylinder (001) direction, and negative IN-PHASE voltage causing VCM current to force the VCM towards cylinder 003. In order to lock-on to cylinder 001, inverted QUADRATURE position is selected. For cylinder 002, IN-PHASE is selected. For cylinder 003, QUADRATURE is selected. And, for cylinders 000, or 004, inverted IN-PHASE is selected.

The servo-pattern magnetic flux as a function of radial position that the servo-head senses and the sum of the demodulated di-pulse amplitudes at any radius is a constant. (Ideally, it should be constant, but the "sawtooth's rounding especially near zero signal values causes some inconsistencies.) An AGC circuit utilizes this fairly constant feature to facilitate amplitude, and hence position gain calibration, such that the overall transduction gain (in volts/inch) is constant. (A magnetically recorded digital signal is amplitude-dependent upon a number of parameters, including relative velocity between the reading-head and disk surface.) The end result is the classical saw-tooth-like position signals as a function of disk radius shown in figure F.

See figure G on page 20. The AGC AMP shown receives an AGC "ERROR" voltage that is generated from the AGC CONTROL FEEDBACK voltage that is 50 % of the demodulated "4's" voltage, and 50 % of the demodulated "3's" voltage due to the "Thevinin divider" summing circuit formed by Ra and Rb. The AGC's "servo-loop's" reference voltage is designed to be a magnitude of 5 volts, therefore the average value of the sum of the demodulated di-pulses will be 5 volts, and since they are nearly a sawtooth, they should have a peak value of 10 volts.

For a track density of 1400 TPI, the position transduction gain, KP, is calculated as follows:

Recall that the IN-PHASE demodulator peak output signal is equal to 20 volts peak-to-peak, "sawtoothing" over twice the servo pattern trackwidth. See figure H on page 21.

$1/1400 \text{ TPI} = 0.0007143 \text{ inches/ data track}$

$\frac{20 \text{ volts}}{(2) * (0.0007143 \text{ inches})} = 14,000 \text{ volts/inch} = \text{KP}$

VELOCITY TRANSDUCTION BY "ELECTRONIC TACHOMETER"

The 14,000 volt/inch, spacially-sloped output of the position transduction system appears as an FM modulated sawtooth waveform when the actuator seeks across the radius of the disk. By time-differentiating this output signal, one obtains an amplitude-modulated waveform as shown in figure I on page 22. The envelope contains amplitude proportional to velocity. FET analog switches that are gated by analog comparator circuits making decisions regarding the instantaneous values of the four demodulated di-pulse-amplitude signals select the appropriate polarity of time-differentiated position voltage, away from any transient shift times, (the vertical edges) in orderly sequence. The same polarity selecting analog comparators select the appropriate position transduction signal, IN-PHASE, inverted IN-PHASE, QUADRATURE, and inverted QUADRATURE. Refer once again to the timing chart on figure H on page 21, and the electronic tachometer subsystem shown in figure J on page 23.

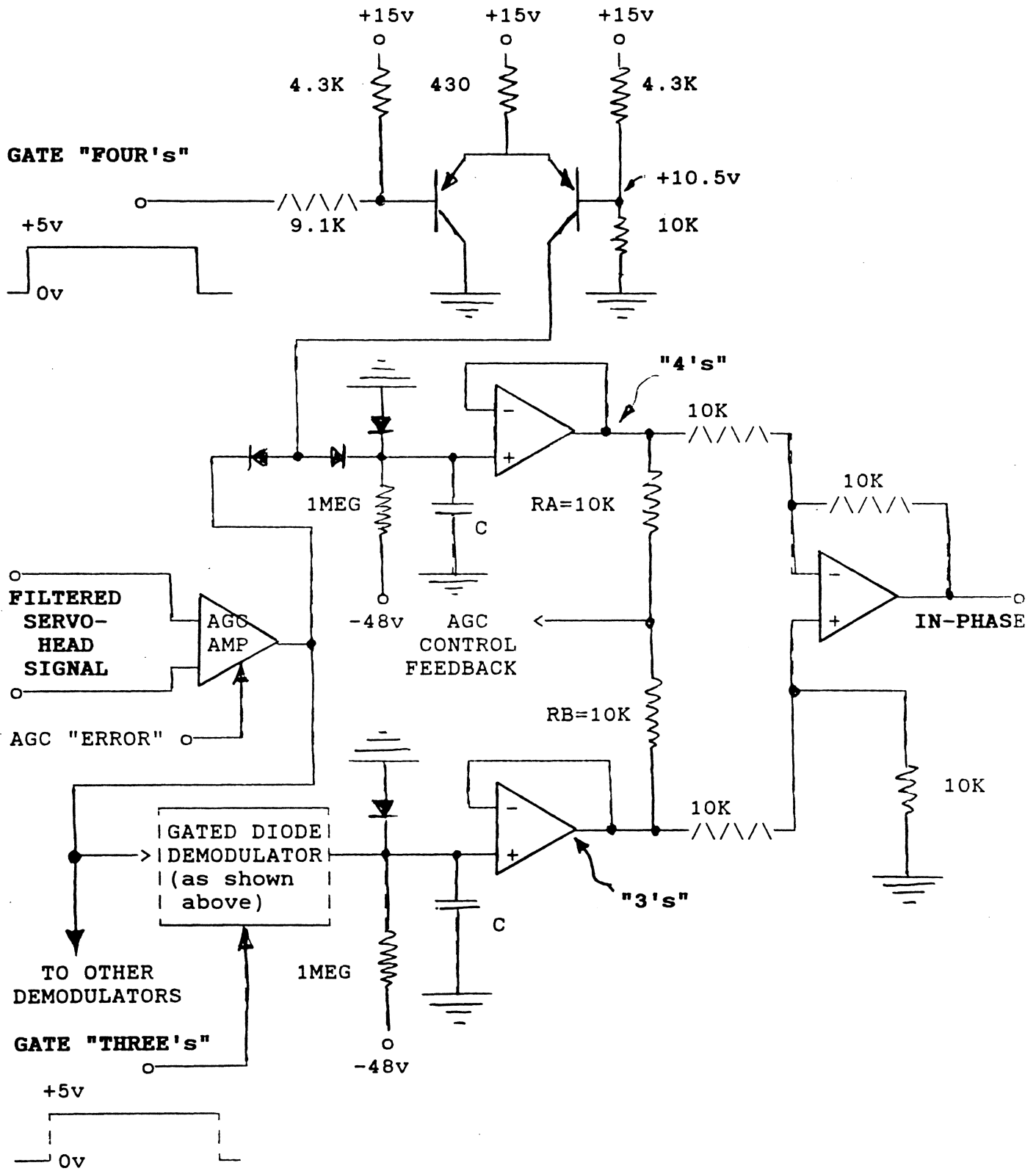


FIGURE F. SERVO POSITION INFORMATION DEMODULATION CIRCUIT

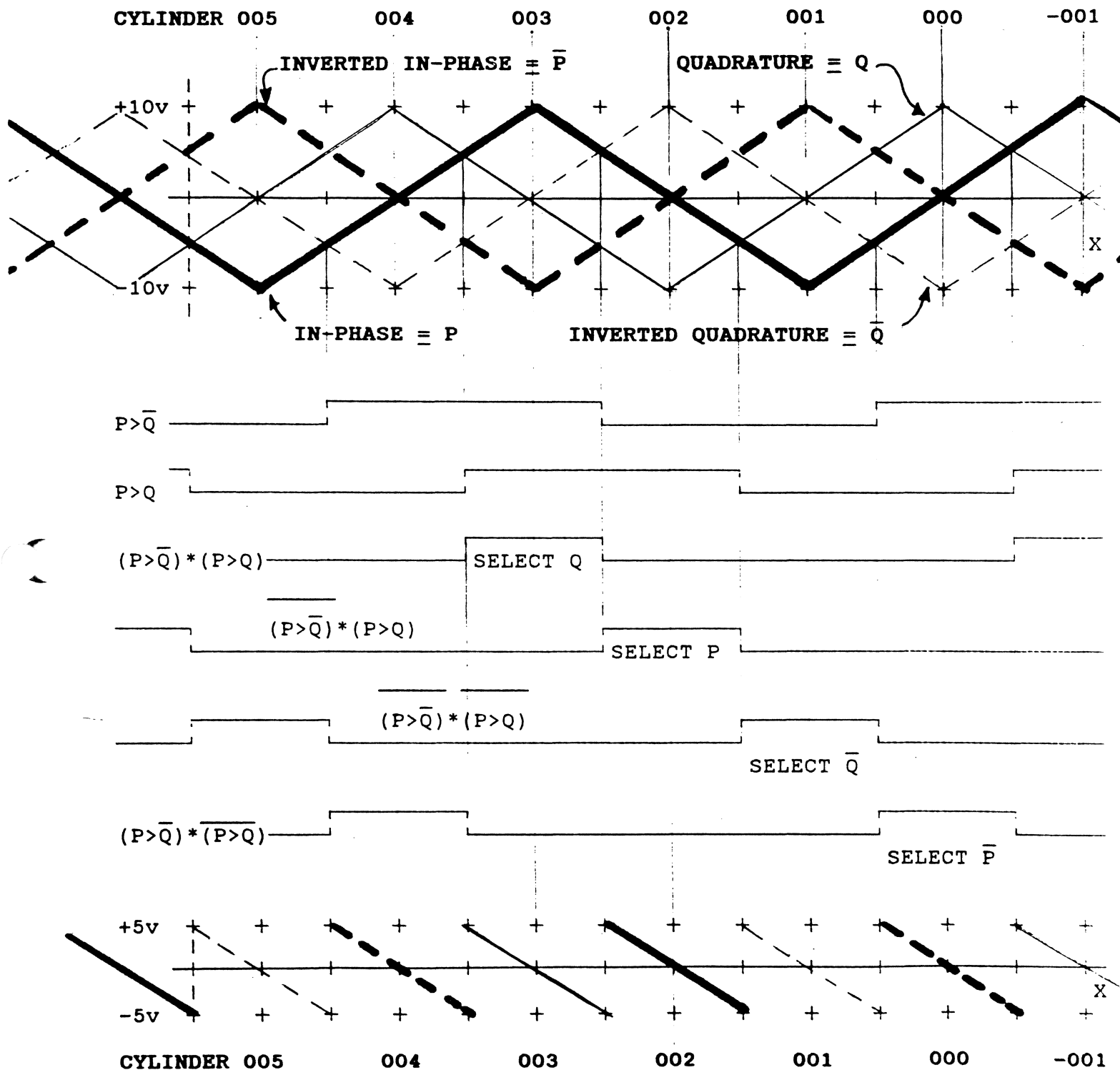
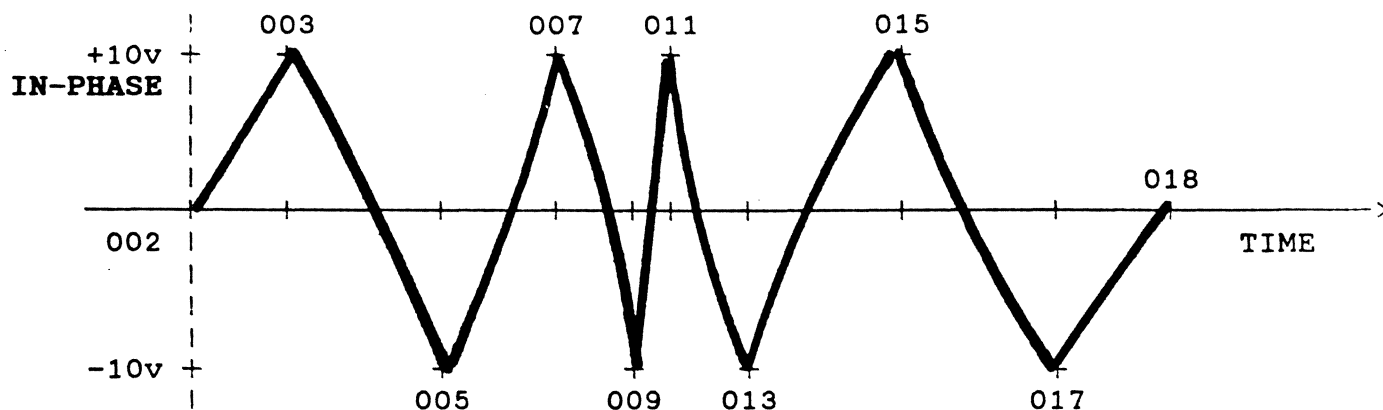
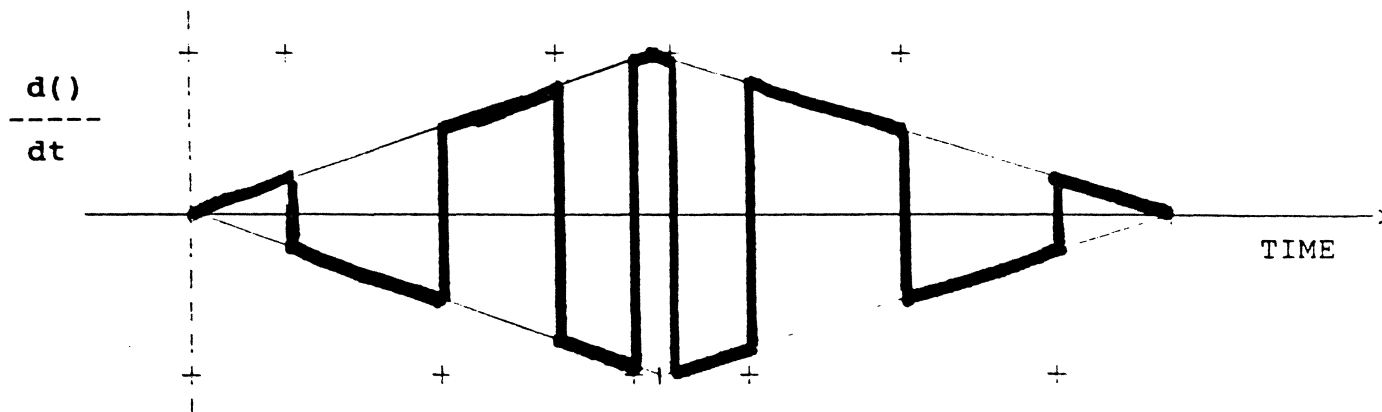


FIGURE H POSITION TRANSDUCER "IN-PHASE", "INVERTED IN-PHASE", "QUADRATURE", AND "INVERTED QUADRATURE" SIGNALS VERSES RADIAL DISK POSITION OR CYLINDER LOCATION; LINEAR REGION SELECTION LOGIC AND CYLINDER COUNTING IN COARSE MODE; AND, SELECTED LINEAR REGION FOR FINE MODE.



The above signal is present at the input to the differentiator circuit as shown in figure J on page 23. (See $E_{in}(s) = IN-PHASE.$)



The above signal is present at the source of the FET analog switch as shown in figure J on page 23.

FIGURE I. POSITION TRANSDUCER "IN-PHASE" OUTPUT AND TIME-DIFFERENTIATION OF SAME FOR 16 CYLINDER SEEK FROM CYLINDER 002 TO CYLINDER 018. (NUMBERS ARE CYLINDERS)

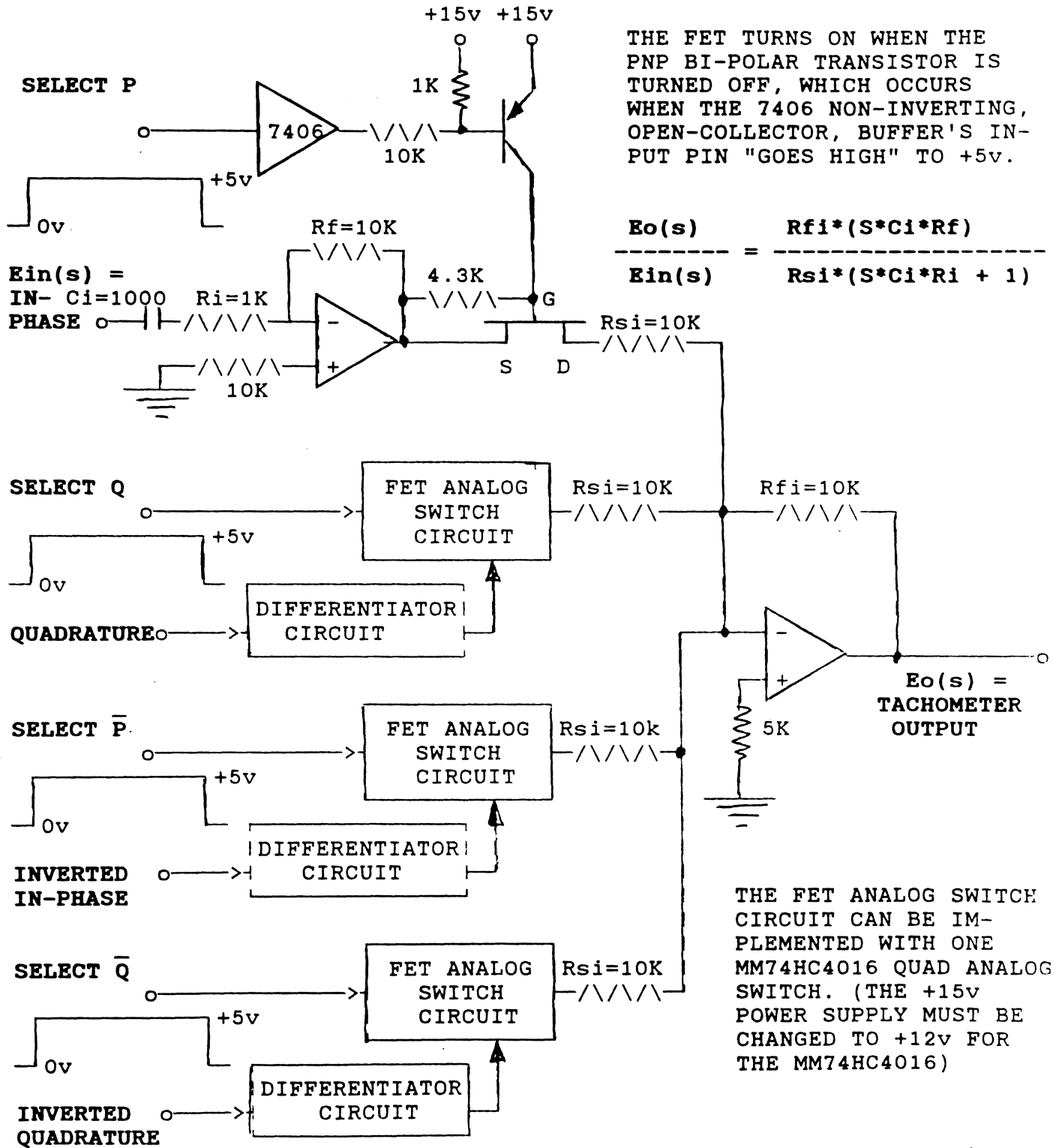


FIGURE J. ELECTRONIC TACHOMETER SUBSYSTEM

NOMINAL SPECIFICATIONS:

$K_T = 10 \times 10^{-6} \cdot K_P = 0.1400 \text{ volt}/(\text{inch}/\text{sec.}) @ K_P = 14000 \text{ volt}/\text{inch};$
 RANGE: $E_o(\text{max}) = \pm 14 \text{ volt} \rightarrow \pm 100 \text{ inch}/\text{sec.}$

COMPONENTS OF MISREGISTRATION OF THE SERVO HEAD WITH RESPECT
TO THE SERVO PATTERN'S DATA-CYLINDER (TRACK) CENTERLINE.

1. DUE TO POSITION TRANSDUCTION AND ELECTRONICS:

a. SERVO WRITER:

- * VIBRATIONS DURING WRITING
- * PATTERN-WRITING HEAD'S AIRBEARING FLIGHT INSABILITIES.

b. SERVO-SURFACE MEDIUM:

- * DEFECT CERTIFICATION
- * CERTIFICATION-PASSED MINOR DEFECTS
- * SIGNAL TO NOISE RATIO (SNR)
- * MODULATION
- * "STRESS ERASURE" DUE TO MOMENTARY HDI (KISSES FROM HEAD)

c. SERVO HEAD

- * GAP IRREGULARITIES ALONG CORE WIDTH CENTERLINE
- * MAGNETIC PARTICLE(S) CONTAMINATING GAP
- * AIR BEARING FLIGHT INSTABILITIES VERSUS RADIUS

d. "SYSTEM NOISE" ENTERING SERVO CHANNEL

- * COUPLING FROM WRITING DATA HEAD
- * COUPLING FROM SPINDLE MOTOR/VCM POWER AMPS, ELECTRONICS

e. DEMODULATOR OFFSET(S)

- * DIODE OFFSETS
- * AMPLIFIERS EVEN HARMONIC DISTORTIONS
- * POSITION COMPONENT SUMMING TOLERANCES

COMPONENTS OF MISREGISTRATION OF THE SERVO HEAD WITH RESPECT TO THE SERVO PATTERN'S DATA-CYLINDER (TRACK) CENTERLINE.

1. DUE TO POSITION TRANSDUCTION AND ELECTRONICS (CONTINUED):

f. DC CHANNEL OFFSET(S)

* DC CHANNEL OP-AMP(S), COMPONENTS, BALANCE ADJUSTMENT(S)

g. SERVO ELECTRONICS PARASITIC OSCILLATIONS

* POWER AMP POWER TRANSISTORS

2. DUE TO EXTERNAL (UNWANTED) FORCES & MOTIONS:

a. EXTERNAL VIBRATIONS & SHOCK

b. DISK SPINDLE RUNOUT

c. BASEPLATE "PUMPING" OR RINGING

* SEEK REPETITION PATTERNS AND RATES

d. MECHANICAL RESONANCES

* ACTIVATED BY SEEKING, FANS, SPINDLE MOTOR, EXTERNAL

e. CARRIAGE FRICTION

f. DISK AIRFLOW PATTERNS

* "WIND" DRAG VERSUS RADIUS IN THE RADIAL DIRECTION

g. BASEPLATE-TO-CARRIAGE ELECTRICAL CONNECTIONS (DRAG)

h. DRIVE SPATIAL ORIENTATION (UPHILL, DOWNHILL)

i. SERVO "FEEDBACK" PARASITIC OSCILLATIONS

**COMPONENTS OF MISREGISTRATION OF THE DATA HEAD WITH RESPECT
TO THE SERVO HEAD'S POSITION.**

1. DUE TO THERMAL GRADIENTS:

- a. HDA AIR FLOW PATTERNS
- b. ONE HEAD ARM HAS UNFAVORABLE PROXIMITY TO SOURCES OF HEAT
 - * SPINDLE BEARING(S)
 - * SPINDLE MOTOR
 - * ACTUATOR
 - * ELECTRONICS CIRCUIT BOARDS
 - * HEAD ARM MOUNTED ICs
- c. INITIAL START-UP/WARM-UP HEAT FLOW/TEMPERATURE PATTERNS

2. DUE TO EXTERNAL (UNWANTED) FORCES & MOTIONS.

- a. CARRIAGE RAIL(S)/BEARING(S) IMPERFECTIONS
- b. MECHANICAL RESONANCES (VIBRATORY DIFFERENCES SERVO/DATA)
- c. DISK SPINDLE TILT
- d. BASEPLATE DEFORMATION
 - * AT ASSEMBLY
 - * OVER TEMPERATURE RANGES
- e. SERVO-HEAD TO DATA-HEAD ALIGNMENT SHIFT
 - * AFTER HITTING CRASH-STOP

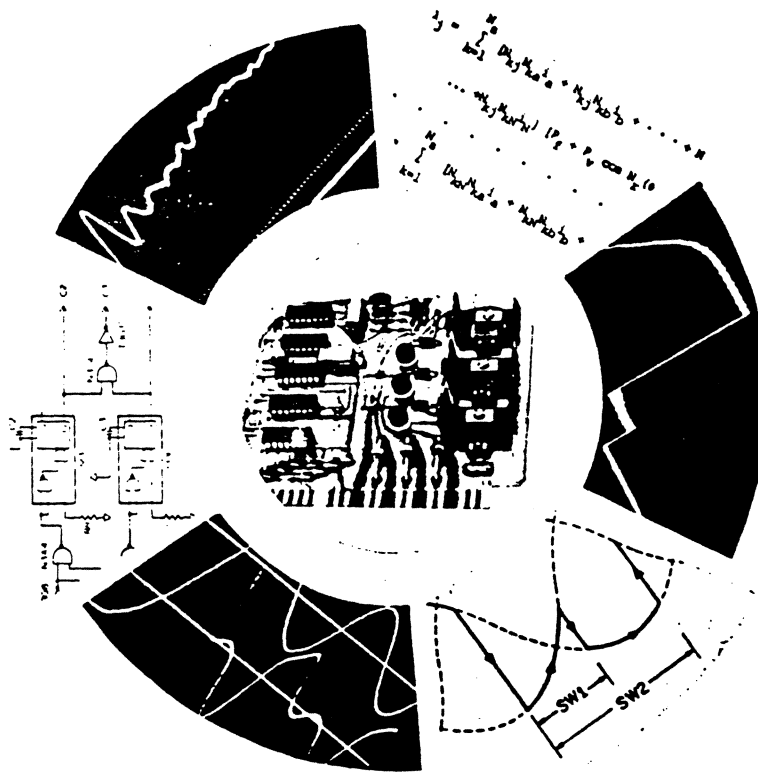
proceedings

Sixth Annual Symposium

incremental motion control systems and devices

Professor B.C. Kuo, Editor

may 24 - 27, 1977



**Department of Electrical Engineering
University of Illinois at Urbana-Champaign**

in cooperation with

Warner Electric Brake and Clutch Company, Beloit, Wisconsin

and

Westool Ltd., Durham, England

MEASUREMENT OF SOLID FRICTION PARAMETERS OF BALL BEARINGS

P. R. Dahl

The Aerospace Corporation
El Segundo, CaliforniaI. INTRODUCTION

A schematic of an electric motor gearbox and inertia load is shown in Figure 1. The system block diagram can be depicted as in Figure 2 where the electrically generated torque T_E drives the motor inertia which, in turn, applies torque through the gearbox to the load inertia. The motor electromechanical characteristics such as back EMF and torque constant are not shown in this diagram. Three forms of friction are present: viscous friction, solid friction, and magnetic hysteresis "friction." The first form, viscous friction, is so familiar it needs no description here. The second form is commonly called Coulomb friction or "stiction," and is referred to in this paper as Solid Friction or SF. A solid friction model (SFM) that aptly describes this type of rolling friction was devised recently [1, 2, 3]. It has the appearance shown in Figure 3 and will be described later in this discussion. The third form is a hysteretic drag torque produced by the permanent magnets and iron in the motor. According to B. G. King [4, 5], it is convenient to think of this as a friction torque. It can be modeled in much the same way as bearing solid friction torque, independent of the electromagnetic impressed torque, as long as the permanent magnets are not demagnetized significantly by the motor windings when current is applied.

The motor angular rate $\dot{\theta}_M$ is input to the gearbox, as is the load angular rate reflected through the gears, to obtain the relative rate with respect to the gearbox input. This relative rate is amplified by the gear ratio to obtain the relative rate with respect to the output shaft. This rate is then integrated to get the angular deflection through the gearbox and output shaft. Most of the torque applied to the load is that transmitted through the box and shaft linear stiffness K . In parallel with the gear shaft stiffness is another solid friction model that takes into account the hysteresis friction of the gearbox. Torque is also applied to the load through this friction. The shape of a typical harmonic

drive-type gear and shaft stiffness and solid friction characteristic without backlash is shown in Figure 4. The case of backlash with hysteretic friction is more difficult to simulate, but some success has been attained by omitting the linear spring and using the friction slope model sketched in Figure 5. This gives the characteristic sketched in Figure 6 where the nominal stiffness is σ and the backlash region has a soft stiffness of σ_0 .

To obtain experimental data on the static stiffness and solid friction hysteresis of the gearbox as shown in Figures 4 and 6, the angle measurements should be taken on the output shaft of the gearbox with the input shaft locked.

Completing the description of Figure 2, the sum of the linear stiffness torque and the gear solid friction torque less the load viscous and solid friction is what drives the load inertia. It is frequently found that the gear hysteretic friction provides a very significant amount of damping to the system.

Solid friction as well as magnetic "friction" is seen to enter the system in very significant ways. We shall show how each of these friction sources can be modeled using three friction model parameters (for each SFM). If a friction source or sources cannot be modeled accurately by a single SFM, multiple SFMs added in parallel can be used. In the following discussion, as an example, it is shown how ball bearing friction parameters are experimentally obtained. Test methods similar to those discussed here can be used to determine parameter values for the other solid friction sources. Raw and reduced test data for bearings are shown.

II. SOLID FRICTION MODEL PARAMETERS

The mathematical model of solid friction is based on deriving the friction torque $T(\theta, t)$ or force $F(x, t)$ from the time derivative of the friction that is a function of x , the angular or linear

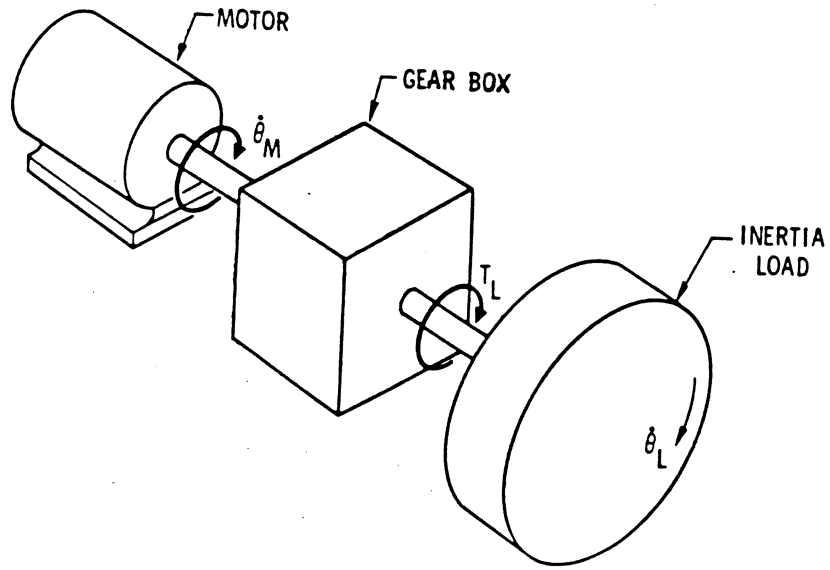


Figure 1. Motor/Gear Box/Load System.

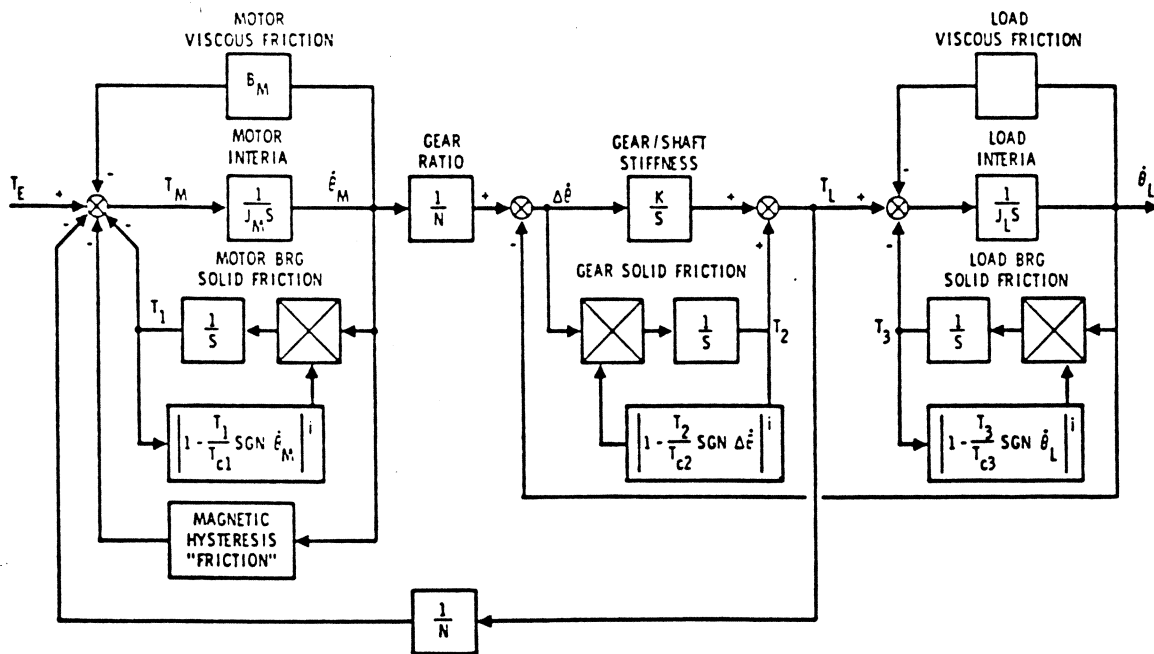


Figure 2. System Diagram.

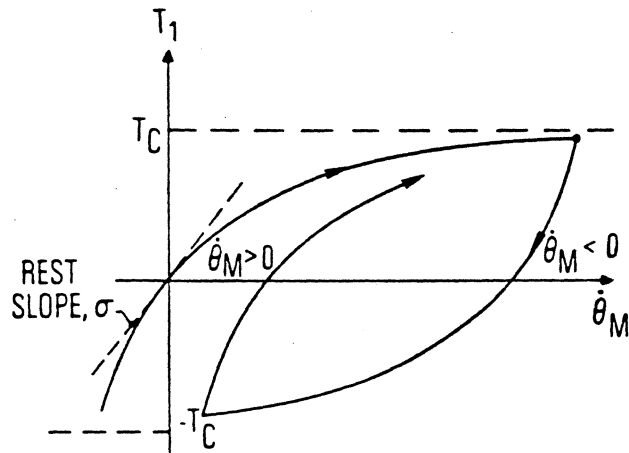


Figure 3. Solid Friction Behavior.

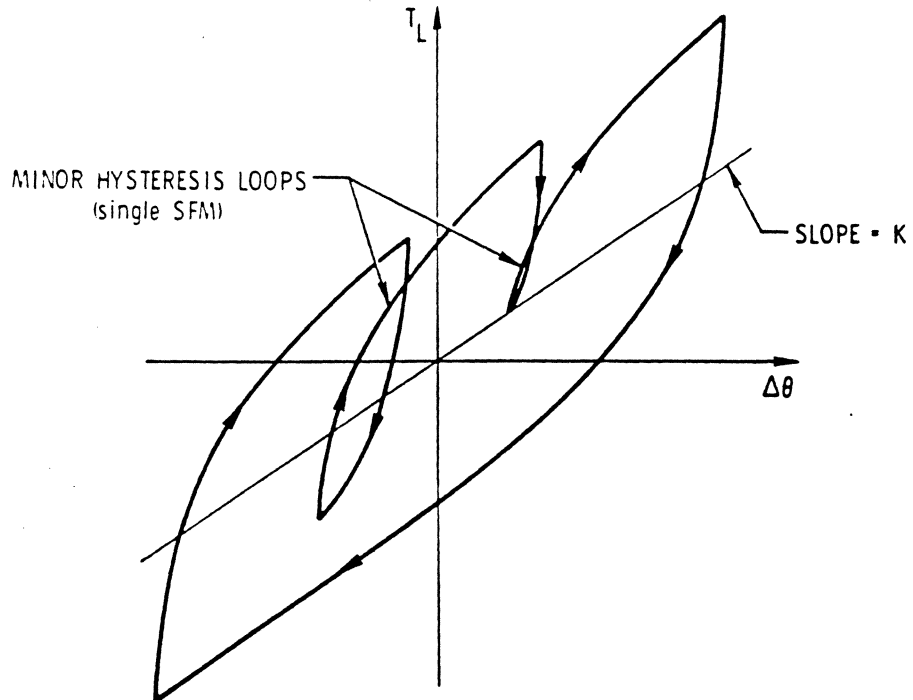


Figure 4. Gear-Shaft Stiffness with Hysteresis (as Measured at Output Shaft).

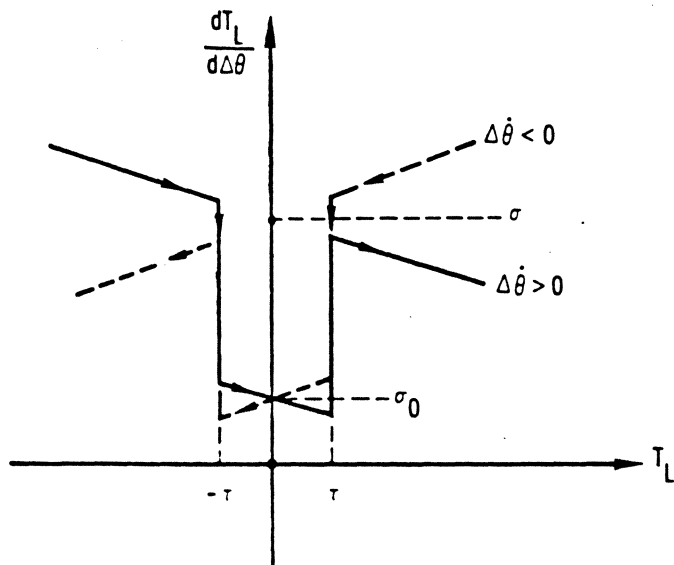


Figure 5. Friction Slope Model for Gear-Shaft Stiffness, Hysteresis, and Backlash.

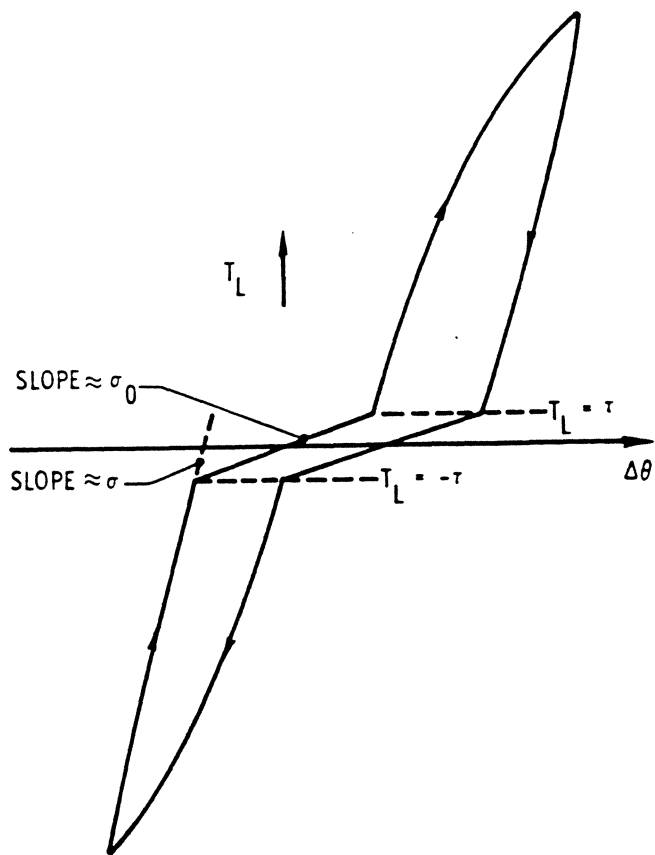


Figure 6. Gear-Shaft Stiffness with Hysteresis and Backlash.

relative displacement between system elements, and time t .

$$\frac{dF(x, t)}{dt} = \frac{dF(x)}{dx} \cdot \frac{dx}{dt} \quad (1)$$

Then, integrating Eq. (1) with respect to time t

$$F(x, t) = \int \frac{dF(x)}{dx} \frac{dx}{dt} dt \quad (2)$$

The derivative of friction force with respect to deflection dF/dx is referred to as the friction slope function. It was found empirically [2] to be generally expressible as

$$\frac{dF}{dx} = \sigma \left| 1 - \frac{F}{F_c} \operatorname{sgn} \dot{x} \right|^i \cdot S \quad (3)$$

where

$$\operatorname{sgn} \dot{x} = \operatorname{sgn} \left(\frac{dx}{dt} \right) = \pm 1 \text{ for } \pm \text{ velocities, respectively}$$

σ = rest stiffness parameter

F_c = Coulomb friction level parameter

i = SFM exponent parameter

S = stabilizing factor, such as $\left| \operatorname{sgn} \left(1 - \frac{F}{F_c} \operatorname{sgn} \dot{x} \right) \right|$ for simulation work. If $i = 1$, then $S = 1$ works.

The slope functions are defined for F/F_c between ± 1 and, although it is not theoretically possible for $|F|$ to exceed F_c , use of a stabilizing factor S is required in some simulations to protect against instability that might occur as a result of factors such as computational roundoff.

The friction slope functions appear as shown in Figure 7 for various values of i for positive velocity $\dot{x} > 0$. The curves for negative velocity $\dot{x} < 0$ are symmetric with the curves shown about the vertical axis $F/F_c = 0$.

Integration of Eq. (3) gives the general friction force-deflection function. In this paper, consideration is given to the cases where the SFM exponent parameter is set equal to 1.0 and 2.0 because the bearing friction data presented show that this parameter lies in this range and because there is an advantage in simulation and analysis using integer exponents. The case of $i = 3/2$ approximates the best fit for the bearing data.

Integrating Eq. (3) with respect to x with $\operatorname{sgn} \dot{x} = +1$ and using the initial condition $F(x) = 0$ at $x = 0$, we get

$$\frac{F}{F_c} = 1 - \left[1 - (1 - i) \frac{x}{x_c} \right]^{1/(1 - i)} \quad (4)$$

where

$$x_c = \frac{F_c}{\sigma} \quad (5)$$

is the characteristic displacement or knee of the force-deflection curve. Note that if $i < 1$, Eq. (4) is valid for $x/x_c < (1/(1 - i))$ and $F/F_c = 1$ for $x/x_c > (1/(1 - i))$.

For $i = 1$:

$$\frac{F}{F_c} = \left(1 - e^{-x/x_c} \right) \quad (6)$$

For $i = 3/2$:

$$\frac{F}{F_c} = 1 - \left(1 + \frac{x}{2x_c} \right)^{-2} \quad (7)$$

For $i = 2$:

$$\frac{F}{F_c} = \frac{x}{x + x_c} \quad (8)$$

The knee parameter x_c can be regarded as an SFM parameter derivable from Eq. (5) if F_c and σ are determined. In any case, two of the three parameters in Eq. (5) need to be found from experimental data.

The shapes of the force-deflection functions given above for positive velocity $\dot{x} > 0$ are evident in Figure 8. When the motion is reversed, $\dot{x} < 0$ and the same shape curves are retraced in the negative direction. The SFM parameters are to be determined for the ball bearings from data that have the appearance of the curves in Figure 8.

III. TEST METHOD

Basically, two test methods are available for use in determining the solid friction parameters: static force-displacement or torque-angular deflection tests, and second-order oscillation decay tests. In both methods, the phenomenon to be observed in the test is hysteresis. In the first method, the hysteresis loop is measured directly. In the second method, it is indirectly determined

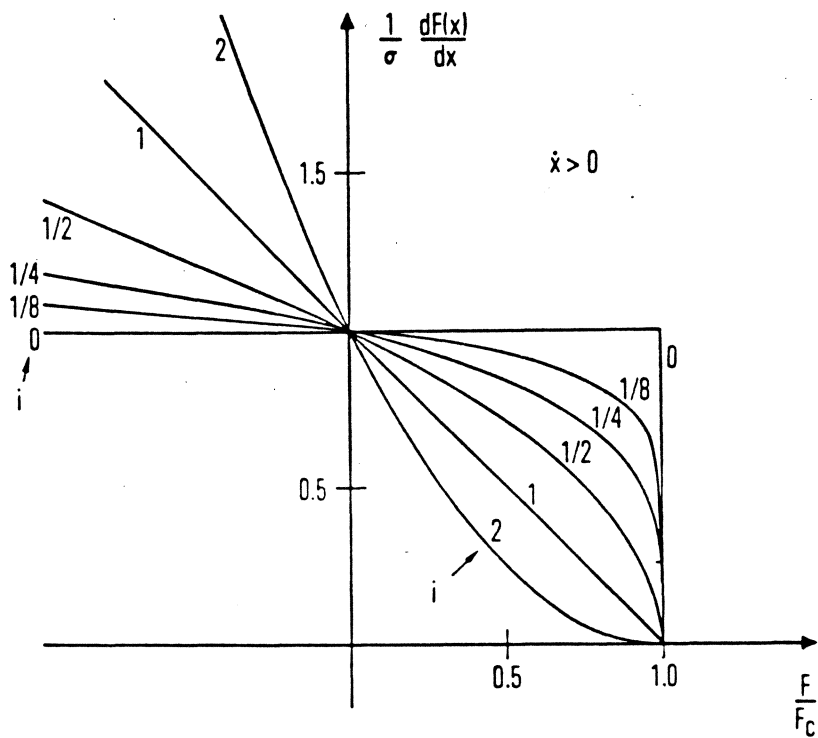


Figure 7. Friction Slope Functions.

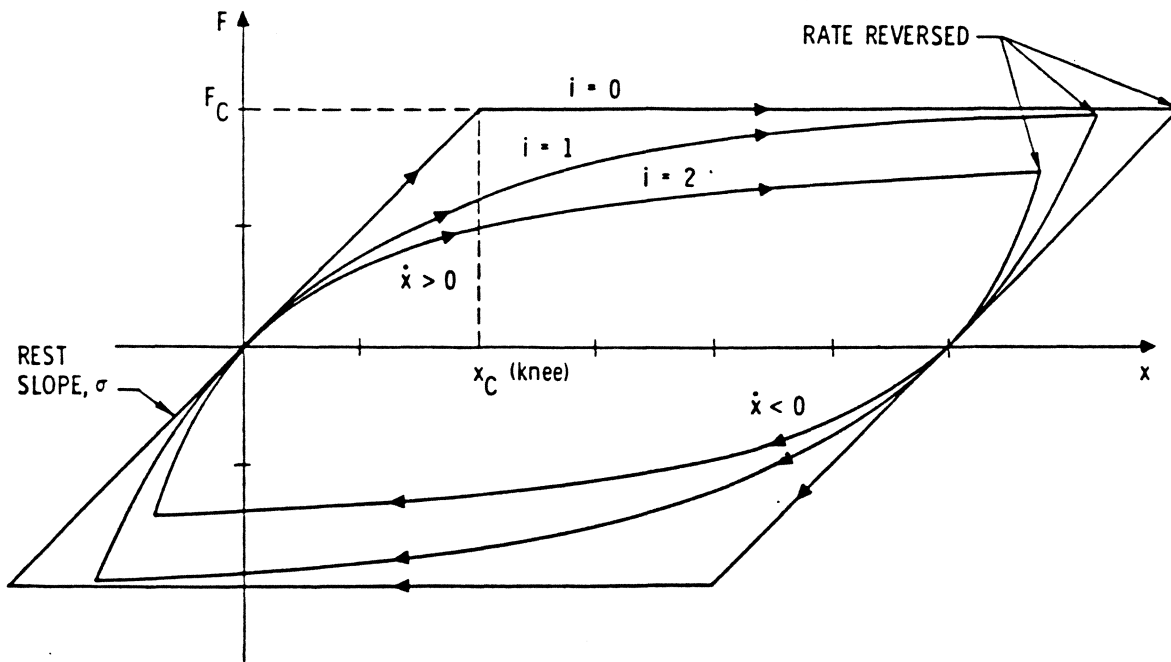


Figure 8. Force Deflection Hysteresis Loops.

power amplifier was also an Inland unit. A Baldwin 18-bit incremental encoder was mounted on the motor and coupled directly to the motor drive shaft. An in-house designed and built digital-to-analog (D/A) converter processed the encoder output signal, and its output was fed to a difference amplifier with compensation circuitry. The 12-bit D/A converter defined the range and quantization bit resolution values available for the drive servo as shown in Table I. The ± 11.25 deg range with the 0.011-deg quantization bit resolution was used for this test. The drive servo position hysteresis for small excursions was less than about 0.001 deg. The bandwidth of the drive servo was about 10 Hz, and the short term noise level was of the same order of magnitude as the position hysteresis, i.e., 0.001 deg. The output of the drive servo was used to drive the x-axis of an x-y recorder, and the torque meter output was used to drive the y-axis.

The duplex bearing pair tested was a Barden 104H, Class 5, with a bore diameter of 20 mm, a ball diameter of 0.25 in., and race width of 12 mm. The bearings had been used in a Bendix Corporation test fixture and indicated significant torque noise as shown by the torque waviness imposed on the hysteresis loop in Figure 10. Inspection of the bearings confirmed the suspicion of worn balls and races, so a new set was obtained. Test runs were made on the new bearings for preloads of 6, 12, 18, 24, 30, and 36 lb. Figure 11 is a typical hysteresis trace obtained with the new bearings for the same preload of 24 lb used for Figure 10.

IV. DATA ANALYSIS

For purposes of analyzing the hysteresis data, it is advantageous to define

$$f = F_c - F \quad (9)$$

and

$$x' = x - x(-F_c) \quad (10)$$

for $\dot{x} > 0$ (or $f = F - F_c$ for $\dot{x} < 0$). Either the increasing or decreasing half of the hysteresis loop or both can be analyzed. The increasing half in Figure 11 is shown with the f and x' axes labeled in graph paper units where the $x' = 0$ axis passes through the rate reversal point. In terms of these

variables and assuming that $f = 2F_c$ at the rate reversal point when $x' = 0$ and that $\dot{x} < 0$, Eqs. (3), (4), (6), and (8) can be written, respectively, as

For $i \geq 0$:

$$\frac{df}{dx'} = \frac{F_c}{x_c} \left(\frac{f}{F_c} \right)^i \quad (11)$$

$$\frac{f}{F_c} = \left[2^{1-i} - (1-i) \frac{x'}{x_c} \right]^{1/1-i} \quad (12)$$

For $i = 1$:

$$\frac{f}{F_c} = 2e^{-x'/x_c} \quad (13)$$

For $i = 2$:

$$\frac{F_c}{f} = \frac{x'}{x_c} + 1/2 \quad (14)$$

Equation (12) can be used in data analysis parameter estimation programs, but it is nonlinear and is not readily put into a linear form by simple changes of variables.

The quantities df/dx' , f/F_c , and F_c/f on the left side of their respective equation can be considered as dependent variables and the variables f and x' on the right side as independent variables. The graph of Eq. (11) plotted as df/dx' versus f on the log-log graph paper is linear as is the plot of f versus x' for Eq. (13) on semi-log graph paper and the plot of $1/f$ versus x' for Eq. (14) on rectangular graph paper. Thus, the least-squares fit linear regression method can be applied to the f , x' data pairs for points on the hysteresis curves. Computer programs are available on large and small computers to analyze data by this method. Other computer programs can be used that fit nonlinear functions such as Eq. (12) to a set of data, but these programs generally are available only on large computers. The programmable Hewlett-Packard hand-held calculators can be utilized to perform the linear regression analysis, and the HP 67 and HP 97 units have curve-fitting program cards that can be used to fit data to straight lines (Eq. [14]), exponential curves (Eq. [13]), logarithmic curves, and power curves (Eq. [11]). Because of its convenience and simplicity, the HP 67 curve-fitting program was used in analyzing the bearing test data. A description of the program is given in the

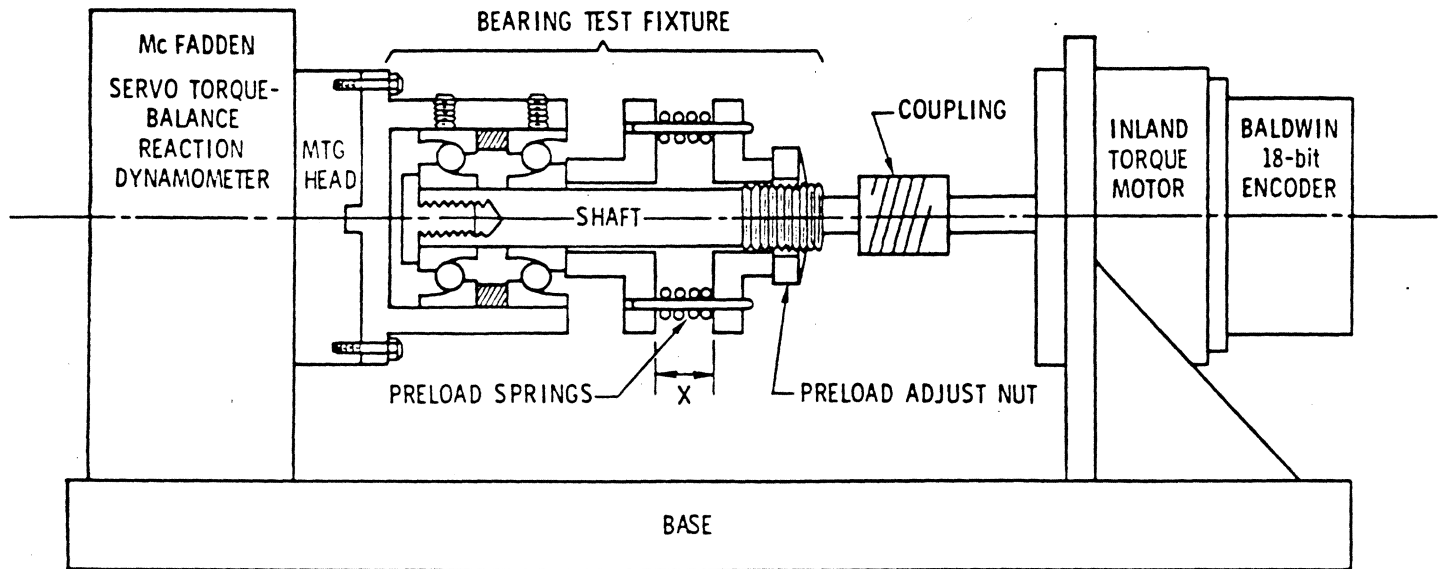


Figure 9. Bearing Static Torque-Deflection Test Setup.

Table I. Drive Servo Range and Resolution.

Range (deg)	Quantization Bit Resolution (deg)	Scale Factor (V/deg)
± 0.703	0.00069	14.222
± 2.81	0.0027	3.555
± 11.25	0.0110	0.8888
± 45.0	0.044	0.2222
± 180.0	0.176	0.05555

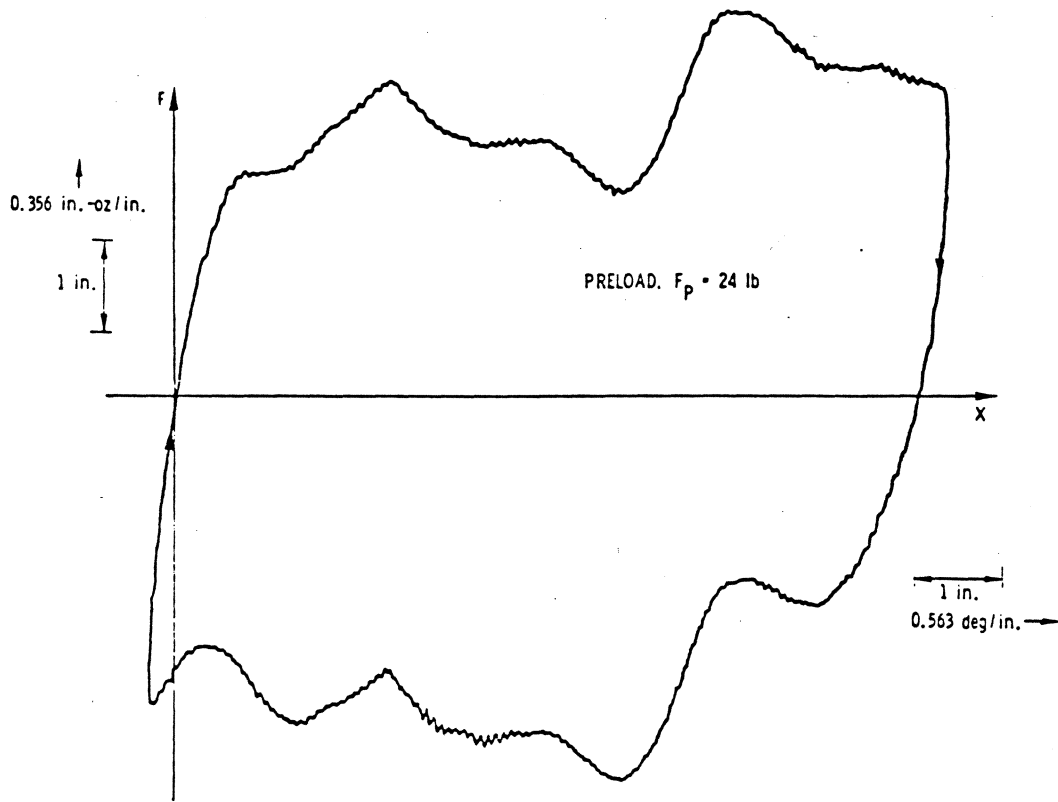


Figure 10. Old Bearing Hysteresis Loop.

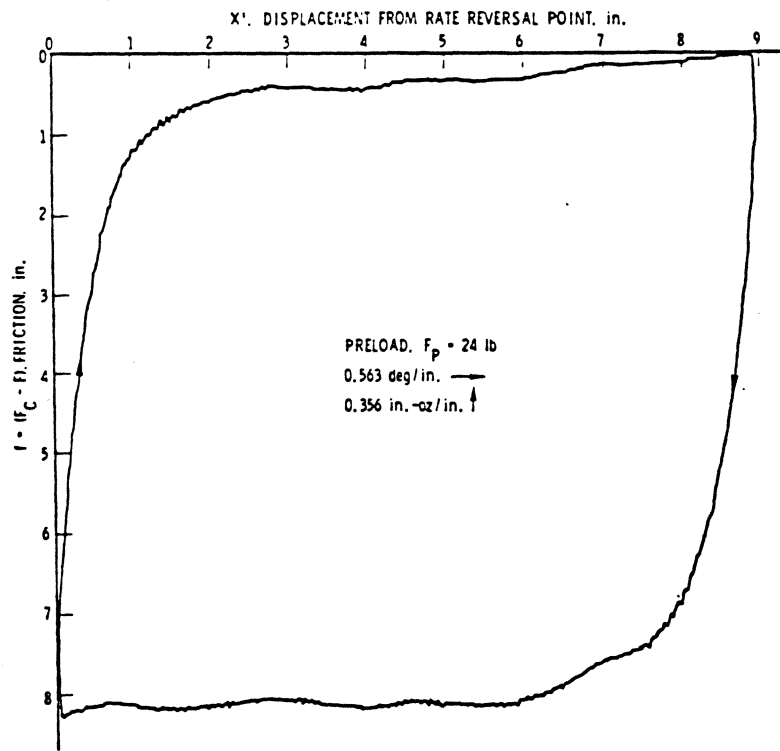


Figure 11. New Bearing Hysteresis Loop.

HP 67 "Standard Pac." Some simple preprocessing of the data to calculate df/dx and $1/f$ was necessary before it could be used in the standard curve-fitting program. The program effectively outputs the parameters i and x_c for Eq. (11) and x_c for Eqs. (13) and (14). The parameter F_c is initially estimated by inspection of the hysteresis curve and is specified by the location of the $f = 0$ and $x' = 0$ axes on the x - y test data plots.

V. RESULTS AND CONCLUSIONS

Test data for the "running" or Coulomb friction were readily obtained by visually estimating the horizontal asymptotes. Results are shown in Figure 12. Both old and new bearing running friction levels were effectively taken as the average of the near asymptotic wavy torque level. The envelope of the old bearing asymptotic wave peaks was only 5 to 15% higher than the average value. Thus, it appears from this data that the wear process increases noise torque but decreases running friction in the mid to high preload range. The friction of the new bearings at the high preload of 36 lb appeared at first to be an outlying data point. However, the old bearing data show the same characteristic of suddenly increasing at 36 lb preload. A 40-lb preload is considered a heavy preload by the manufacturer.

Results of the curve-fitting data analysis are presented in Table II for the new bearings. The characteristic angular displacement x_c was found from the plots by drawing the tangent or the rest slope $\sigma = F_c/x_c$ to the curves at $F = 0$, and is designated with the heading $x_c = F_c/\sigma$. The curve fit program was used to find the parameters i and x_c from the power fit for Eq. (11) as well as the parameter x_c from the exponential fit for Eq. (13) and from the linear fit for Eq. (14). Results are listed in the table with the coefficient of determination r^2 , which indicates goodness of fit, and the friction range where the fits are good, $f_{LIM} < f < 2F_c$. The curve fits deviate from the experimental curves for f values below f_{LIM} .

It seemed important for each curve fit to have approximately the correct value of rest slope σ , and so the data for $f < f_{LIM}$ were deleted because the value of x_c determined from the fit deviated excessively from the rest slope value if that data

were included. Thus, even though the $i = 1$ and $i = 2$ fits have better coefficients of determination than the power curve fit, they will not fit the data over as wide a range and still have the correct rest slope. With this in mind, it is observed that: values of x_c for the power fit curves are about 15% below the graphical x_c , $i = 1$ fit curves have values for x_c slightly higher than the graphical values, and the $i = 2$ fit curves have values for x_c that are about 50% below the graphical values.

It is concluded, as a result of this testing, that the $i = 2$ fit curves are not as accurate as the $i = 1$ and $i \approx 1.5$ fit curves. A useful observation is that the $i = 1$ fit curves give good results over about 85% of the range of friction change from $-F_c$ to $+F_c$. They also give a good fit for the rest slope.

It is important to observe that the value of x_c is approximately constant and independent of preload.

Another important conclusion that can be drawn from these data is that the SFM exponent parameter i is approximately constant and has an average value of about 1.5.

REFERENCES

1. P. R. Dahl, A Solid Friction Model, TOR-0158(3107-18)-1, The Aerospace Corporation, El Segundo, Calif. (May 1968).
2. P. R. Dahl, "Solid Friction Damping of Spacecraft Oscillations," Paper No. 75-1104, Paper presented at the AIAA Guidance and Control Conference, Boston, Mass., August 1975.
3. P. R. Dahl, "Solid Friction Damping of Mechanical Vibrations," AIAA Journal, **14** (12), 1675-1682 (December 1976).
4. B. G. King, Ball Bros. Research Corp., Boulder, Colo., Private correspondence, June 1976.
5. B. G. King, "Simulation of D.C. Torque Motor Magnetic Hysteresis and Cogging Effects," Paper to be presented at the Sixth Annual Symposium on Incremental Motion Control Systems and Devices, University of Illinois, Urbana-Champaign, Illinois, May 1977.

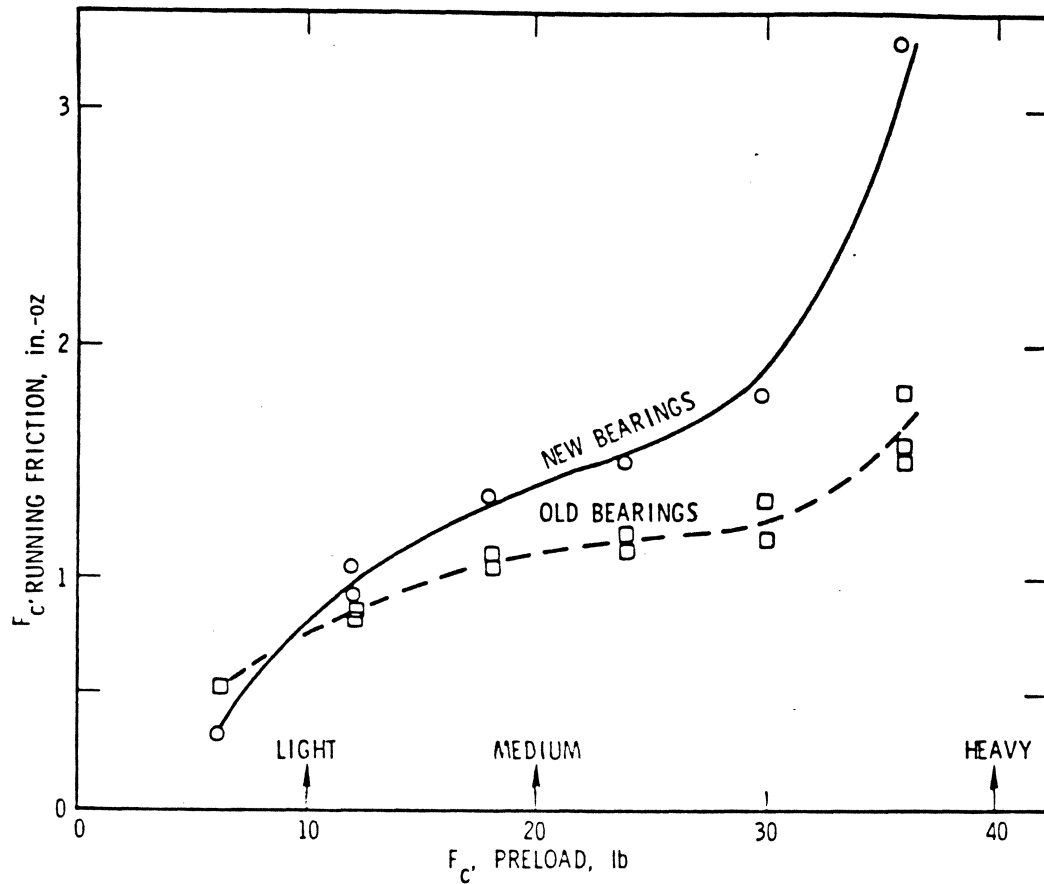


Figure 12. Running Friction versus Preload.

Table II. Bearing Pair SFM Parameters.

Preload F_P (hr)	Running Friction F_c (in-oz)	Rest Stiffness σ (in-oz/deg)	Graph $\frac{F_c}{\sigma}$ x_c (deg)	i Estimated (power fit) ^a				i = 1 (exponential fit)			i = 2 (linear fit)		
				i	x_c (deg)	r^2	Fit Good for $f > f_{LIM}$ (in-oz)	x_c (deg)	r^2	Fit Good for $f > f_{LIM}$ (in-oz)	x_c (deg)	r^2	Fit Good for $f > f_{LIM}$ (in-oz)
6	0.30	1.3	0.23	1.44	0.20	0.89	0.06	0.26	0.99	0.03	0.13	0.95	0.06
12	0.91	3.1	0.29	1.66	0.23	0.98	0.08	0.31	0.99	0.20	0.17	0.97	0.27
18	1.34	4.6	0.29	1.71	0.25	0.97	0.18	0.30	0.99	0.34	0.18	0.99	0.21
24	1.50	4.8	0.31	1.64	0.26	0.98	0.18	0.30	0.99	0.54	0.21	0.96	0.54
30	1.78	5.9	0.30	1.44	0.23	0.98	0.08	0.31	0.99	0.26	0.21	0.97	0.80
36	3.26	12.5	0.26	1.36	0.21	0.97	0.08	0.28	0.99	0.79	0.15	0.96	0.79

^a $i_{ave} = 1.54 \pm 0.15$ (1 sigma)

Note: ± 2.5 deg imposed triangular waveform at 20-sec period. Amplitude was approximately $10 x_c$.

TRACK MISREGISTRATION (TMR)

AND

OFF-TRACK CAPABILITY (OTC)

MIKE HATCH

IIST SHORT COURSE

SANTA CLARA UNIVERSITY

MARCH 22-24, 1988

TOPICS TO BE COVERED
-----TMR

DEFINITION OF WRITE-TO-WRITE (W/W) AND WRITE-TO-READ (W/R) TMR

TMR FLOWCHART

TMR CATALOG

SIMPLE CLOSED-FORM EXAMPLE

MONTE-CARLO EXAMPLE

OTC

OTC FLOWCHART

OFF-TRACK CONDITIONS

747 CURVES

747 CURVES - ERROR RATE EFFECTS

747 CURVES - HEAD WIDTH EFFECTS

COMBINING TMR AND OTC

HEAD WIDTH EFFECTS

ERROR RATE AND TMR SURFACES

AVERAGE ERROR RATE CALCULATION UNDER OFF-TRACK CONDITIONS

TMR FACTORS

MRH 3-7-88

WHY TMR AND OTC ?

TMR / OTC PROVIDES A METHODOLOGY FOR:

1) ENSURING COMPATIBILITY BETWEEN SERVO/MECHANICAL
AND READ/WRITE SYSTEMS

2) SETTING DESIGN GOALS AND TOLERANCE LIMITS FOR
CRITICAL AREAS OF THE DRIVE:

MECHANICAL

SERVO

R/W

SERVOWRITER

3) CHOOSING OPTIMUM HEAD WIDTH

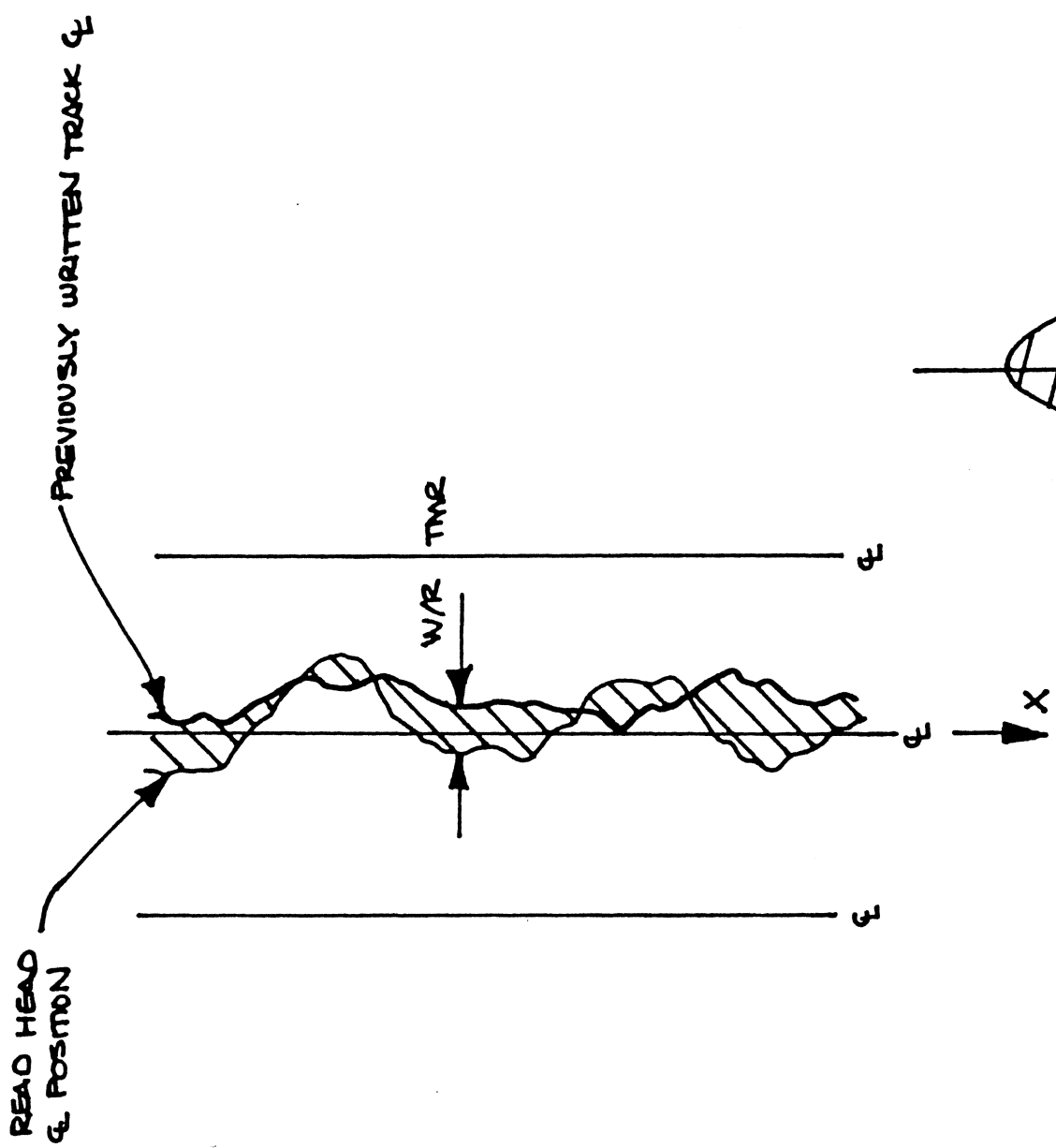
4) PREDICTING ERROR RATE UNDER OFF-TRACK CONDITIONS

AND, TMR/OTC PROVIDES A METHOD OF VISUALIZING AND COMMUNICATING
DESIGN TRADEOFFS BETWEEN SERVO, MECHANICAL, AND R/W GROUPS.

MRH 3-7-88

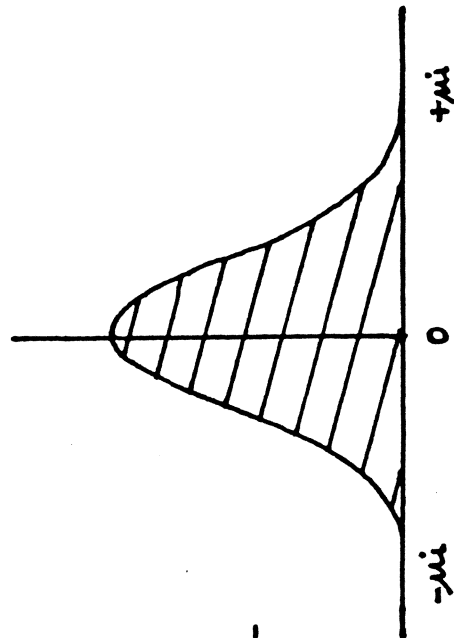
WRITE-TO-READ TOLERANCE (W/R)

MEASURE OF MISREGISTRATION WHEN READING
A PREVIOUSLY WRITTEN TRACK



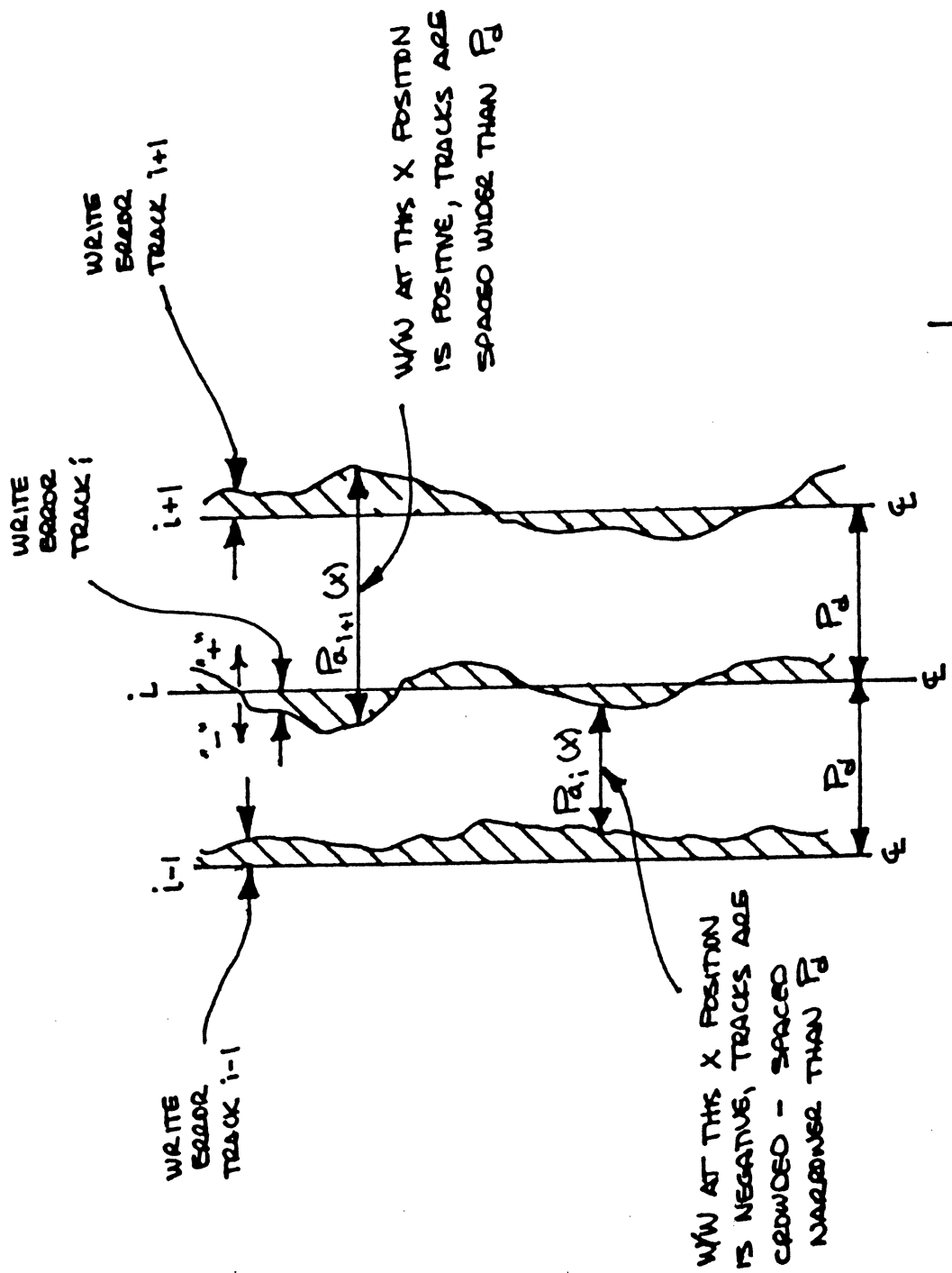
RESULTING W/R P.D.F.

W/R = READ POSITION (X)
- WRITE POSITION (X)



WRITE - TO - WRITE TOLERANCE (W/W)

MEASURE OF ADJACENT TRACK CROWDING



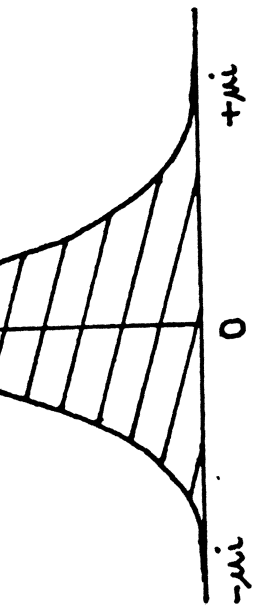
P_d - DESIGN TRACK PITCH, $1/TPI$

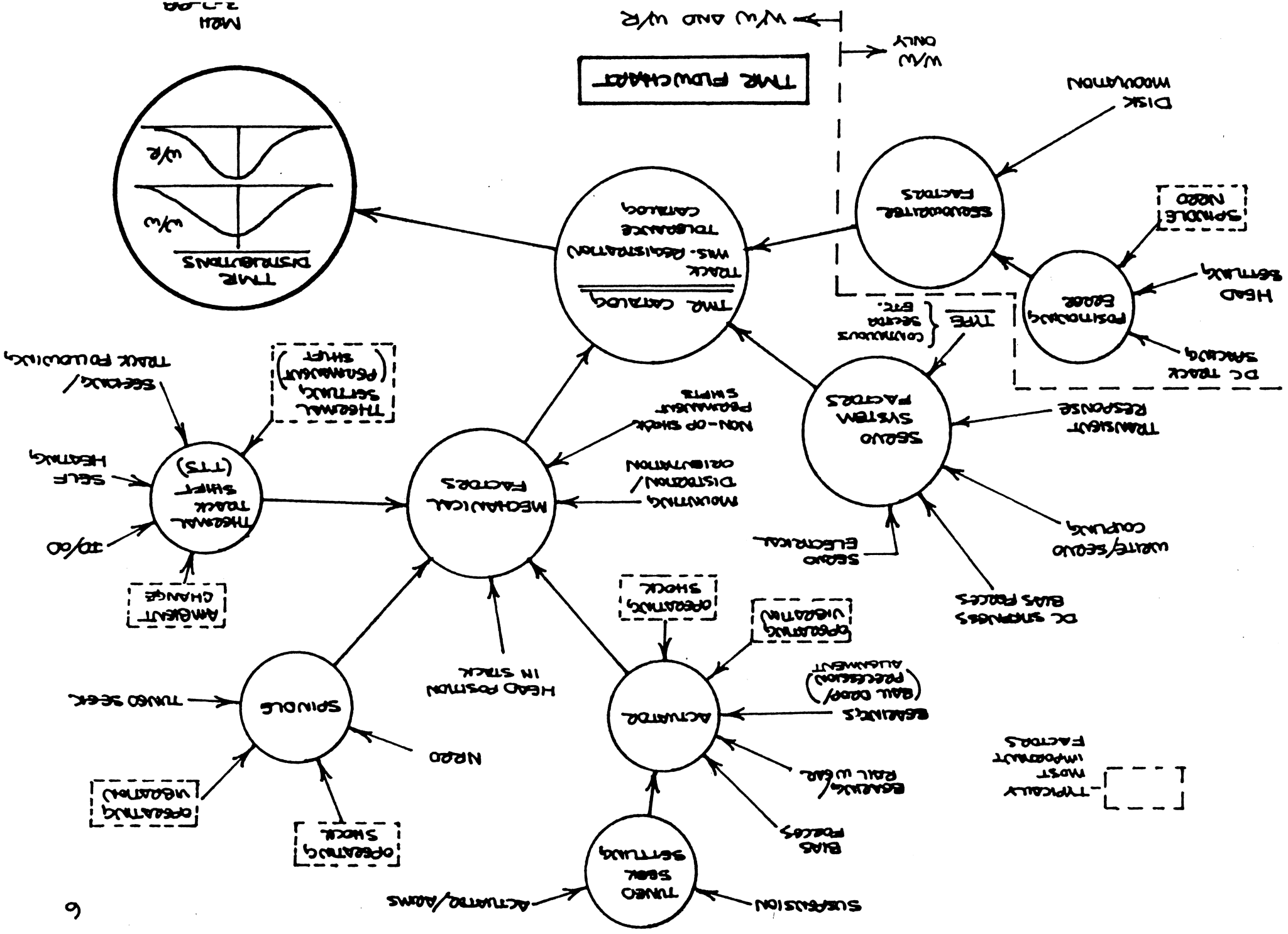
$P_a(x)$ - ACTUAL TRACK PITCH BETWEEN TRACKS i AND $i-1$

$$P_{a_i}(x) = (\text{WRITE ERROR})_{i+1} - (\text{WRITE ERROR})_i + P_d$$

$$(W/W)_i(x) = P_{a_i}(x) - P_d$$

RESULTING W/W PDF.





CLOSED-FORM W/W AND W/R TOLERANCE STUDY
 (ALL TOLERANCES GAUSSIAN)

TMR CATALOG

TOLERANCE NUMBER	DESCRIPTION	W/W TOL'S	W/R TOL'S
1	TOLERANCE 1 (HOW MEASURED, CALC'D, HOW MANY SAMPLES, CONFIDENCE LEVEL)		
2	TOLERANCE 2		
3	TOLERANCE 3		
4	TOLERANCE 4		— NONE —

FIRST WASTE OPERATION:

$$\bar{x}_{w1} = \bar{x}_1 + \bar{x}_2 + \bar{x}_3 + \bar{x}_4$$

$$\sigma_{w1} = (\sigma_1^2 + \sigma_2^2 + \sigma_3^2 + \sigma_4^2)^{1/2}$$

SECOND WASTE OPERATION:

$$\bar{x}_{w2} = \bar{x}_{w1}$$

$$\sigma_{w2} = \sigma_{w1}$$

W/W: $\bar{x}_{w1} = \bar{x}_{w1} - \bar{x}_{w2}$

$$\sigma_{w1} = (\sigma_{w1}^2 + \sigma_{w2}^2)^{1/2}$$

W/R SUMMATION

FIRST WASTE OPERATION:

$$\bar{x}_w = \bar{x}_1 + \bar{x}_2 + \bar{x}_3$$

$$\sigma_w = (\sigma_1^2 + \sigma_2^2 + \sigma_3^2)^{1/2}$$

READ OPERATION:

$$\bar{x}_R = \bar{x}_w$$

$$\sigma_R = \sigma_w$$

W/R: $\bar{x}_{w/R} = \bar{x}_w - \bar{x}_R$

$$\sigma_{w/R} = (\sigma_w^2 + \sigma_R^2)^{1/2}$$

W/R SUMMATION

MONTE CARLO TMR SIMULATION

TMR CATALOG

TOLEANCE NUMBER	DESCRIPTION	w/w TOL'S	w/R TOL'S
1	TRUNCATED GAUSSIAN		
2	UNIFORM		
3	WEIBULL		
4	ARBITRARLY (DEFINE CDF)		
	SUMMATION		

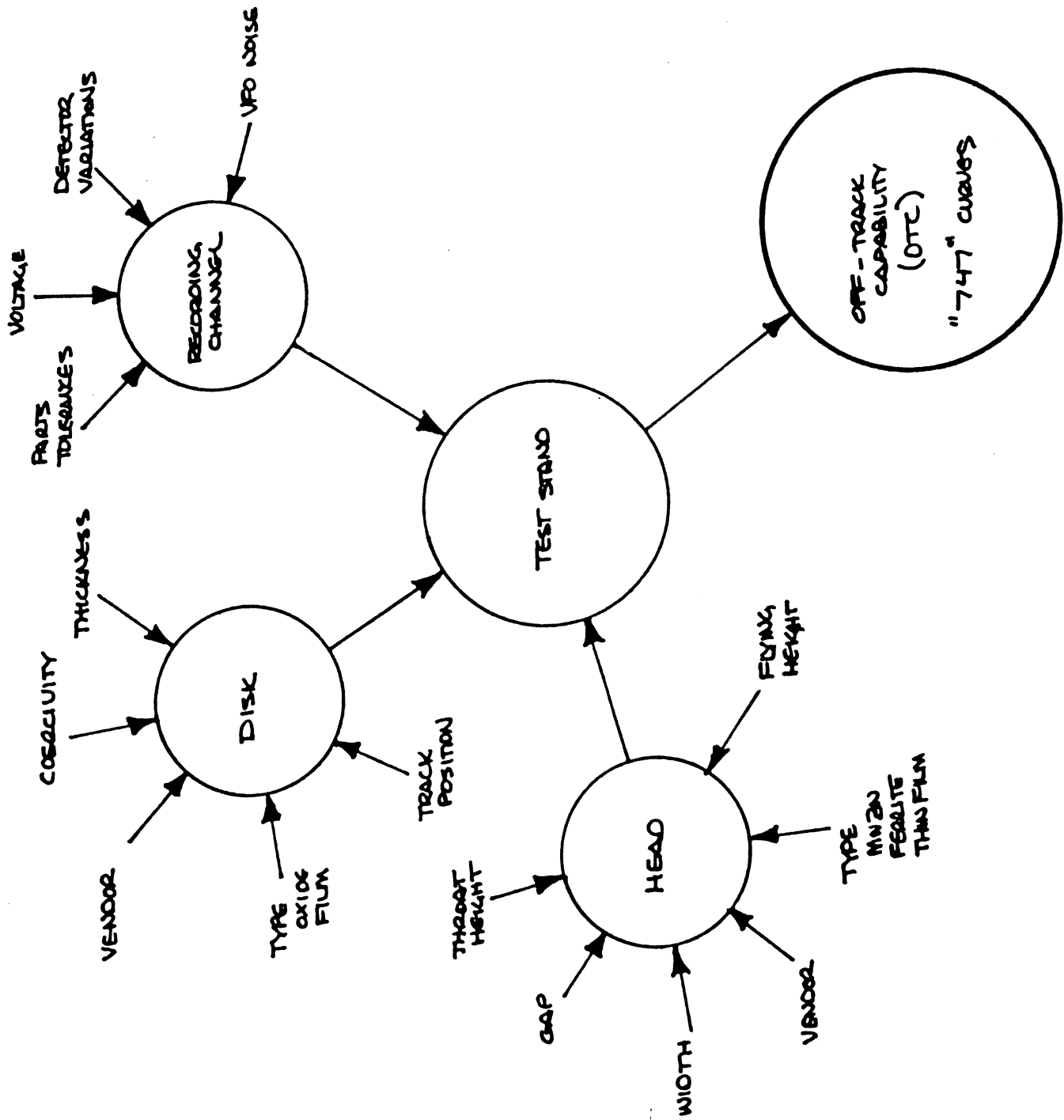
FIRST PASS THROUGH ALL TOL'S : $\sum w_{ij} = ()$ $\sum w_j = ()$

SECOND PASS THROUGH ALL TOL'S : $\sum w_{ij} = ()$ $\sum R_j = ()$

$w/w_j = \sum w_{ij} - \sum w_{2i}$ $w/R_j = \sum w_j - \sum R_j$

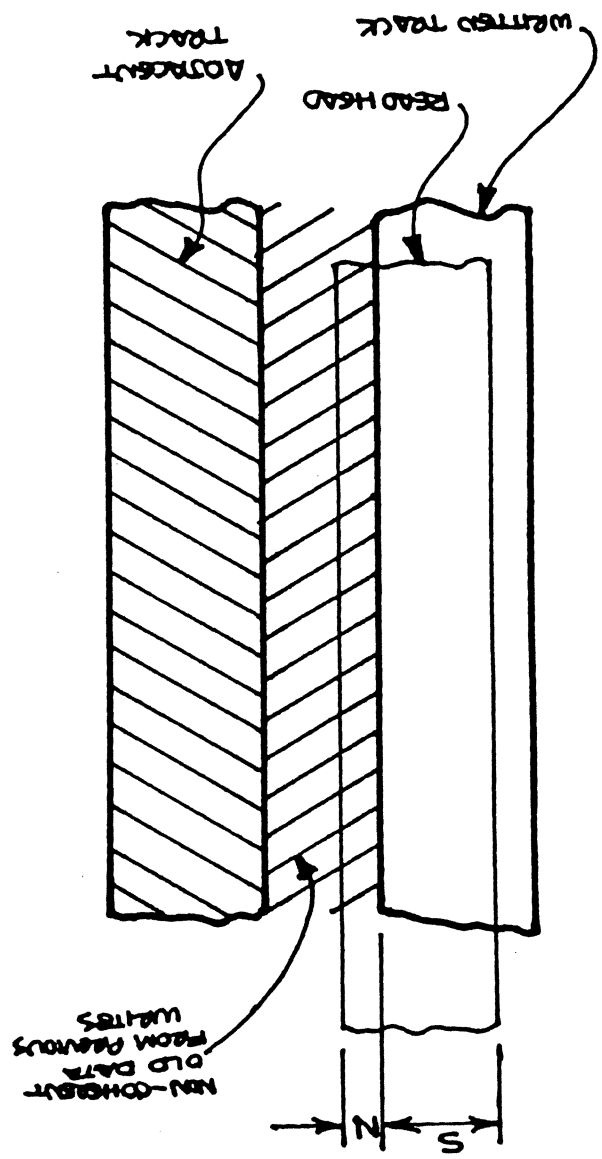
ENTER w/w_j INTO w/w HISTOGRAM

ENTER w/R_j INTO w/R HISTOGRAM

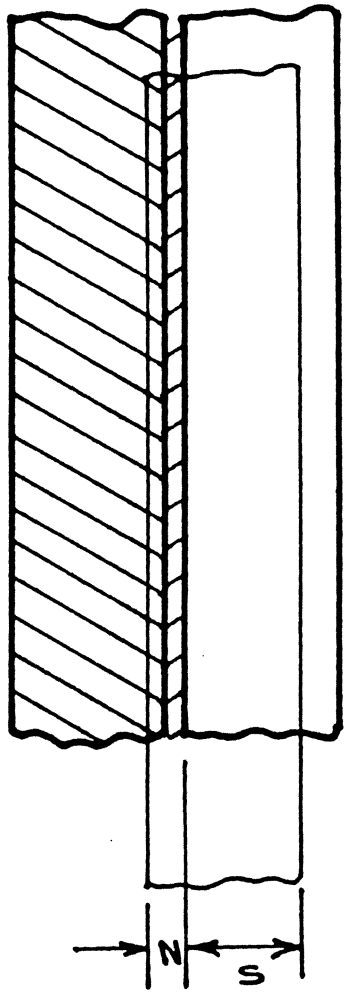


OTC FLOWCHART

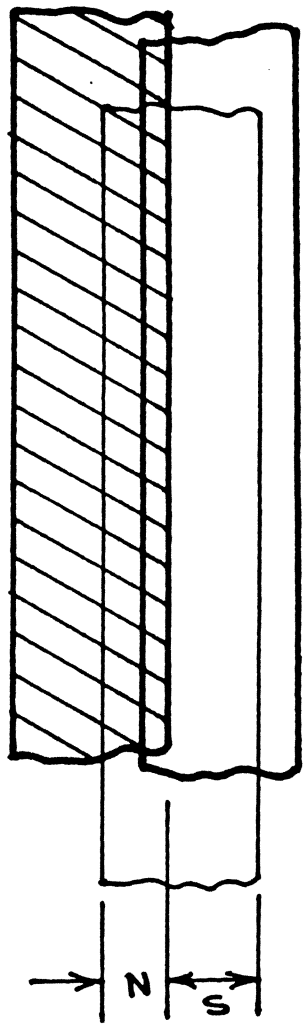
OFF TRACK CONDITIONS - GEOMETRICAL S/N



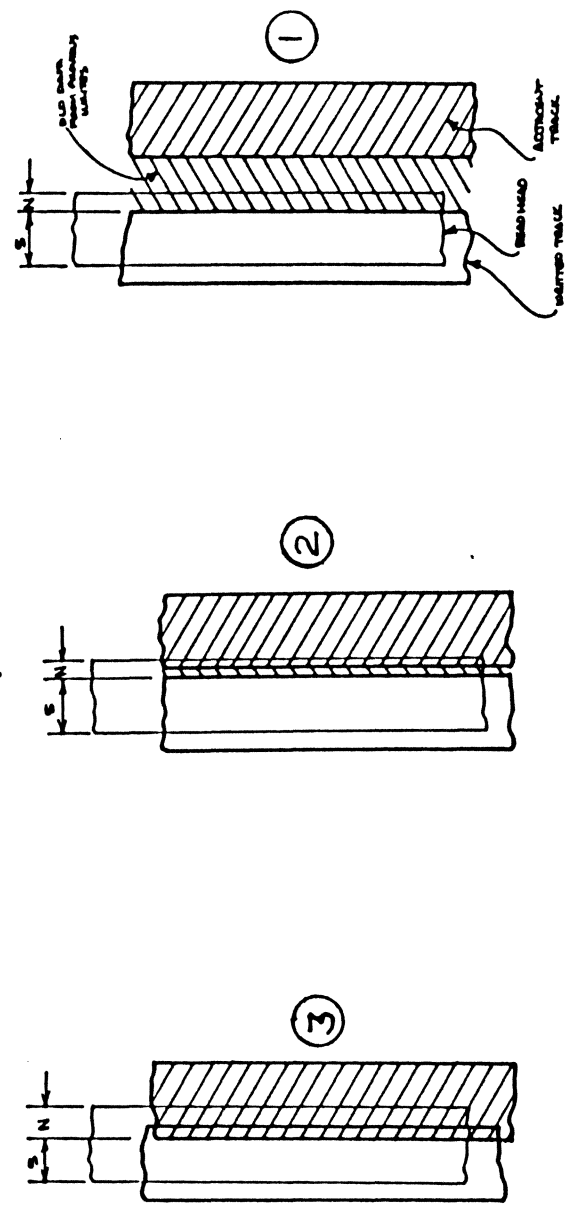
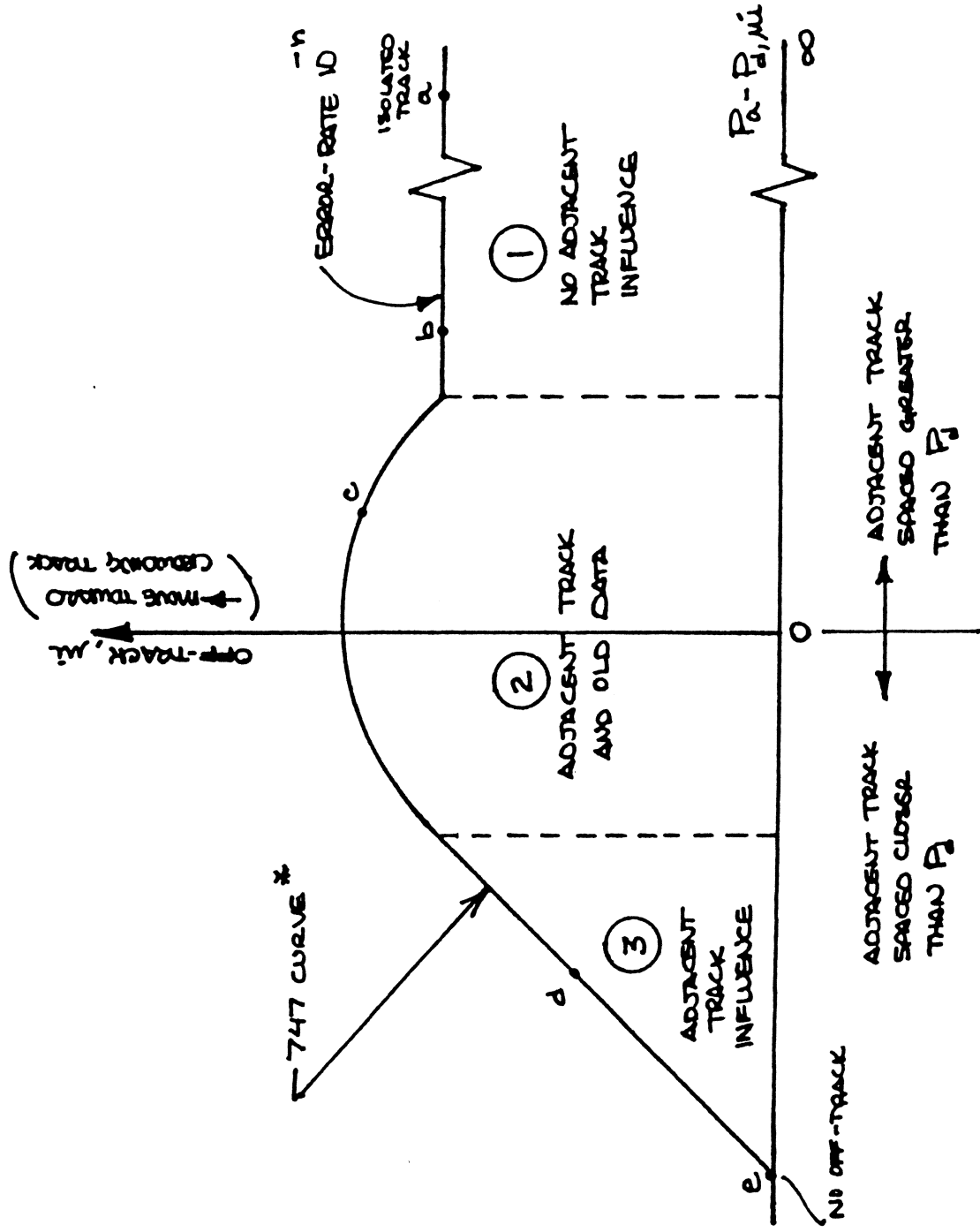
② HEAD READING OLD DATA AND ADJACENT TRACK



③ HEAD READING ADJACENT TRACK ONLY, NO OLD DATA INFLUENCE

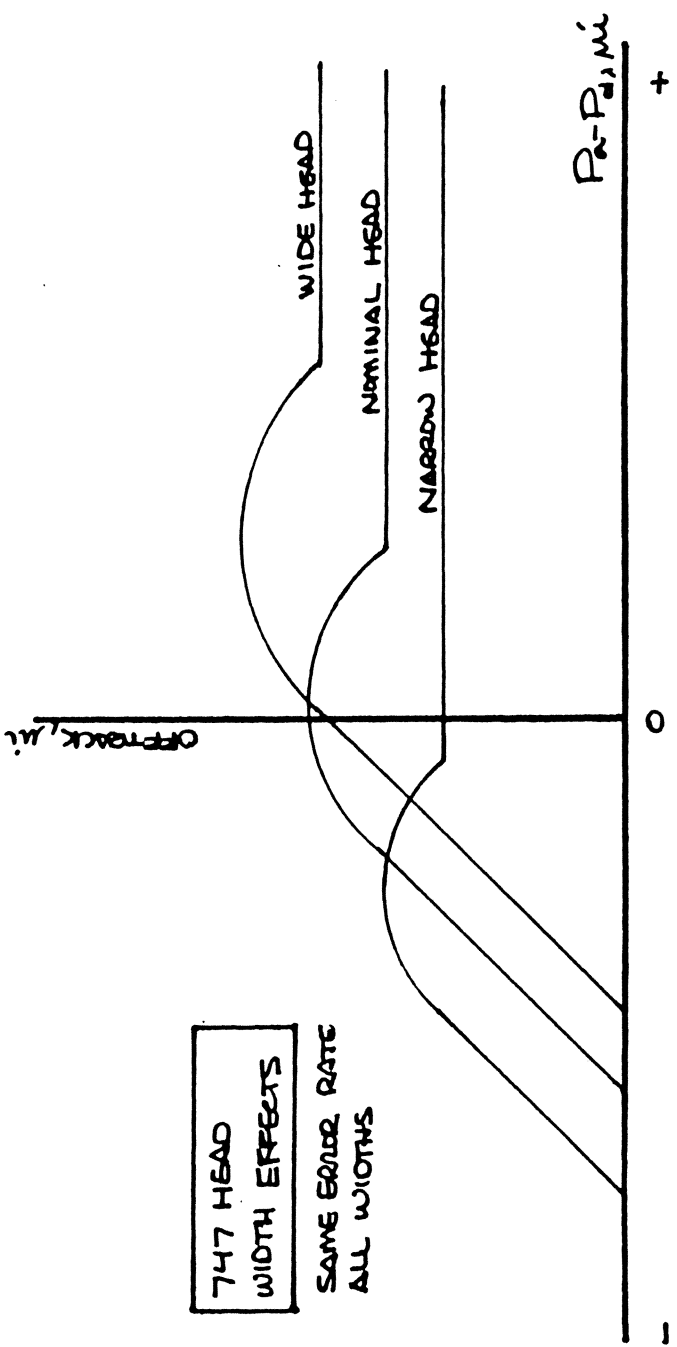
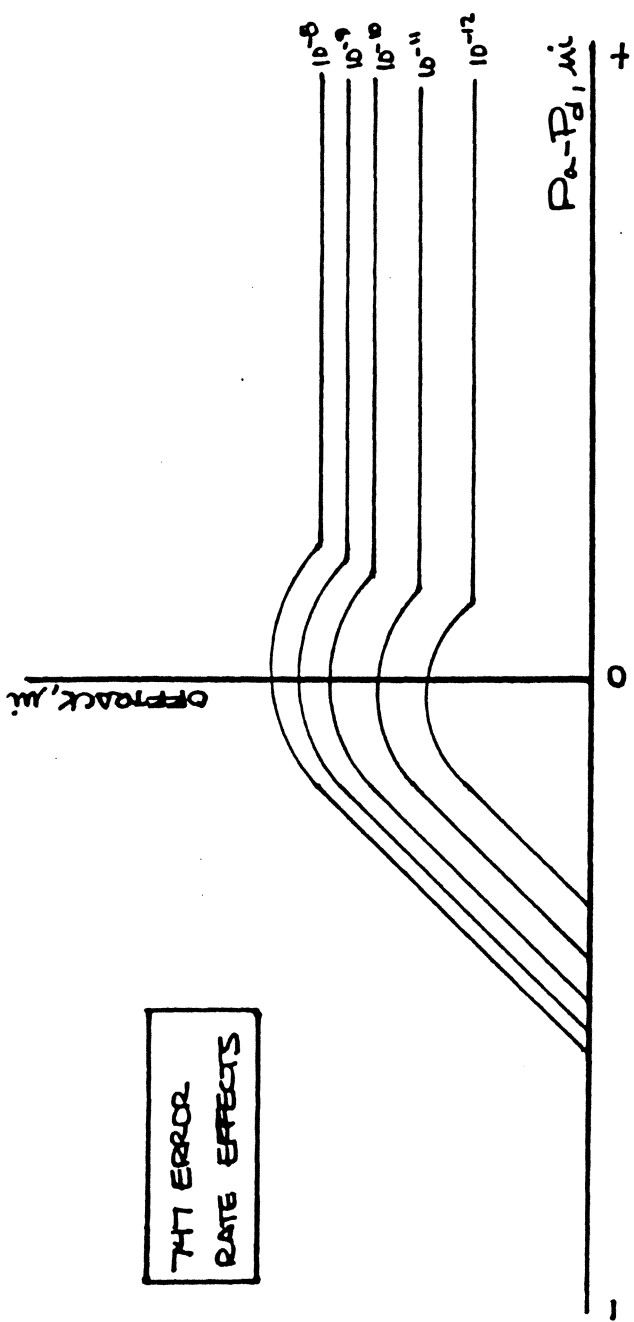


747 OTC CURVE



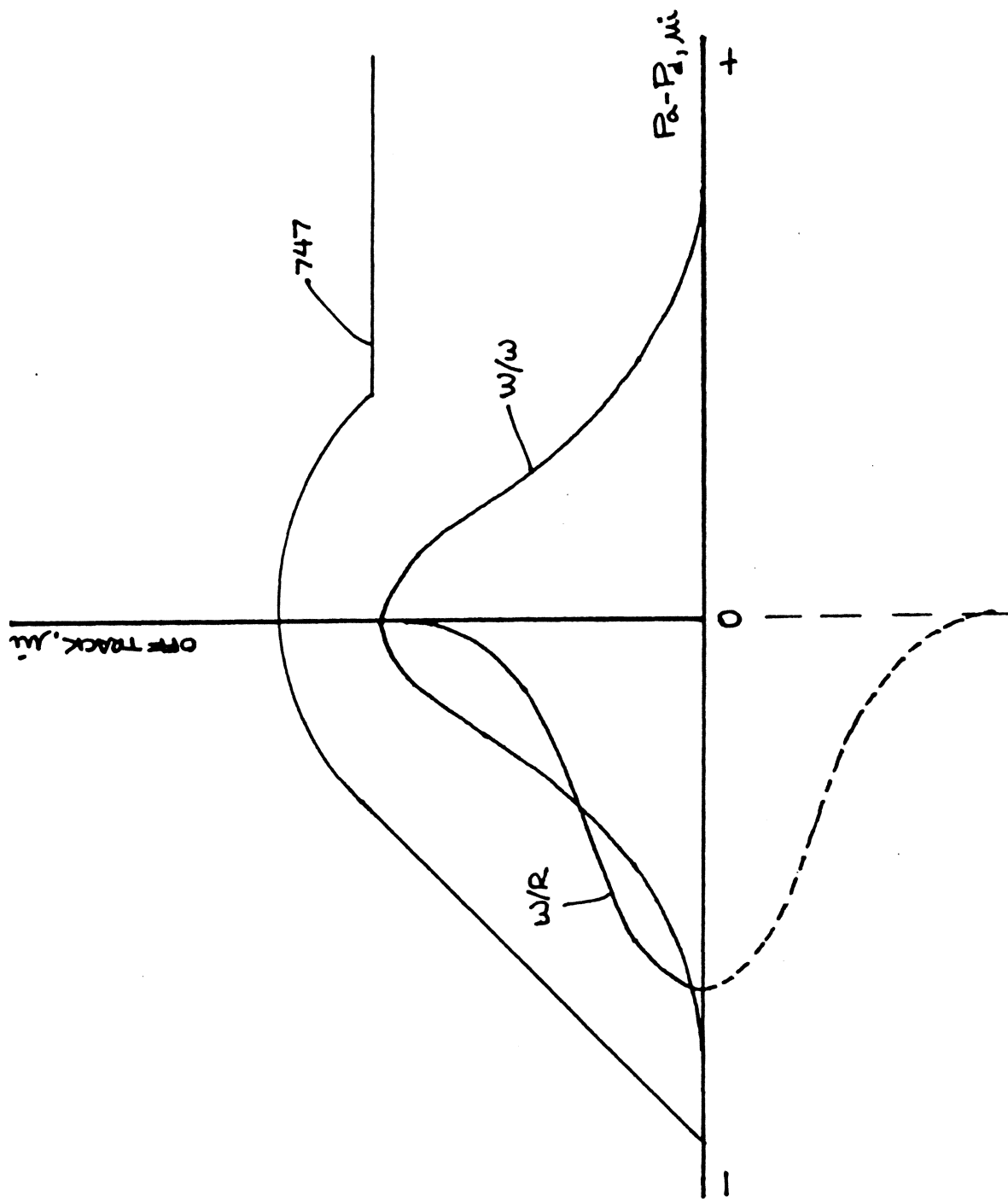
* GURK TESTER SOFTWARE GENERATES AUTOMATICALLY

MRH

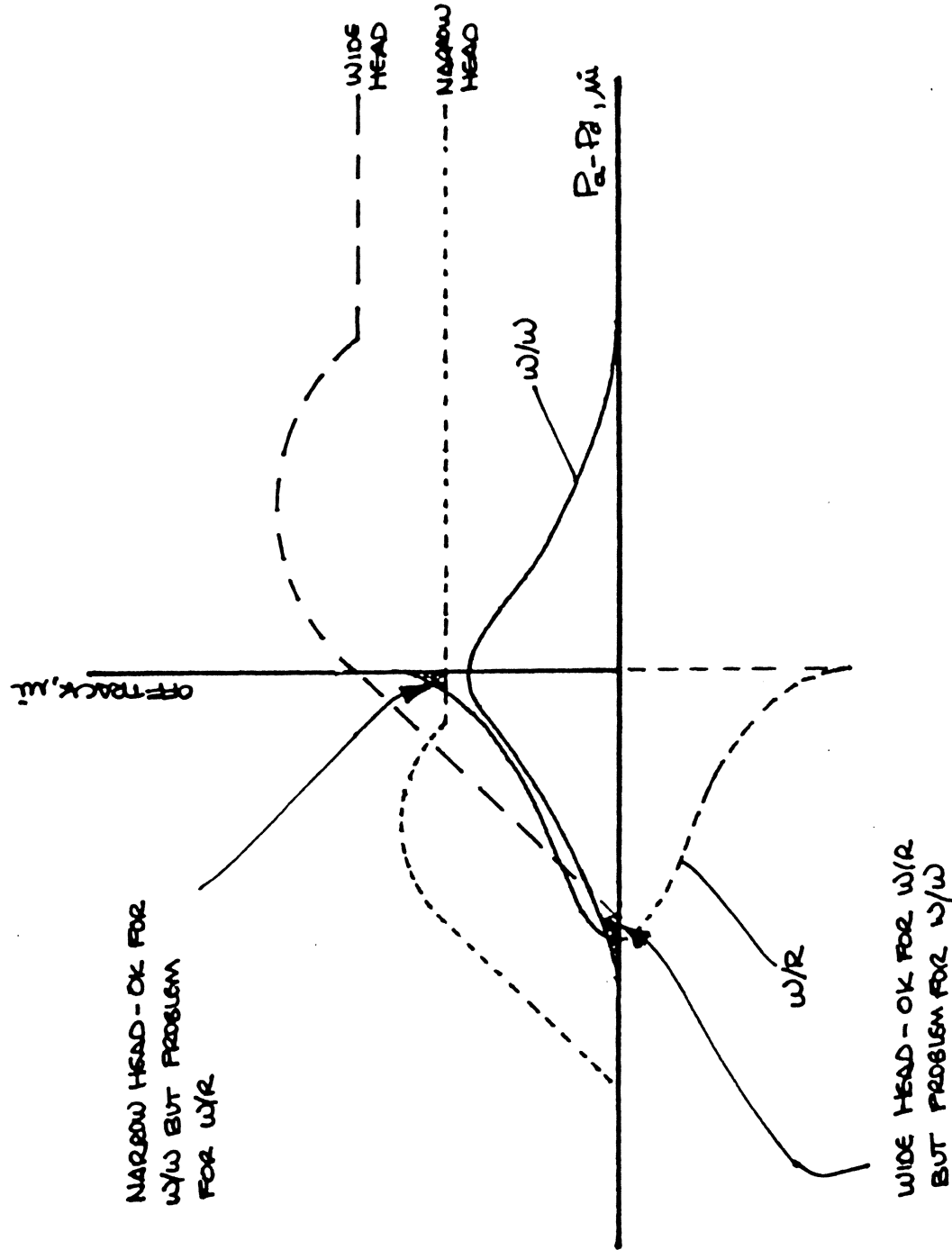


MRH
3-7-68

COUPLING TIME AND CTC

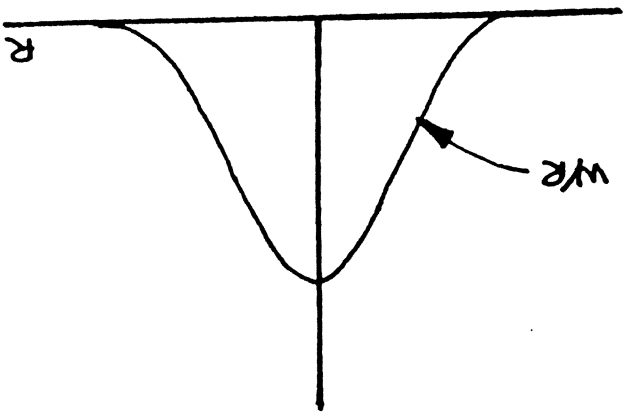
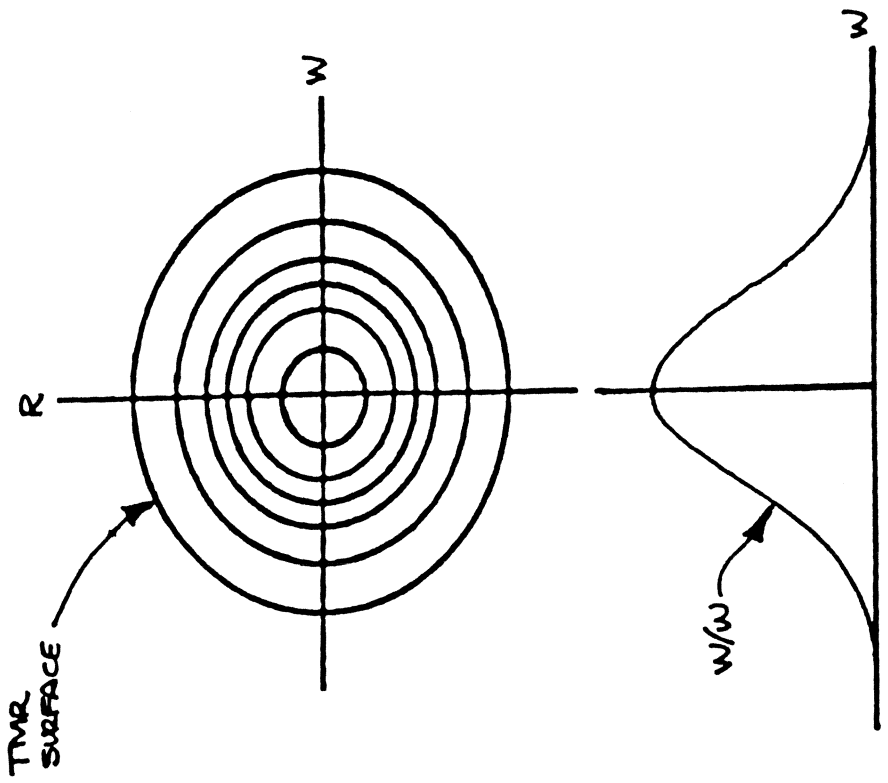
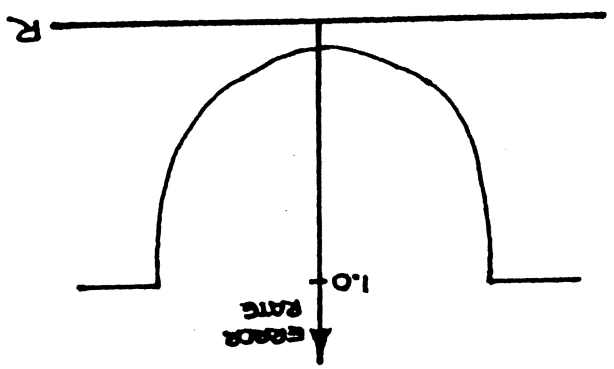
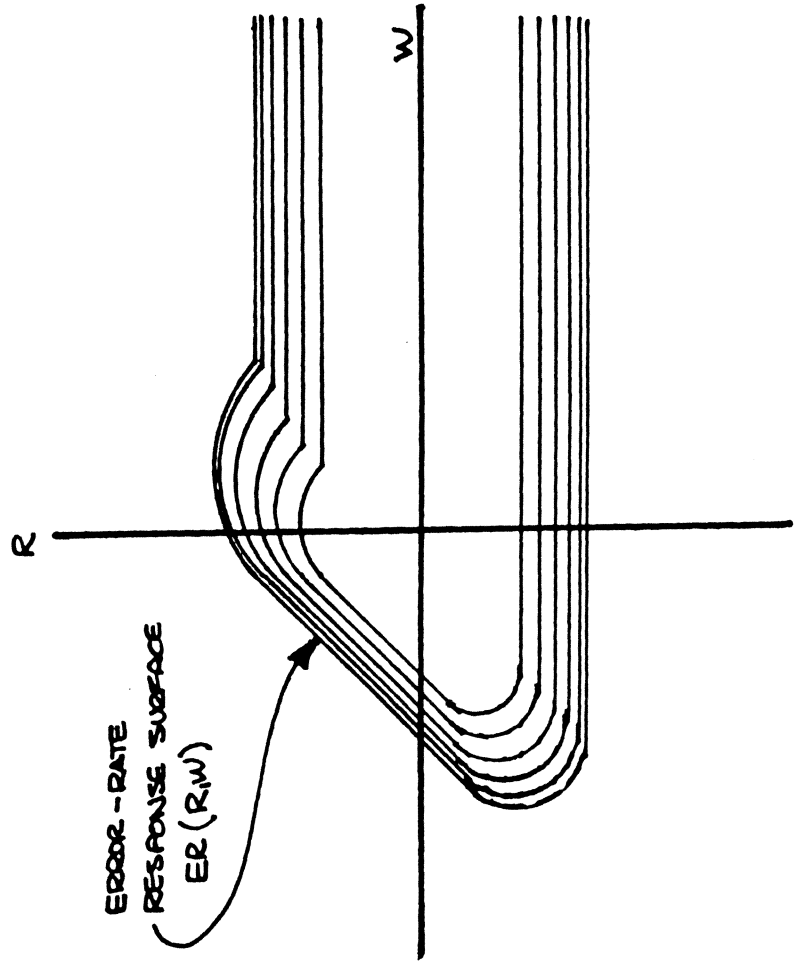


COUPLING, TMR AND OTC --
HEAD WIDTH EFFECTS



MRH
3-7-66

ERROR RATE AND TMR SURFACES



MRH
3-7-68

AVERAGE ERROR RATE CALCULATIONUNDER OFF-TRACK CONDITIONS

$$ER_{\text{AVG}} = \frac{\int_{-\infty}^{\infty} \int_{-\infty}^{\infty} [ER(R, w) \cdot TMR_R dR] TMR_w dw}{\int_{-\infty}^{\infty} \int_{-\infty}^{\infty} TMR_R TMR_w dR dw^*}$$

* DENOMINATOR IS NORMALIZATION FACTOR

TMR FACTORS
-----**SERVOWRITER TMR FACTORS: (PROVIDES W/W TOLERANCES ONLY)**
-----**DISK MODULATION TMR:**

DISK MODULATION IS AN AC ERROR IN THE POSITION OF SERVO TRACKS CAUSED BY NON-UNIFORM MAGNETIZATION OF THE DISK. IT CAN BE MEASURED BY MOVING THE SERVOWRITER HEAD TO THE AVERAGE SERVO NULL POSITION BETWEEN ADJACENT SERVO TRACKS AND PASSING THE RESULTING PES THROUGH A FILTER WHICH SIMULATES THE CLOSED-LOOP RESPONSE OF THE DRIVE SERVO SYSTEM. THE ERROR DISTRIBUTION CAN BE PLOTTED FOR AN INDIVIDUAL TRACK OR TWO ADJACENT NULL POSITIONS CAN BE RECORDED AND SUBTRACTED, KEEPING RELATIVE CIRCUMFERENTIAL POSITIONS INTACT, TO GIVE THE W/W TOLERANCE FOR THE TWO TRACKS DIRECTLY.

THIS TOLERANCE WILL BECOME MORE IMPORTANT AS TRACK DENSITIES APPROACH THE 1500 TO 2000 TPI RANGE, AND CORRECTION ALGORITHMS MAY HAVE TO BE BUILT INTO SERVOWRITERS TO LIMIT THE MAGNITUDE OF THE ERRORS.

DC TRACK SPACING TMR:

FOR OPEN-LOOP STEPPER MOTOR SYSTEMS, THIS TOLERANCE IS DEFINED BY THE STEPPER MOTOR STEP ERROR. FOR CLOSED-LOOP SYSTEMS WITH SERVO SURFACES, THE TOLERANCE IS DEFINED BY THE DC SPACING ACCURACY OF THE SERVOWRITER.

HEAD SETTling TMR:

HEAD SETTling TMR IS VIBRATION OF THE SERVOWRITER ACTUATOR/HEAD FOLLOWING A MOVE TO WRITE A NEW TRACK.

SPINDLE NRRO TMR:

NON-REPEATABLE RUNOUT (NRRO) OF THE SPINDLE MOTOR WILL CONTRIBUTE AN AC ERROR TO EACH WRITTEN TRACK. ACTUAL NRRO ON WELL DESIGNED SPINDLES CAN BE IN THE 10-20 MICROINCH P-P RANGE, HOWEVER, SPINDLES WITH RESONANCES CLOSE TO THE BALL BEARING DEFECT FORCING FREQUENCIES CAN EASILY REACH 30-100 MICROINCHES P-P. THE TREND TOWARD FIXED-SHAFT SPINDLES, CLAMPED ON BOTH ENDS, IS REDUCING THE AMOUNT OF NRRO COMPARED TO THAT SEEN ON CANTILEVERED SPINDLES.

SERVO SYSTEM TMR FACTORS:
-----**TYPE OF SERVO USED:**

THE TYPE OF SERVO SYSTEM USED, IF ANY, IS THE PRIMARY FACTOR TO BE TAKEN INTO ACCOUNT IN ANY TMR STUDY. DEPENDING ON THE TYPE OF SYSTEM USED, SOME TOLERANCES MAY BE COMPLETELY ELIMINATED, OTHERS MAY BE INCREASED OVER THE NO-SERVO CASE, AND OTHERS MAY EXIST NO MATTER WHICH TYPE OF SERVO IS USED.

TRANSIENT RESPONSE TMR:

THIS IS THE TOLERANCE WHICH DESCRIBES THE SETTLING CHARACTERISTICS OF THE SERVO SYSTEM. THOUGH THE AVERAGE LATENCY IS 8.33ms, SOME READING AND WRITING CAN OCCUR IMMEDIATELY AFTER SEEK COMPLETE IS SET, AND THE OVER/UNDERSHOOT SETTLING CHARACTERISTICS OF THE SERVO NEED TO BE TAKEN INTO ACCOUNT.

WRITE/SERVO COUPLING TMR:

ANY SERVO SYSTEM IN WHICH SIMULTANEOUS READING OF SERVO INFORMATION AND WRITING OF DATA OCCURS IS SUBJECT TO COUPLING OF WRITE NOISE INTO THE SERVO, CREATING POSITIONING ERROR.

DC STIFFNESS/BIAS FORCES:

THE SERVO SYSTEM SHOULD HAVE ENOUGH DC STIFFNESS TO MINIMIZE THE EFFECTS OF DRIVE ORIENTATION, CABLE BIAS FORCES, AND OTHER BIAS FORCES. THE FACT THAT ALL BALL-BEARING SUPPORTED MECHANICAL STRUCTURES DO NOT ACT AS RIGID BODIES BUT ACT AS MASS-SPRING- HYSTERETIC DAMPER SYSTEMS WITH LOW RESONANT FREQUENCIES REQUIRES ADDITIONAL COMPENSATION TO RE-ESTABLISH DC GAIN.

SERVO ELECTRICAL EFFECTS TMR:

VOLTAGE TOLERANCES, COMPONENT TOLERANCES, VCM FORCE CONSTANT VARIATIONS, AND OTHER FACTORS WHICH CAN CHANGE SERVO TRACK FOLLOWING OR SETTLING CHARACTERISTICS SHOULD BE INCLUDED AS APPROPRIATE.

MECHANICAL TMR FACTORS - ACTUATOR:
-----**OPERATING SHOCK TMR:**

TYPICAL OPERATING SHOCK SPECIFICATIONS ARE 5-10g HALF-SINE WITH 11ms PULSE WIDTH. BOTH BECAUSE SMALL DRIVES ARE USED IN MOVEABLE SYSTEMS AND BECAUSE THEIR SMALL SIZE MAKES THEM EASY TO TEST, DRIVE USERS ARE REQUIRING GOOD SHOCK AND VIBRATION PERFORMANCE.

SINCE THE 11ms SHOCK PULSE CONTAINS LOW FREQUENCY ENERGY RELATIVE TO THE TYPICAL LOWEST NATURAL FREQUENCY OF THE ACTUATOR SYSTEM, THE RESPONSE OF THE ACTUATOR IS DEFINED BY THE STATIC STIFFNESS. FOR A LINEAR ACTUATOR, THE PRIMARY STIFFNESS IS THAT OF THE BEARING/GUIDE ROD SYSTEM. "CANTILEVER" TYPE SYSTEMS WITH THE BEARING SYSTEM AT THE BOTTOM OF THE CARRIAGE AND THE CARRIAGE CENTER OF MASS ABOVE THE SUPPORT SYSTEM WILL HAVE GREATER SHOCK MOVEMENTS THAN ACTUATORS WITH BEARINGS AT TOP AND BOTTOM. ALSO, THE BEARING PRELOAD SHOULD BE SUCH THAT THE CARRIAGE IS NEVER UNLOADED DURING OPERATING SHOCK. FOR A ROTARY ACTUATOR, THE BEARING/SHAFT STIFFNESS AS WELL AS BALANCE ABOUT THE PIVOT CONTRIBUTE TO MOTION. AS ROTARY ACTUATORS MOVE TOWARD BEING CONSTRAINED AT THE TOP AND BOTTOM OF THE SHAFT, DRASTICALLY REDUCING SHAFT BENDING, BALANCE ABOUT THE PIVOT BECOMES THE PRIMARY OFFTRACK INFLUENCE.

HIGH-BANDWIDTH CONTINUOUS SERVO SYSTEMS CAN REDUCE THE ERROR CONSIDERABLY AT THE SERVO HEAD, BUT IF THE MOTION INCLUDES A TILT, SOME OF THE DATA HEADS CAN BE IN ERROR EVEN IF THE THE SERVO HAS NONE.

ROTARY ACTUATOR SYSTEMS WHICH HAVE BASE ROTATION OCCURRING DURING SHOCK CAN HAVE OFF TRACK ERROR AS THE BASE ROTATES EVEN IF THE ACTUATOR IS PERFECTLY BALANCED. THIS BASE ROTATION IS CAUSED BY THE SHOCK MOUNT AND FRAME STIFFNESS RELATIVE TO THE CENTER OF MASS OF THE SYSTEM.

OPERATING VIBRATION TMR:

TYPICAL OPERATING VIBRATION SPECIFICATIONS ARE 0.5g P-P FROM 5-500 Hz. THIS VIBRATION LEVEL IS LOW ENOUGH THAT THE PRIMARY CONCERN IS NOT STATIC STIFFNESS BUT THE EXISTENCE OF ANY RESONANCES WHICH CAN BE EXCITED AND THEREBY INCREASE THE MOTION. STEPPER MOTOR SYSTEMS TYPICALLY HAVE A RIGID-BODY MODE IN THE 200-300 Hz RANGE WHICH CAN BE EXCITED. MOTION AT SHOCK-MOUNT RESONANT FREQUENCIES ESSENTIALLY INCREASE THE ACCELERATION LEVELS SEEN BY THE ACTUATOR. ROTARY ACTUATOR SYSTEMS CAN HAVE ERRORS CAUSED BY BASE ROTATION DURING OPERATING VIBRATION AS DESCRIBED ABOVE UNDER OPERATING SHOCK TMR.

BEARING TMR FACTORS:

BALL BEARING SUPPORT STRUCTURES FOR THE ACTUATOR CAN CONTRIBUTE TO ERROR, WITH THE EFFECT BEING MUCH LARGER FOR LINEAR ACTUATORS THAN FOR ROTARY. LINEAR ACTUATOR BEARINGS HAVE SEVERAL EFFECTS TO BE CONSIDERED: OUTER RING RUNOUT, BALL-DROP (THE RAISING AND LOWERING OF THE SHAFT AS THE BALL COMPLEMENT ROTATES), OUTER RING BENDING, AND NON- REPEATABLE EFFECTS IF THE BEARING IS NOT ALIGNED WELL AND ROLLS AND SLIDES INSTEAD OF ROLLING ONLY. EACH BEARING IN A LINEAR ACTUATOR SYSTEM SHOULD BE CONSIDERED INDIVIDUALLY FOR ITS CONTRIBUTION TO TMR, RESULTING IN A TMR TOLERANCE FOR EACH BEARING. BECAUSE BEARING ERRORS IN LINEAR ACTUATORS CREATE TILT EFFECTS, THE TMR ERROR WILL INCREASE AS THE DISTANCE FROM THE BEARING SUPPORT STRUCTURE TO THE HEAD INCREASES OR AS THE DISTANCE FROM THE SERVO HEAD TO THE DATA HEADS INCREASE.

ROTARY ACTUATOR BEARINGS CONTRIBUTE VERY LITTLE TO TMR AS THE ONLY TOLERANCE WHICH OCCURS (IF ALL RINGS ARE CONSTRAINED FROM PRECESSING) IS THAT CAUSED BY BALL DIAMETER TOLERANCES AS THE BALL COMPLEMENT PRECESSES. IF, HOWEVER, A RING IS FREE TO PRECESS, THEN THE RUNOUT OF THAT RING CAN CONTRIBUTE TO TILT OF THE ACTUATOR.

BEARING/RAIL WEAR TMR:

SHOULD BEARING MIS-ALIGNMENT RESULT IN WEAR OF THE BEARING/ RAIL INTERFACE, THE EFFECT SHOULD BE INCLUDED IN THE TMR.

BIAS FORCE TMR EFFECTS:

ANY BIAS FORCES WHICH CAN VARY WITH TIME AT A GIVEN TRACK POSITION CAN CREATE OFF-TRACK AT THAT POSITION AND SHOULD BE CONSIDERED. FLEX-CABLE BIAS FORCES WHICH CAN CHANGE WITH TEMPERATURE IS ONE EXAMPLE.

TUNED SEEK SETTling TMR:

"TUNED SEEK" REFERS TO A WORST CASE EXCITATION OF THE STRUCTURE BY CHOOSING COMBINATIONS OF SEEK LENGTH AND DELAY BETWEEN SEEKS TO EXCITE THE STRUCTURE. THE MOTION OCCURRING UNDER THIS WORST CASE EXCITATION CAN BE COMPARED WITH THE MOTION OCCURRING UNDER A RANDOM EXCITATION AND THE APPROPRIATE VALUE USED IN THE TMR STUDY.

BOTH ACTUATOR RESONANCES AND SUSPENSION RESONANCES CAN CONTRIBUTE TO TUNED SEEK SETTling TMR. TYPICALLY ONLY RESONANCES IN THE FREQUENCY RANGE UNDER 1KHz ARE IMPORTANT BECAUSE OF THEIR LOW STIFFNESS AND RESULTING HIGHER AMPLITUDE OF MOTION. HOWEVER, WITH ROTARY ACTUATORS USING THE 3370 SUSPENSION IN THE "SIDEWINDER" ORIENTATION, SIGNIFICANT MOTION OF THE HEAD MAY OCCUR, REQUIRING A DAMPING TREATMENT TO BE APPLIED.

MECHANICAL TMR FACTORS - SPINDLE:
-----**NRRO TMR:**

NON-REPEATABLE RUNOUT (NRRO) AS DISCUSSED EARLIER UNDER THE SERVOWRITER SECTION AFFECTS THE AC POSITION OF THE SERVO HEAD, AND HENCE W/W TMR. NRRO OF THE SPINDLE DURING READING AND WRITING OF DATA WILL CONTRIBUTE TO W/R ERROR. DEPENDING UPON THE BANDWIDTH AND TYPE OF SERVO USED, IF ANY, THE ERROR CREATED BY NRRO CAN BE INCREASED BY THE CLOSED-LOOP GAIN EFFECT OF THE SERVO SYSTEM. TYPICAL CLOSED-LOOP SERVO SYSTEMS HAVE CLOSED-LOOP TRANSFER FUNCTION PEAKING IN THE 200-600Hz RANGE, WHICH IS THE SAME FREQUENCY RANGE THAT MOST BEARING DEFECT CAUSED NRRO OCCURS.

OPERATING SHOCK TMR:

AS FOR THE ACTUATOR, SPINDLE DEFLECTION UNDER OPERATING SHOCK IS DEFINED BY THE STATIC STIFFNESS CHARACTERISTICS OF THE SPINDLE. DEPENDING ON THE SPINDLE DESIGN, ERRORS CAUSED BY OPERATING SHOCK CAN BE VIRTUALLY ZERO TO OVER 100 MICROINCHES FIXED SHAFT MOTORS WITH BOTH ENDS CONSTRAINED AND WITH THE BEARINGS SYMMETRICALLY LOCATED AXIALLY RELATIVE TO THE ROTATING MASS CENTER OF GRAVITY HAVE LOWER OFF-TRACK THAN CANTILEVERED DESIGNS UNDER SHOCK.

OPERATING VIBRATION TMR:

SPINDLES WILL HAVE "ROCKING" OR COMBINED "LATERAL" AND "ROCKING" MODES BETWEEN ROUGHLY 200 AND 500 Hz FOR CANTILEVERED SPINDLES AND ROUGHLY BETWEEN 400 AND 1000 Hz FOR FIXED-SHAFT DESIGNS WITH BOTH ENDS CONSTRAINED. IF THE ROCKING MODE EXISTS IN THE 5-500 Hz RANGE, THE MODE CAN BE EXCITED BY THE EXTERNAL VIBRATION INPUT.

TUNED SEEK TMR:

VOICE COIL MOTOR (VCM) REACTION FORCE CAN ACT AS A FORCING FUNCTION, EXCITING SPINDLE RESONANCES. BECAUSE THE SPINDLE RESONANCE WILL BE ASYNCHRONOUS WITH THE SPINDLE ROTATION, THE VIBRATION WILL APPEAR AS ADDITIONAL NRRO TO THE SERVO SYSTEM.

THERMAL TRACK SHIFT (TTS) TMR FACTORS:

THERMAL TRACK SHIFT IS THE ERROR CAUSED BY CHANGES IN TEMPERATURE, EITHER INTERNALLY OR EXTERNALLY GENERATED. ALL COMPONENTS OF THE DRIVE MUST BE CONSIDERED AS POTENTIAL SOURCES OF TTS: ACTUATOR, SPINDLE, BASE, COVER, ETC. TTS MEASUREMENT SHOULD BE CONSIDERED EARLY IN THE DEVELOPMENT PROGRAM AND A MEANS OF MEASURING ERRORS AT EVERY HEAD POSITION PROVIDED. TTS WILL VARY CONSIDERABLY FROM DRIVE TO DRIVE, NECESSITATING TESTING ON A MINIMUM OF 10-20 DRIVES TO DEFINE THE RANGE TO BE EXPECTED.

SELF HEATING TTS TMR:

THE SELF HEATING TTS TOLERANCE OCCURS AS THE DRIVE HEATS ITSELF UP AFTER BEING POWERED UP FROM AN INITIAL UNIFORM TEMPERATURE STATE. TTS OCCURS DUE TO TWO INFLUENCES, TEMPERATURE GRADIENTS AND DIFFERENTIAL THERMAL EXPANSION. AS THE DRIVE HEATS ITSELF UP DUE TO THE DISKS SPINNING, THE SPINDLE MOTOR HEATING, THE ACTUATOR HEATING, AND THE PCB HEATING, TEMPERATURE GRADIENTS ARE CREATED. THESE GRADIENTS CAUSE NON-UNIFORM EXPANSIONS THROUGHOUT THE STRUCTURE. THE GRADIENTS ARE HIGHEST IMMEDIATELY AFTER STARTUP AND DECREASE AS CONDUCTION AND CONVECTION TEND TO FORCE THE DRIVE TO A MORE UNIFORM TEMPERATURE.

IN ADDITION TO THE GRADIENT EFFECT, THE MIS-MATCH OF COEFFICIENTS OF THERMAL EXPANSION IN VARIOUS COMPONENTS OF THE DRIVE CREATES ADDITIONAL ERROR AS THE DRIVE WARMS ITSELF UP. TTS ERROR SHOULD BE MONITORED DURING THE ENTIRE WARM-UP PERIOD, AS TYPICALLY TTS WILL BE HIGHEST DURING THE FIRST 5 MINUTES AND THEN LATER AS THE DRIVE REACHES ITS EQUILIBRIUM TEMPERATURE DISTRIBUTION. THE TTS DURING THE FIRST 5 MINUTES IS CAUSED BY RAPID HEATING OF THE DISKS RELATIVE TO THE SUSPENSIONS AND OTHER COMPONENTS IN THE DRIVE.

AMBIENT CHANGE TTS TMR:

AMBIENT CHANGE TTS TMR OCCURS AS A RESULT OF CHANGES IN AMBIENT TEMPERATURE WHICH OCCUR AFTER THE DRIVE HAS SELF HEATED AND REACHED AN EQUILIBRIUM STATE. TYPICAL MAXIMUM SPECIFIED RATE OF CHANGE OF AMBIENT TEMPERATURE IS 10 DEGREES C PER HOUR, A CHANGE WHICH IS SLOW ENOUGH TO NOT SIGNIFICANTLY CHANGE THE EQUILIBRIUM TEMPERATURE GRADIENTS THROUGHOUT THE DRIVE. AS A RESULT, THE ERRORS WHICH OCCUR DURING AMBIENT CHANGE ARE DRIVEN NOT BY CHANGING TEMPERATURE GRADIENTS BUT BY DIFFERENTIAL THERMAL EXPANSION CAUSED BY MIS-MATCHES OF COEFFICIENTS OF THERMAL EXPANSION IN VARIOUS COMPONENTS OF THE DRIVE.

WORST-CASE AMBIENT SWING TTS OCCURS UNDER CONDITIONS OF WRITING COLD AND READING HOT, OR VICE VERSA.

ID/OD TTS TMR:

THIS ERROR IS CAUSED BY DIFFERENCES IN TEMPERATURE GRADIENTS WHICH OCCUR WITH ACTUATOR POSITION. IF THE ACTUATOR IS POSITIONED AT THE ID FOR A LONG PERIOD OF TIME AND THEN SEEKED TO THE OD, THE INITIAL RELATIVE POSITIONS OF THE HEADS AND DISKS WILL BE DIFFERENT FROM THAT REACHED WHEN THE SYSTEM HAS REACHED ITS EQUILIBRIUM TEMPERATURE STATE AT THE OD.

STEPPER MOTOR SYSTEMS USING BAND TYPE DRIVES WILL TYPICALLY HAVE AN ERROR ASSOCIATED WITH BAND EXPANSION DIFFERENCES AT ID AND OD POSITIONS, NECESSITATING SOME SORT OF THERMAL COMPENSATION LINK IN THE SYSTEM.

SEEKING/TRACK FOLLOWING TTS TMR:

THE EQUILIBRIUM TEMPERATURE STATE WHEN TRACK FOLLOWING IS DIFFERENT FROM THAT WHICH OCCURS WHEN RAPIDLY SEEKING. THE DIFFERENT TEMPERATURE AND TEMPERATURE GRADIENTS CAN CONTRIBUTE A TTS ERROR.

PERMANENT SHIFT TTS TMR:

PERMANENT SHIFT TTS IS THE ERROR CREATED BY PERMANENT CHANGES IN POSITION OF COMPONENTS CAUSED BY THERMALLY CYCLING THE DRIVE. SHIFTING OF ARMS RELATIVE TO CARRIAGE, SUSPENSIONS RELATIVE TO ARMS, DISKS RELATIVE TO THE ORIGINAL AXIS OF ROTATION, SPINDLE MOTOR RELATIVE TO BASE, AND WARPING OF THE BASE/COVER ASSEMBLY ARE COMMON, ESPECIALLY FOLLOWING SHIPPING TEMPERATURE LIMIT EXPOSURE.

MECHANICAL - MISCELLANEOUS TMR EFFECTS:

MOUNTING DISTORTION / ORIENTATION TMR:

IF THE SHOCK MOUNT SYSTEM WHICH ISOLATES THE HDA FROM FRAME DISTORTION IS TOO STIFF OR NON-EXISTENT, DISTORTIONS IN THE FRAME CAUSED BY MOUNTING IN THE CUSTOMERS BOX MAY BE TRANSFERRED TO THE HDA, CREATING OFF TRACK ERROR.

DRIVES WITH RELATIVELY FLEXIBLE SPINDLE AND/OR ACTUATOR SYSTEMS CAN HAVE SMALL ERRORS DEPENDING UPON THE DIRECTION OF ORIENTATION OF THE DRIVE AND THE RESULTING GRAVITY EFFECTS.

NON-OPERATING SHOCK TMR:

NON-OPERATING SHOCK, TYPICALLY SPECIFIED IN THE 40-75g RANGE, CAN CREATE ERRORS DUE TO PERMANENT SHIFT OF COMPONENTS OR DUE TO INCREASES IN NRRO DUE TO SPINDLE BEARING DAMAGE.

POSITION SENSING, HEADS,
MEDIA SERVO PATTERNS

EDGAR WILLIAMS

READ-RITE CORP.

IIST SHORT COURSE
MARCH 22-24, 1988

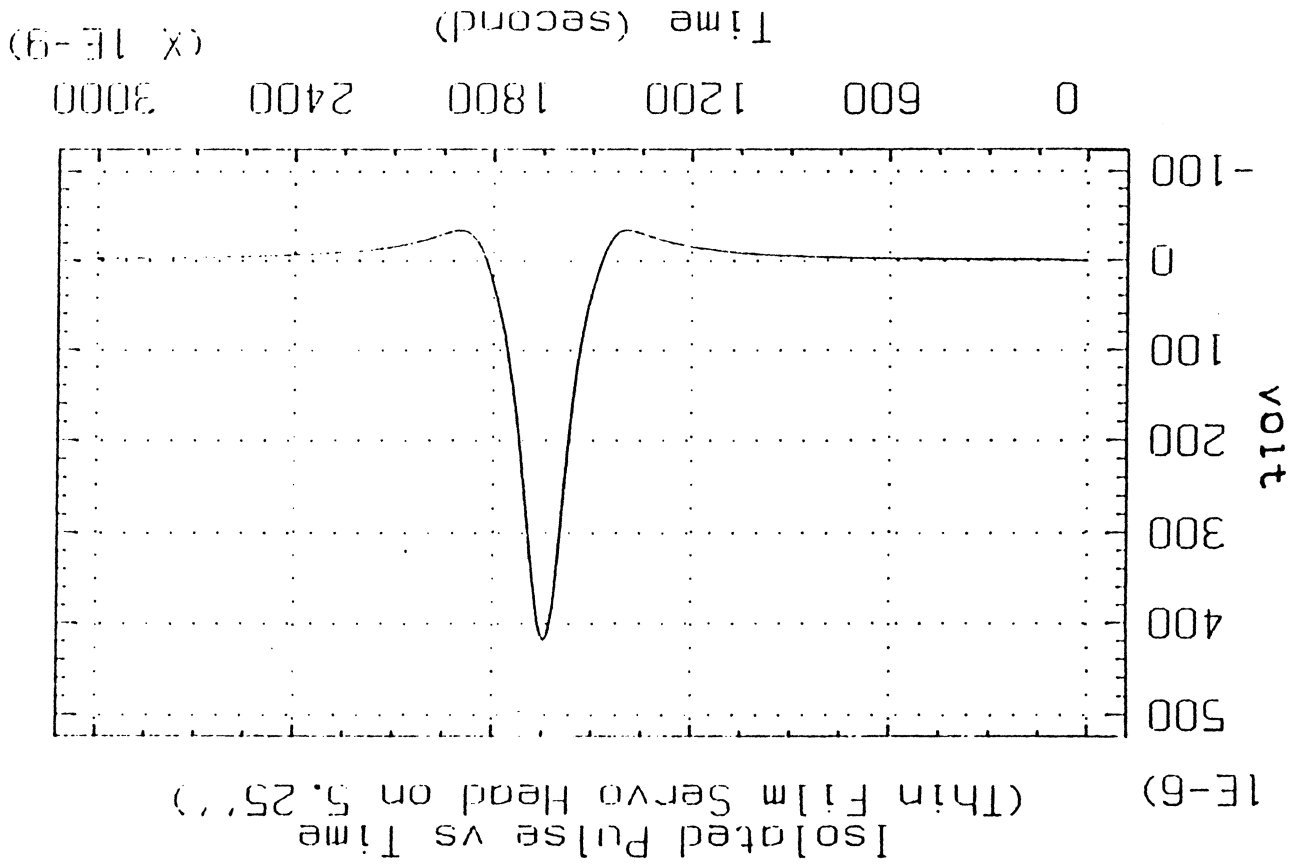
SANTA CLARA UNIVERSITY
SANTA CLARA, CALIF.

Position Sensing: Heads, Media, Servo Patterns

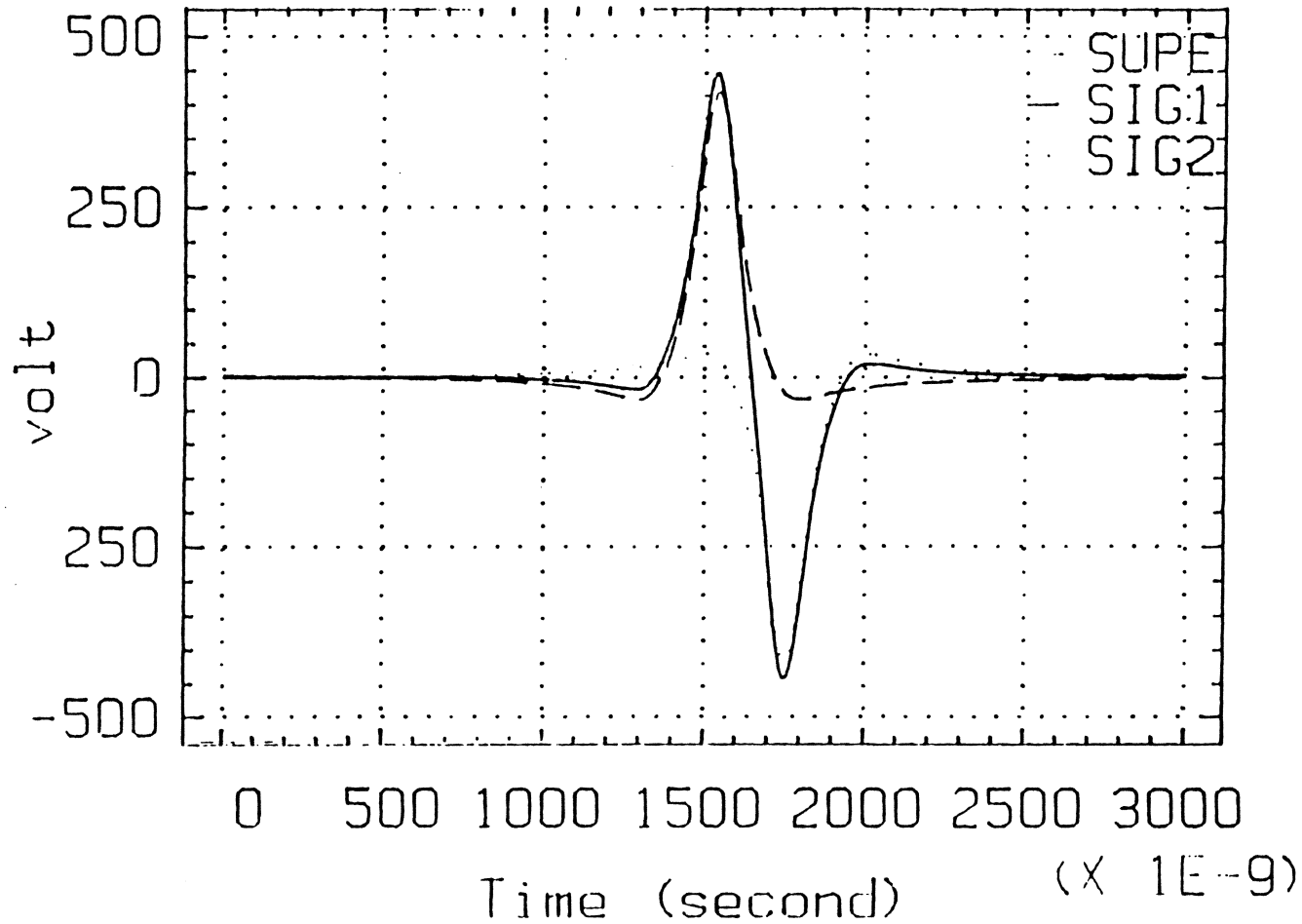
- * Isolated Pulses
- * Di-bits and Linear Superposition
- * Side-writing
- * Side-reading
- * Isolated Track Profiles
- * Quadrature Servo Patterns

EMWilkins
3/8/88
READ-RITE CORP.

SM Williams
3/8/88
READ-RITE CORR.

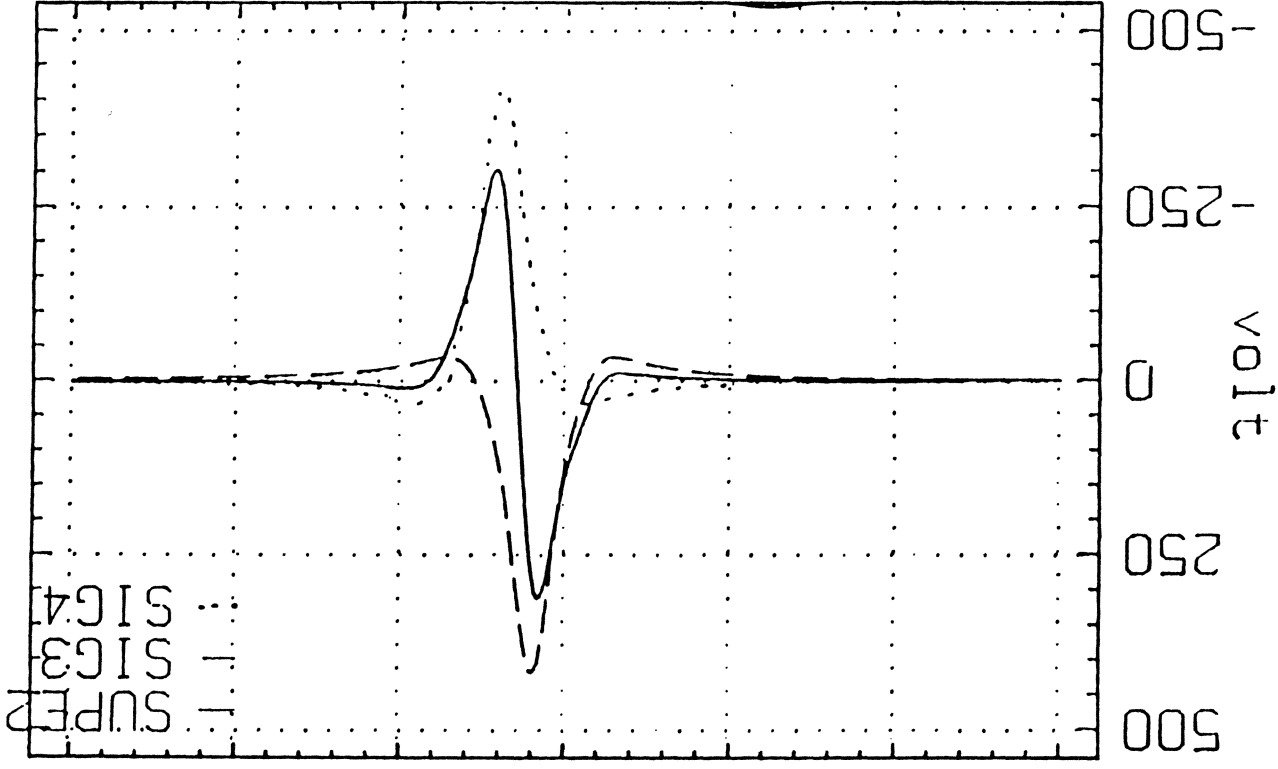


Superposition of Isolated Pulses
(X 1E-6) (Di-Bit Interval = 200 nsec)



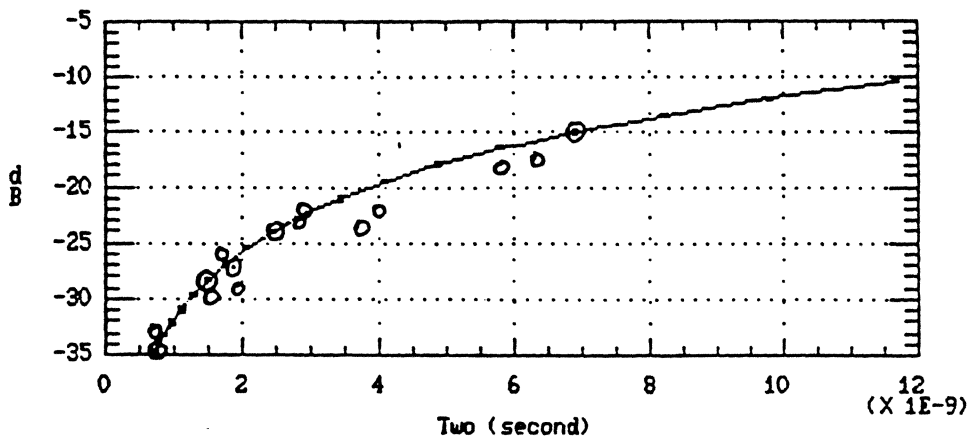
Smilkins
3/8/88
READ-RITE CORP.

Superposition of Isolated Pulses
(X 1E-6) (Di-Bit Interval = 100 nsec)



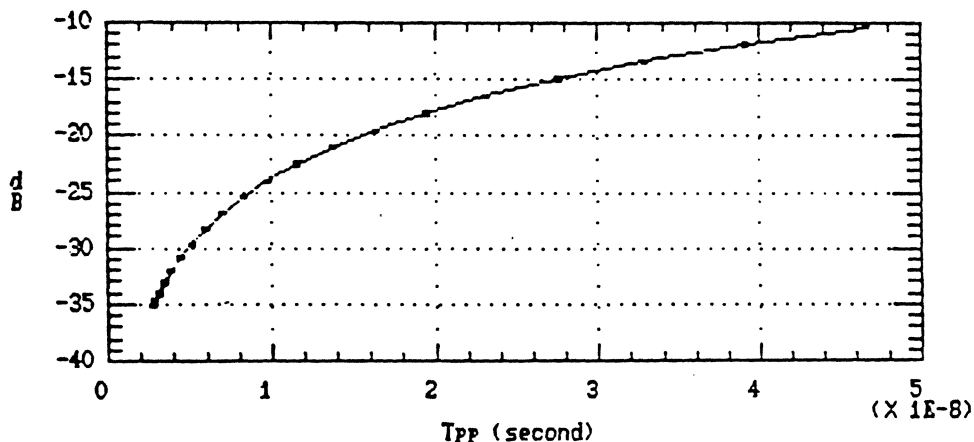
3/8/88
Rcmd-rite corp
Mullikin

Overwrite vs Write-induced Shift



— Theory
 ○ Experiment

Overwrite vs Pulse-pairing



$T_{pp} = 4T_{wo}$

$$T_{wo} = \frac{H_c T_0}{H_m}$$

$$OW(dB) = 20 \log_{10}(\Delta\phi)$$

$$\Delta\phi = 2\pi f \cdot T_{wo}$$

$$R = HF/LF \text{ S}$$

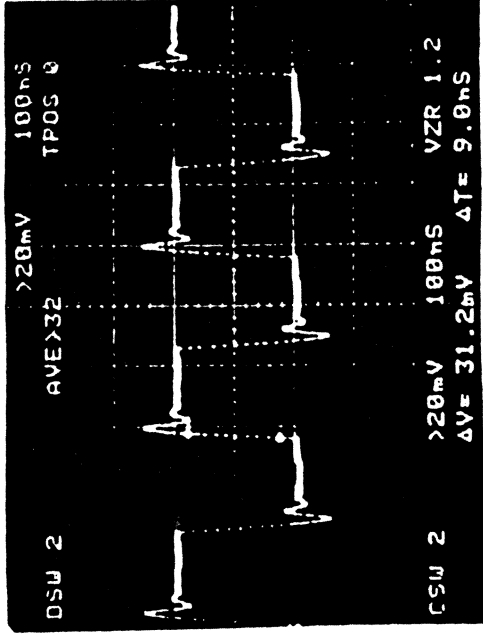
H_m = max. recording field at medium

T_0 = 0-50% rise time of written field.



Emil Wilham
 5/13/87
 READ-RITE CORP.

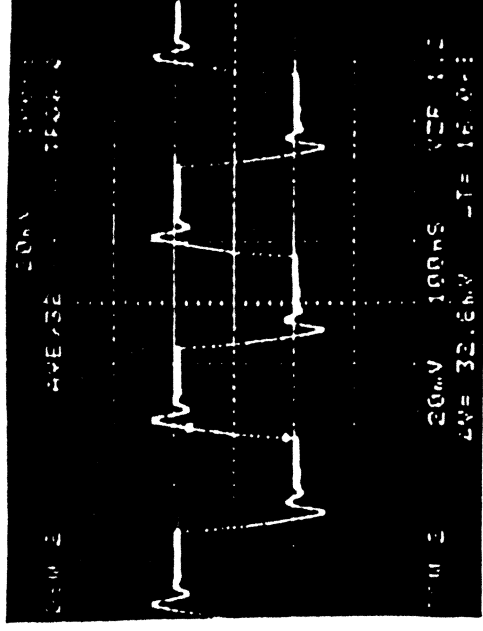
WRITE CURRENT RISE TIME



24 Turns

$$L \approx 500 \text{ nH}$$

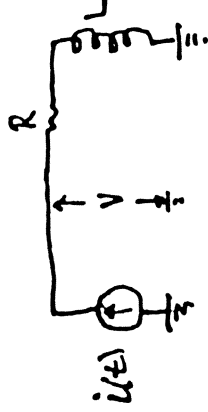
$$t_r \approx 9.0 \text{ ns} \quad (10\% - 90\%)$$



30 Turns

$$L \approx 900 \text{ nH}$$

$$t_r \approx 16.0 \text{ ns}$$



$$V = L \frac{di}{dt}$$

$$\approx L \frac{\Delta I}{T_0}$$

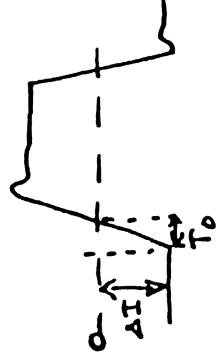
If $V = V_0$, a write-driver limited constant,

then

$$T_0 \approx \frac{L \Delta I}{V_0}$$

e.g. Let $V_0 = 2.5 \text{ Volts}$
 then $T_0 \approx \frac{5 \times 10^{-7} \times 0.02}{2.5} = 4 \times 10^{-9} \text{ s}$

or $T_0 \approx \frac{9 \times 10^{-7} \times 0.02}{2.5} = 7.2 \times 10^{-9} \text{ s}$



$$T_0 \approx \frac{t_r}{2}$$

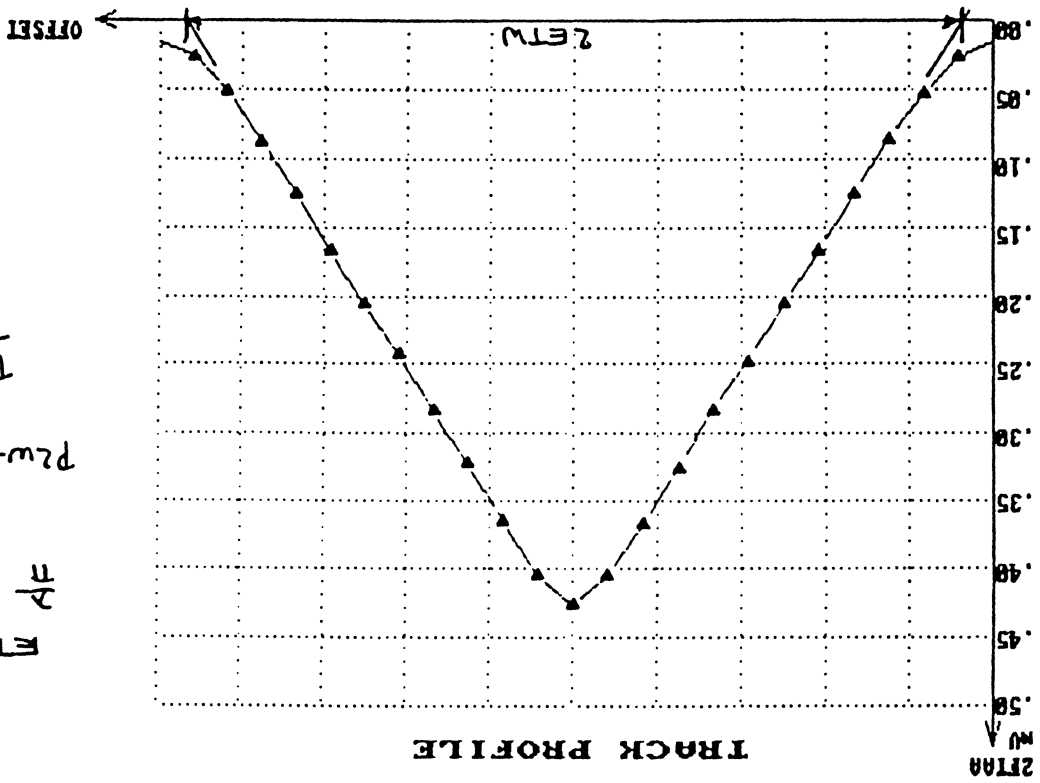
{mWilkins
READ-RITE

READ-RITE CORP.

3/8/88
Mullins

5257-6-004 ID: P61/CY11 TRAK: 1398 HEAD: 0 CLOCK: 200 ns
03/04/87 01:02:20

Steps 300 240 180 120 60 0 240 480 720 960 1200
inches -1200 -960 -720 -480 -240 0 240 480 720 960 1200



$$FTW = 139 \mu\text{m} = 28.9 \mu\text{m}$$

$$\frac{\pi}{2} = \frac{1215}{\pi \times 1.5 \times 10^6} = 3.1 \mu\text{m}$$

$$p2w + 2\sigma + \frac{\pi}{2} = 29.6 \mu\text{m}$$

$$\frac{\text{Theory}}{\text{Exp.}} = \frac{29.6}{28.9} = 1.02$$

Effective Track Width

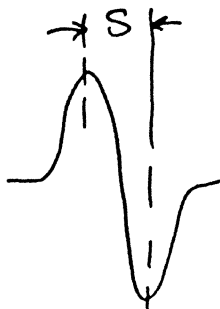
$$ETW = P2W + G + 2S/\pi$$

where P2W = geometrical read width

P2W + G = written track width

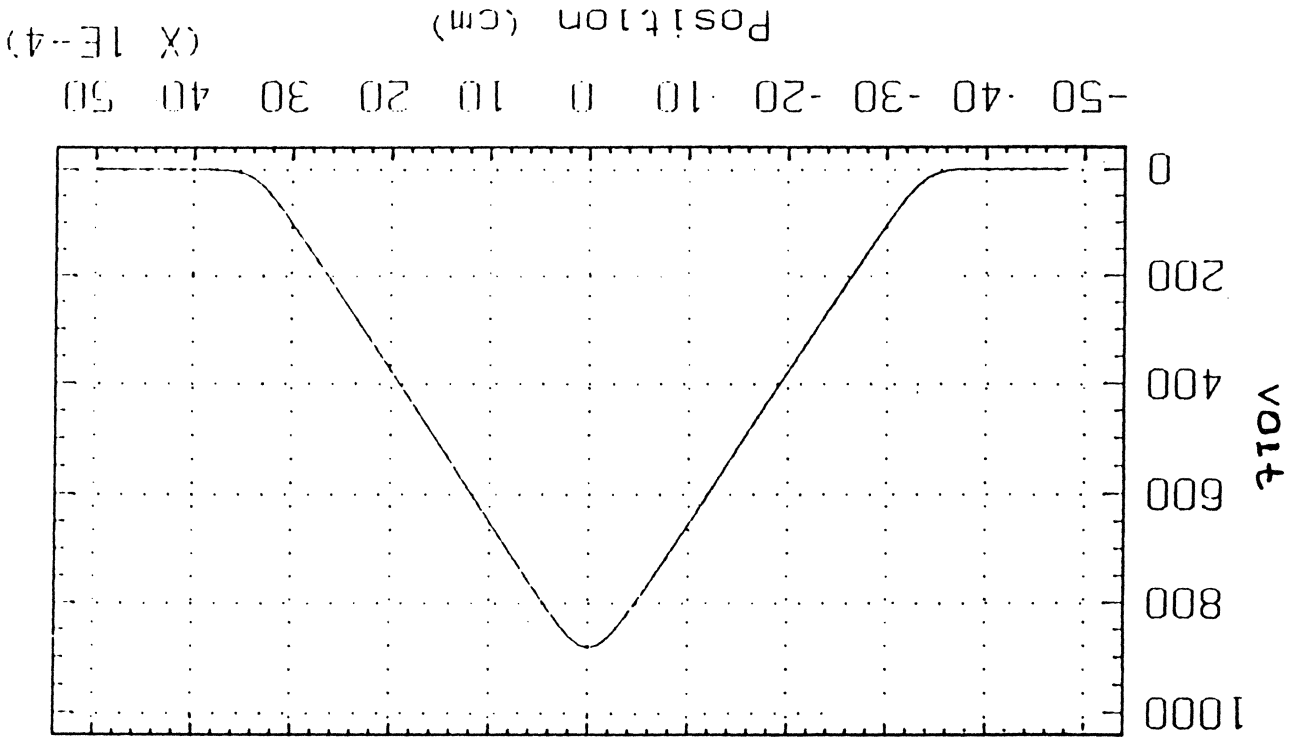
$2S/\pi$ = electrical broadening

arising from dipulse interval



E. M. Williams
3/8/88
READ-RITE Corp.

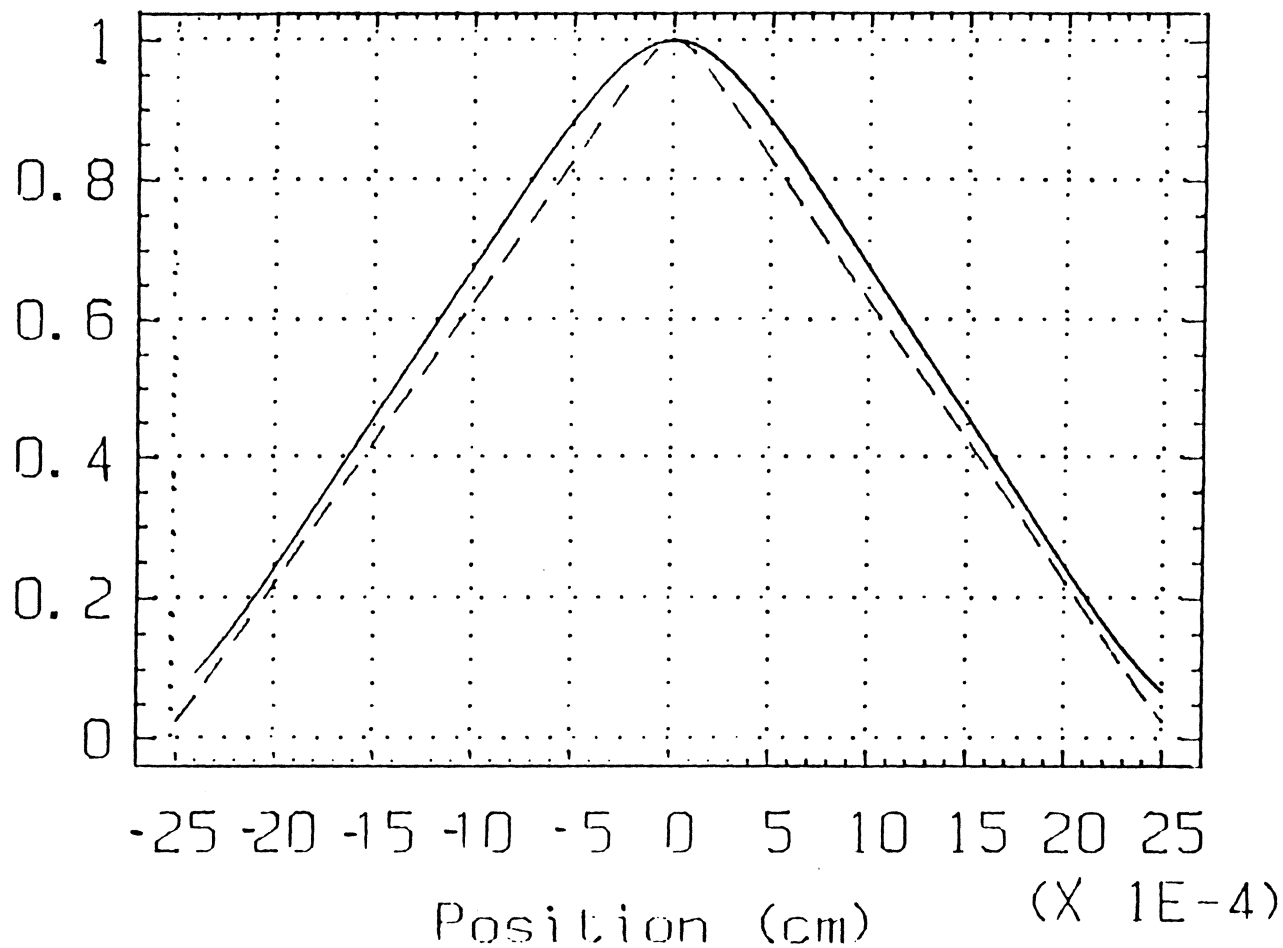
Signal vs Head Position Across Track
 (Pole Width = 33 microns)
 (1E-6)



Emulsion
 3/8/88
 READ-RITE cap.

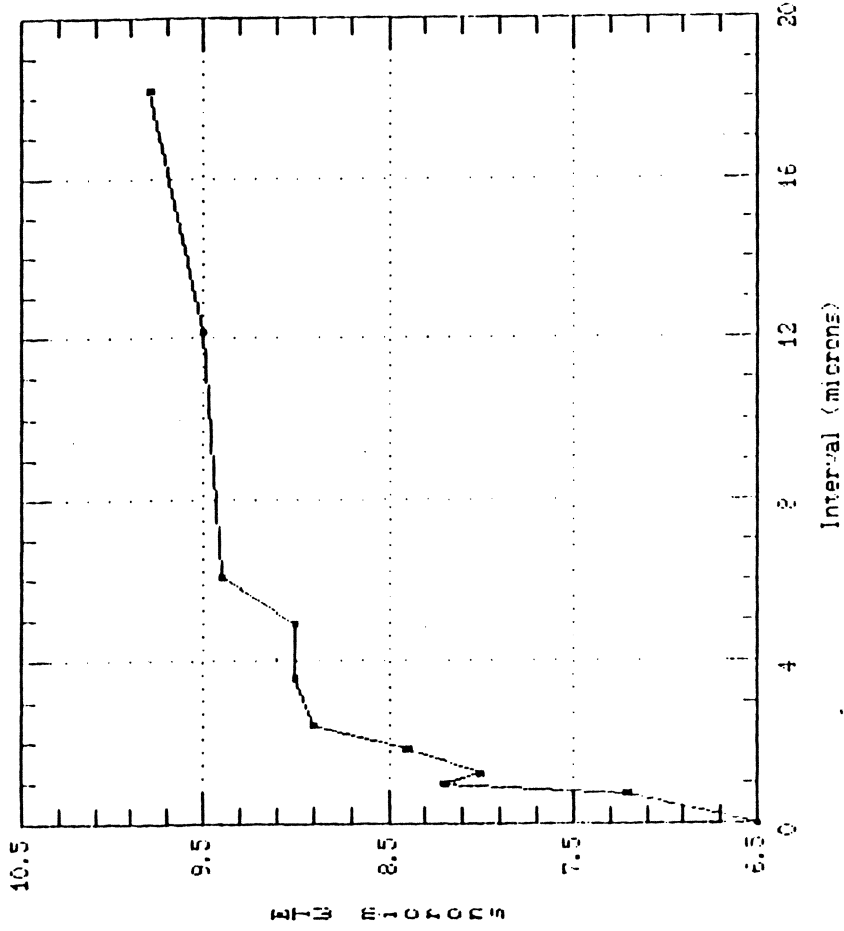
Servo Track Profiles

(Di-pulse intervals = 1, 5 microns)

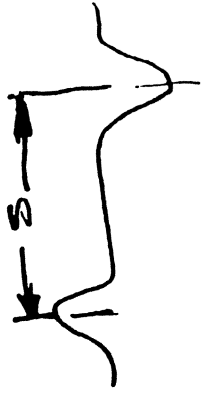


EM Williams
3/8/88
READ-RITE CORP.

Plot of ETW vs Pulse Interval
 (P2W = 6.1 um; G = 0.2 um)

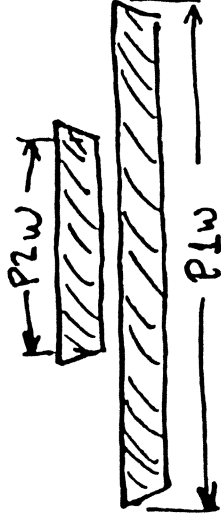


Pulse Interval



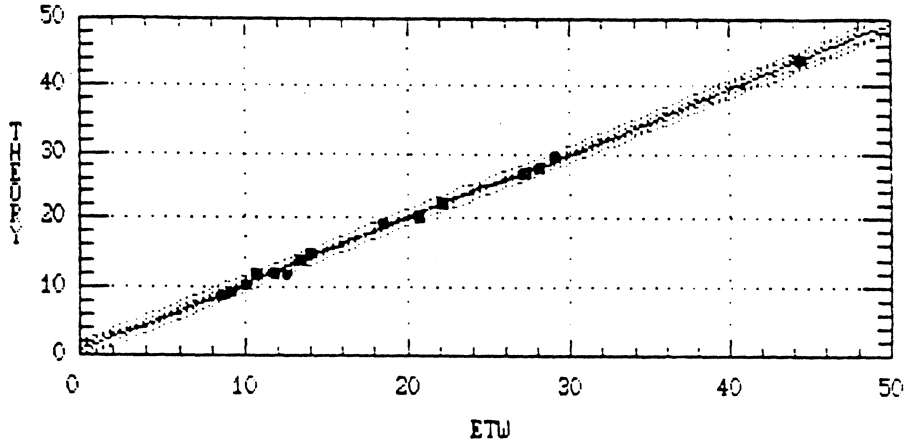
$$P2W + 2G = 6.5 \mu m$$

$$P1W = 15.0 \mu m$$

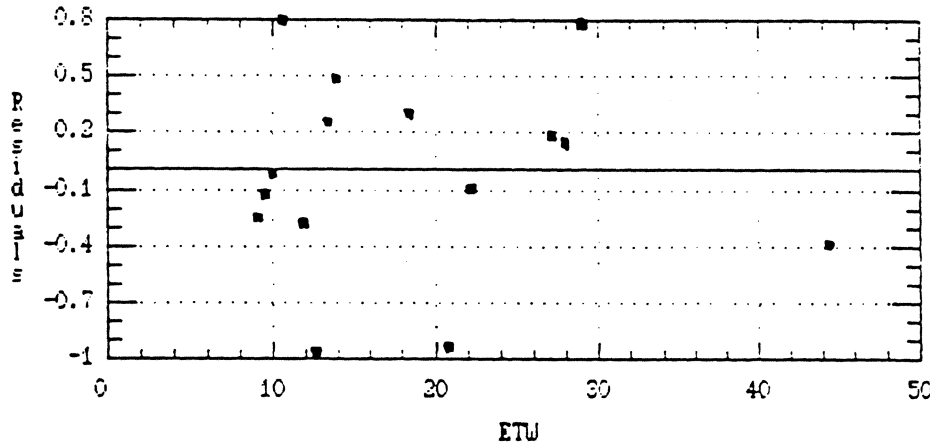


S. M. Johnson
 READ-RITE CORP
 11/12/87

Regression of THEORY on ETW



Regression of THEORY on ETW



Em Wilkins
3/8/88
READ RATE CORR.

Regression Analysis - Linear model: $Y = a + bX$

Dependent variable: THEORY				Independent variable	
Parameter	Estimate	Standard Error	T Value	Prob. Level	
Intercept	0.687339	0.305424	2.25044	0.042373	
Slope	0.973019	0.014538	66.9294	0	

Analysis of Variance

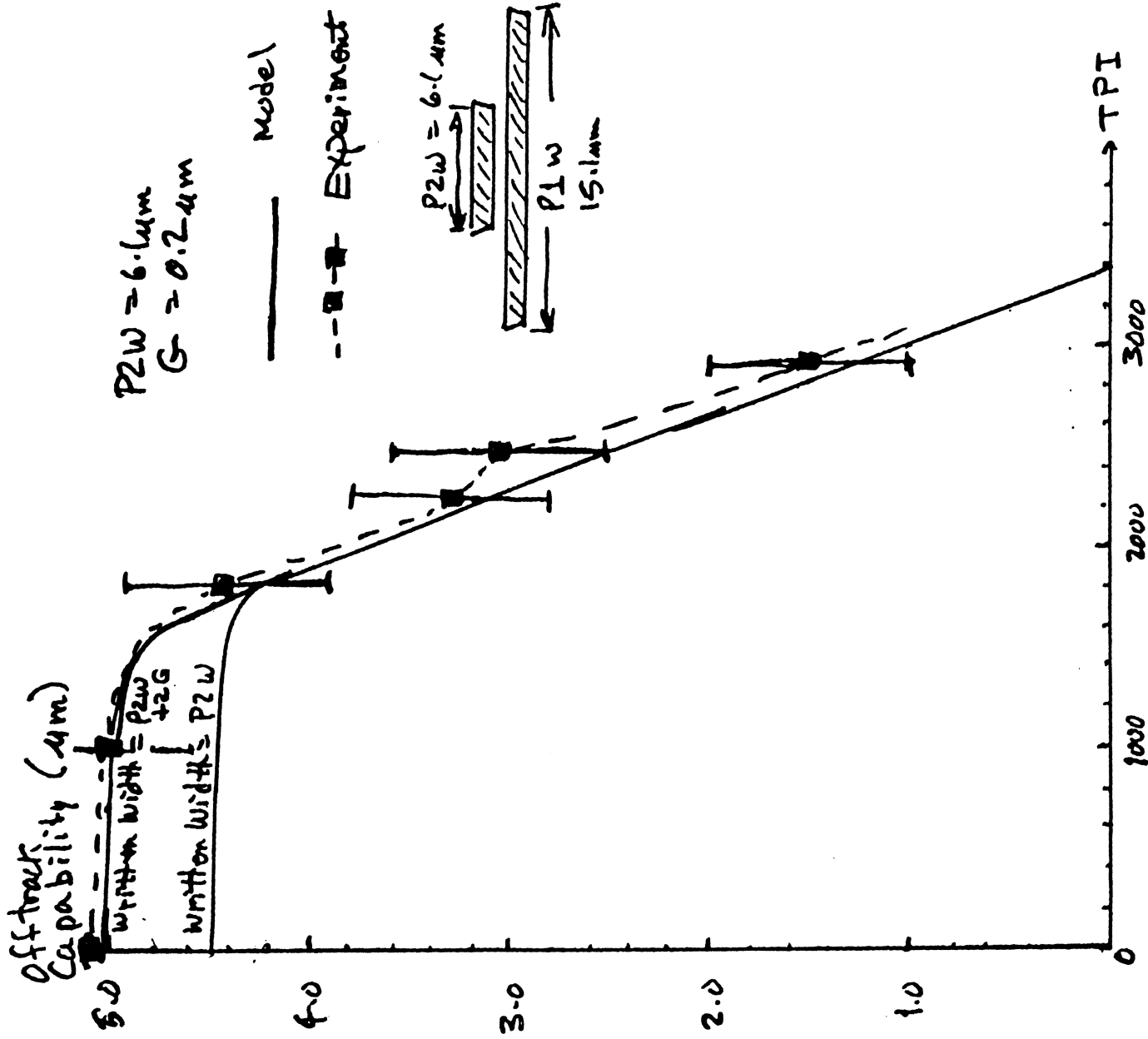
Source	Sum of Squares	Df	Mean Square	F-Ratio	Prob. Le
Model	1312.5432	1	1312.5432	4479.5432	.00
Error	3.809108	13	.293008		
Total (Corr.)	1316.3523	14			

Correlation Coefficient = 0.998552
Std. Error of Est. = 0.541302

R-squared = 99.71 percent

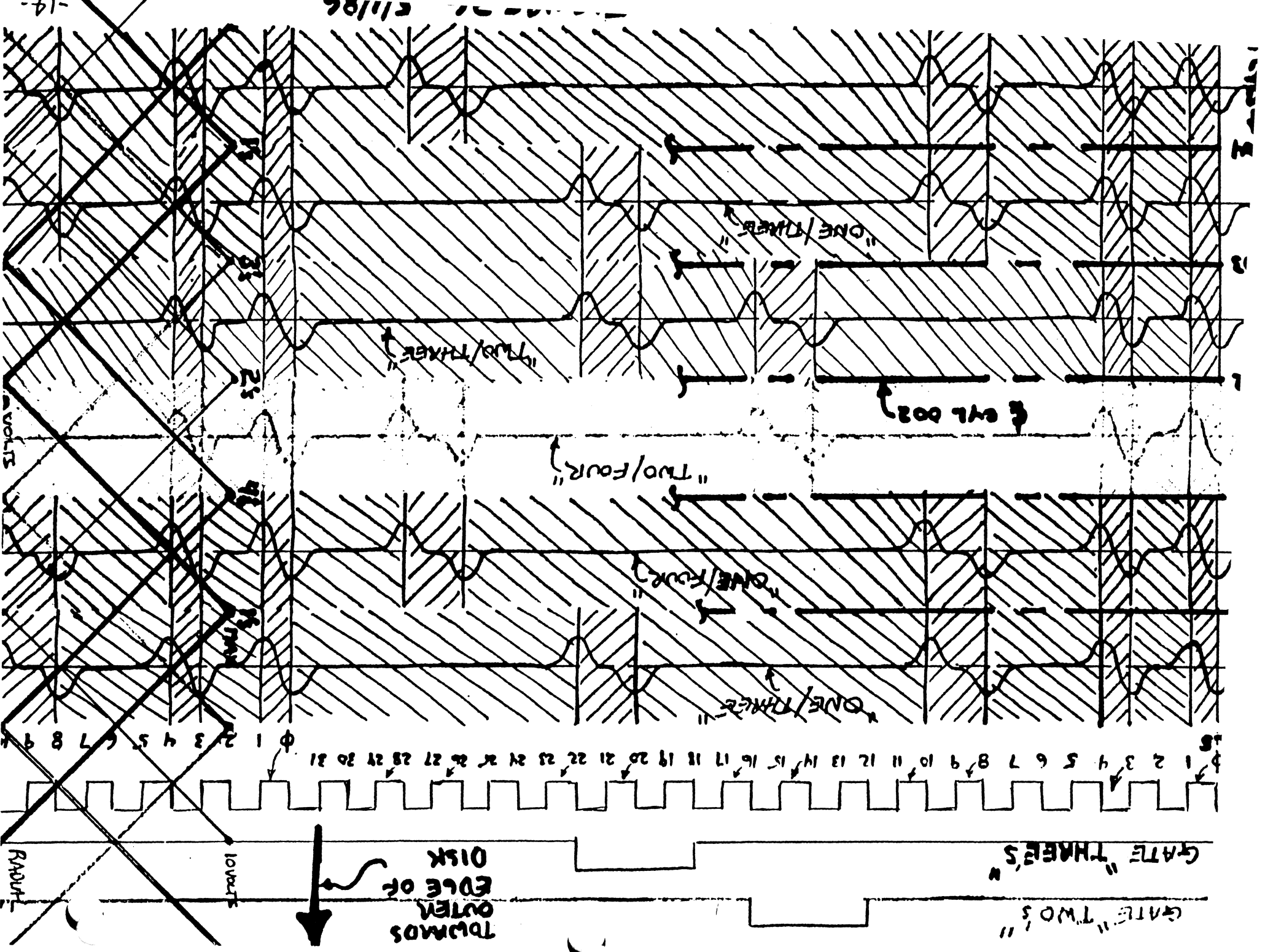
NARROW TRACK RECORDING

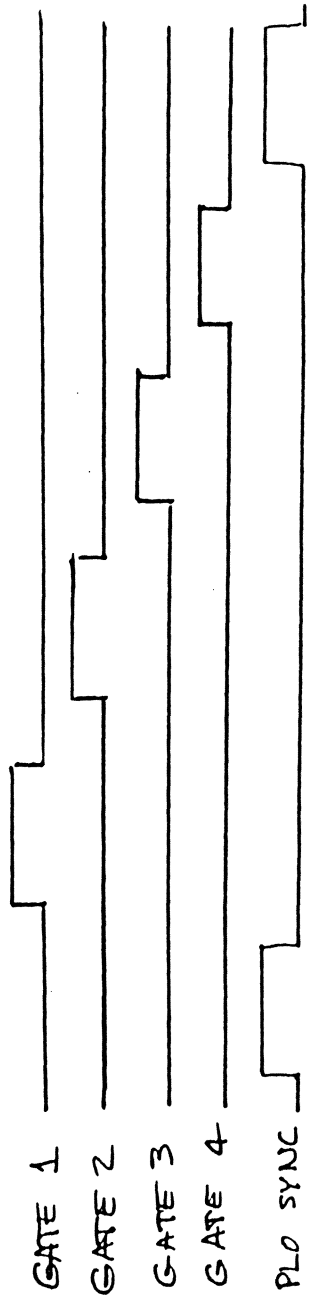
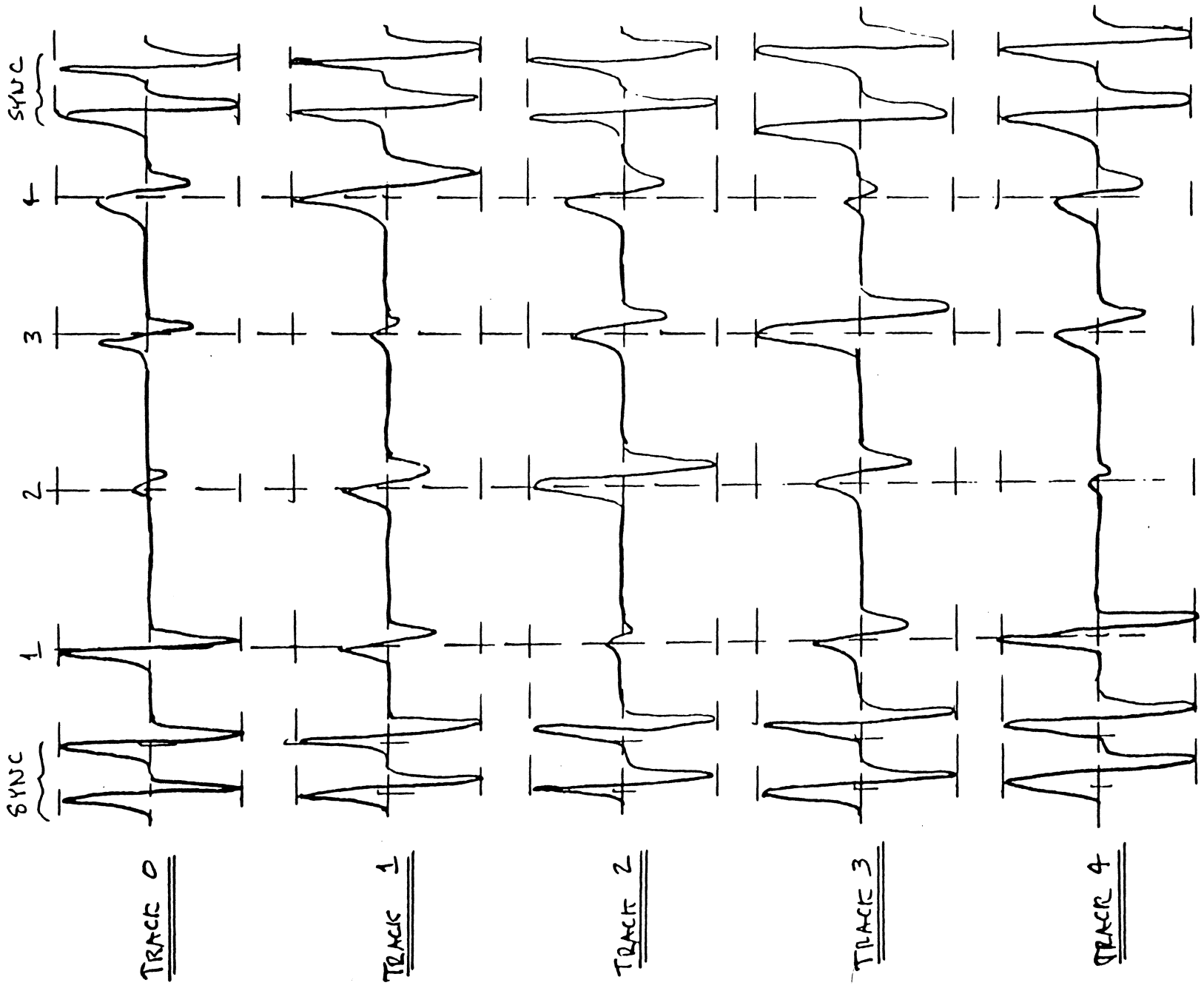
Ed Williams, READ-RITE CORP.



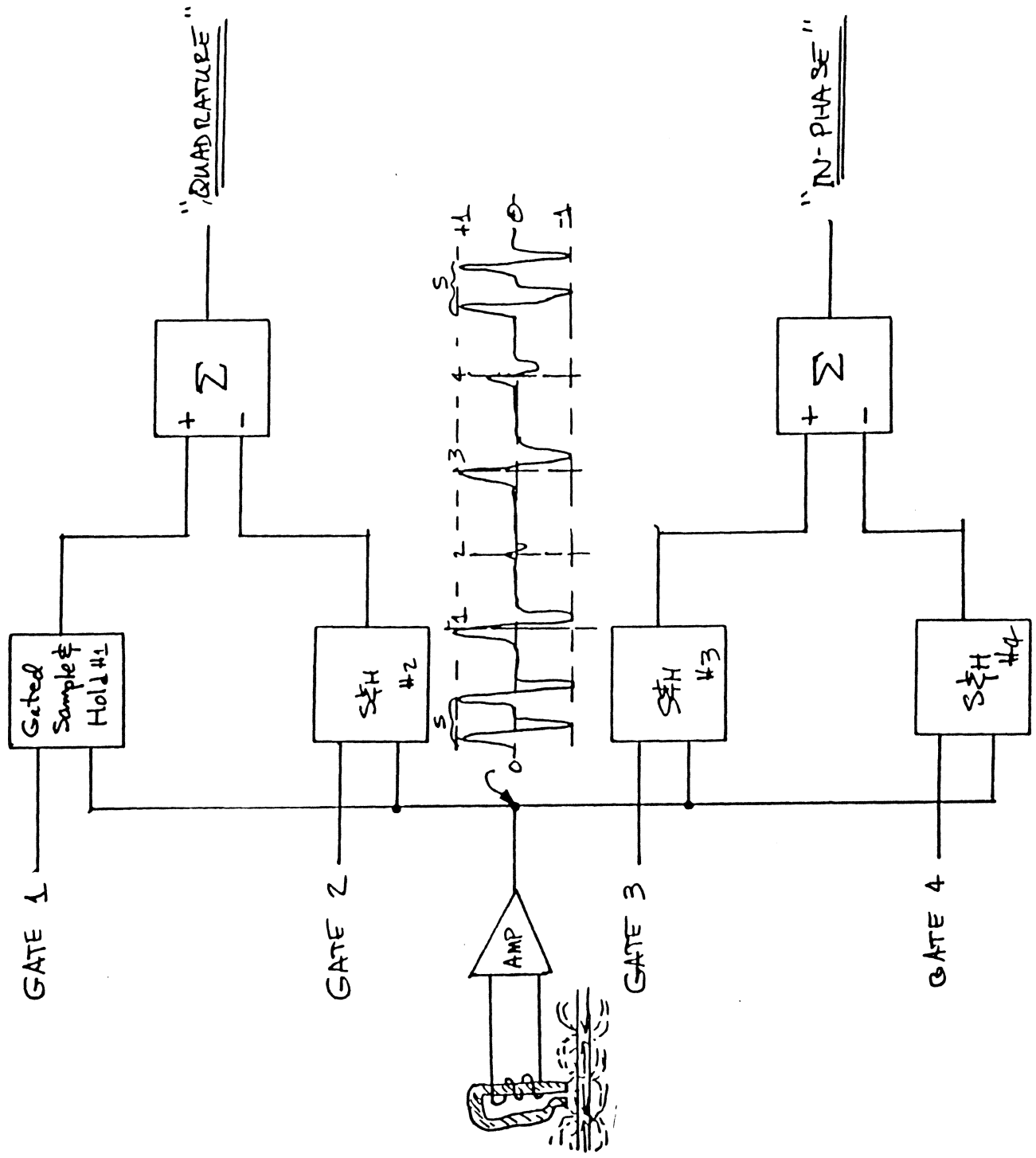
OTC = distance moved off-track to just consume detector window margin at 10^{10} soft error rate

Ed Williams
READ-RITE CORP.



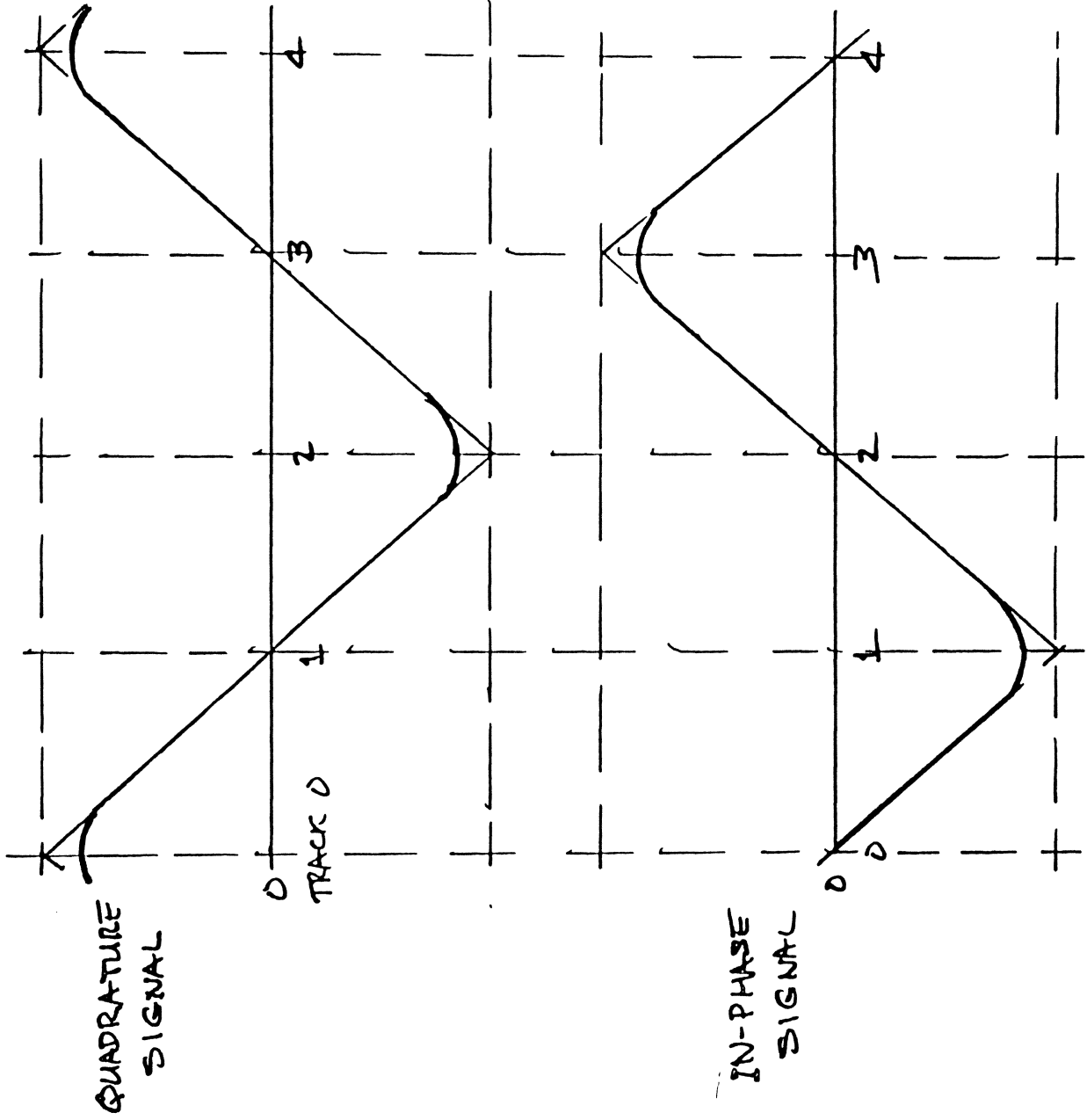


DEMODULATION SCHEME



From F. Sordello

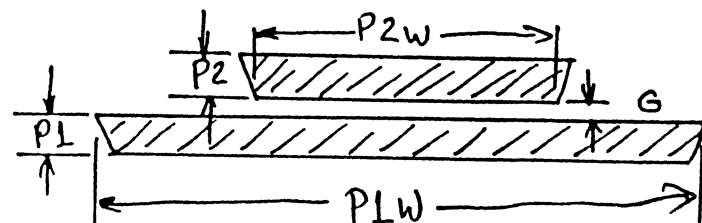
QUADRATURE DETECTION SCHEME



Emulsion
3/8/88
READ-RITE CORP.

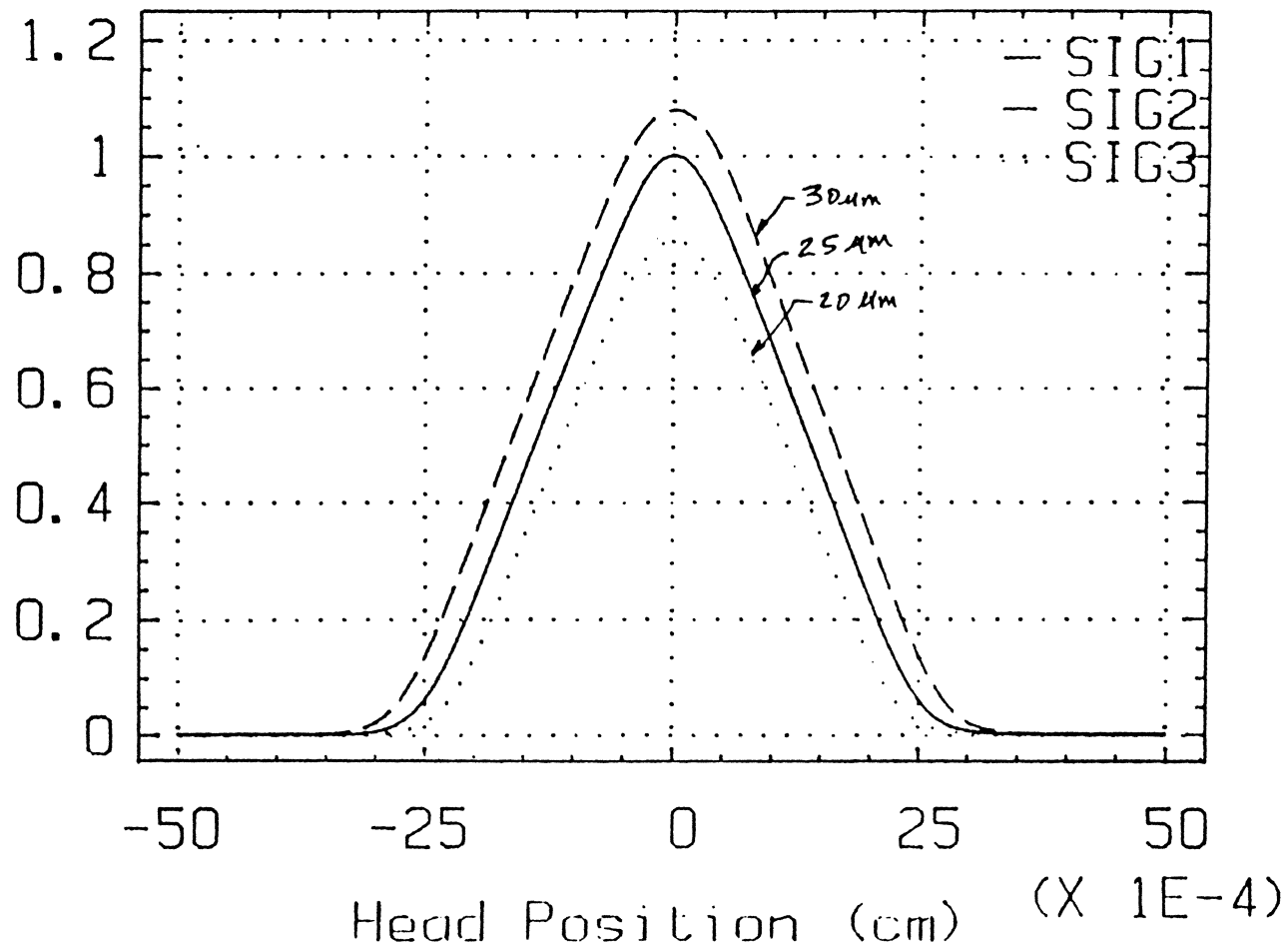
Quadrature Servo Head Design Guides

- * $P2W \cong 2.00/TPI$ for minimum rounding
- * Thin Film Servo Heads: $P1W$ not critical
- * $P1$ and $P2$ chosen for optimum dipulse signal
- * Overwrite: not critical
- * Resolution: not critical



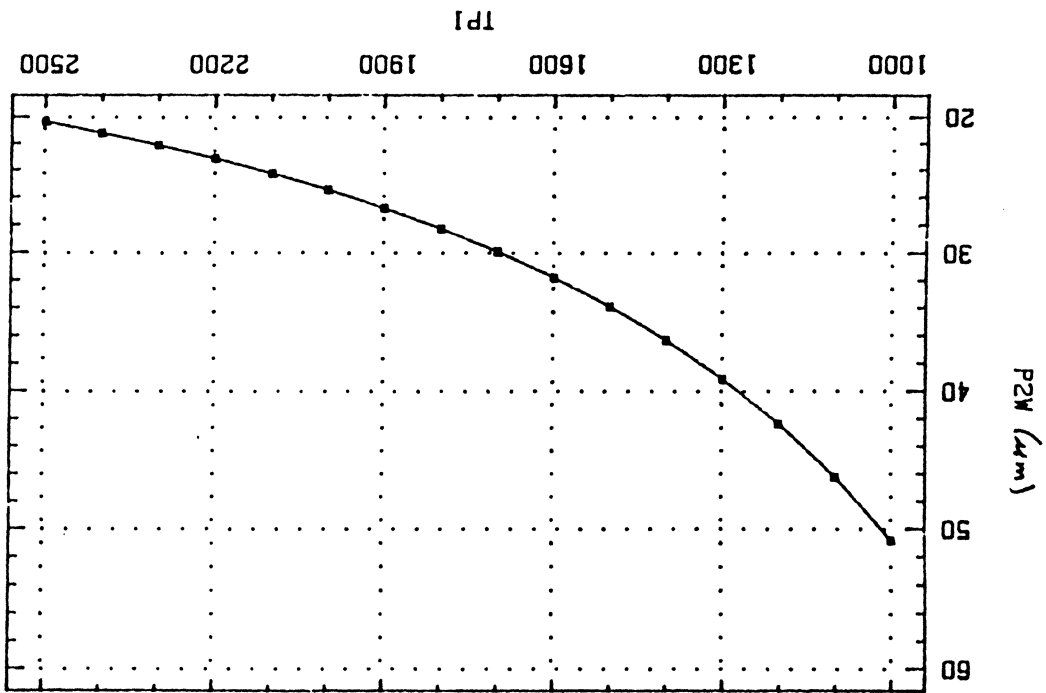
EmWilliam
READ-RITE CORP
3/8/88

Track Profiles for Different Written
Track Widths (Servo Head = 25 microns)



Em Williams
READ-RITE CORP

Smulkin
READ RATE CORR.
3/8/88



Plot of P2W vs TP1

THE SERVO CHANNEL

R. K. OSWALD
898 JANSEN AVE.
SAN JOSE, CA 95125
408-295 0094

PART I

A) THE TRACK FOLLOWING CONTROLLER

THE PRIMARY OBJECTIVE OF THE TRACK FOLLOWING CONTROLLER IS TO MAINTAIN THE RECORDING HEAD'S LOCATION PRECISELY ABOVE THE DESIRED RECORDING TRACK ON THE DISK. MANY OF THE EFFECTS THAT CAUSE DEVIATIONS FROM THIS DESIRED POSITIONING RELATIONSHIP HAVE BEEN PREVIOUSLY DISCUSSED. NOW I WOULD LIKE TO EXAMINE IN SOMEWHAT MORE ANALYTICAL DETAIL THE CONTROL SYSTEM THAT DOES THIS JOB. IT IS DESCRIBED BY THE FOLLOWING BLOCK DIAGRAM.

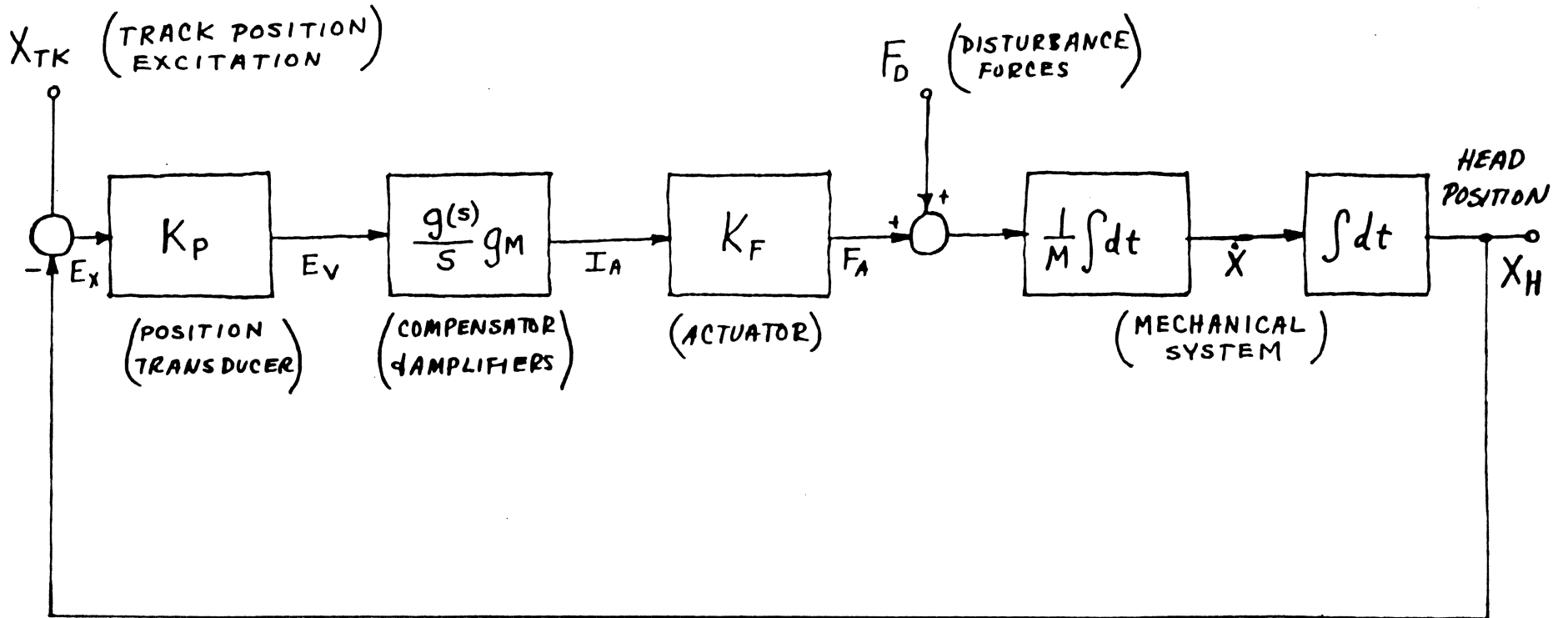
ONCE THE RECORDING HEAD IS LOCATED AT THE CENTER OF THE DESIRED TRACK (BY THE ACCESS CONTROLLER TO BE DESCRIBED LATER), THERE ARE TWO MAJOR SOURCES OF DISTURBANCE THAT CAUSE MISPOSITION ERROR: TRACK POSITION EXCITATION AND FORCE DISTURBANCES.

- TRACK POSITION EXCITATION CONSISTS OF:

1. REPEATABLE AND NON-REPEATABLE SPINDLE BEARING RUNOUT
2. DISK CENTERING ERROR (IN REMOVABLE BUT ALSO NON-REMOVABLE DISK DRIVES)
3. STATIC AND DYNAMIC DISK DEFLECTIONS
4. SERVO WRITER AND MEDIA CAUSED RECORDING TRACK POSITION NON-CONCENTRICITY ERROR
5. ELECTRO-MECHANICAL NOISE IN THE POSITION TRANSDUCER

- MECHANICAL DISTURBANCE FORCE SOURCES INCLUDE:

1. DISK AIR FLOW WINDAGE ON THE CARRIAGE STRUCTURE
2. FLEX CIRCUIT BENDING FORCE BIAS
3. CARRIAGE BEARING "FRICTION" AND PRELOAD
4. HOST ENCLOSURE MOTION, VIBRATION, AND SHOCK
5. GRAVITY (IN LINEAR AND UNBALANCED ROTARYS)
6. RETRACT AND PARK MECHANISMS
7. ACTUATOR MAGNETIC BIAS



TRACK FOLLOWING SERVO

CHARACTERIZATION OF TRANSFER FUNCTIONS FOR THE "FIXED" BLOCKS OF THE TRACK FOLLOWING SYSTEM

1) THE POSITION TRANSDUCER USED IN DISK DRIVES CAN HAVE SEVERAL DIFFERENT IMPLEMENTATIONS SUCH AS AN OPTICAL ENCODER, POTENTIOMETER, LVDT, MAGNETIC ENCODER, LASER INTERFEROMETER, ETC, BUT BY FAR THE MOST USED IN VOLUME PRODUCTION HIGH DENSITY DISK DRIVES IS THE SERVO HEAD-PRE-RECORDED SERVO DISK SURFACE-DEMULATOR ELECTRONICS COMBINATION. THERE ARE MANY KINDS OF CODING AND SEVERAL TYPES OF DEMODULATION USED, BUT ALL RESULT IN A PIECEWISE LINEAR, AT LEAST NOMINALLY TRIANGULAR VOLTAGE VERSUS POSITION SIGNAL. FOR THE OFF TRACK DISTANCES EXPECTED TO BE ENCOUNTERED IN TRACK FOLLOWING, IT CAN BE CHARACTERIZED AS A CONSTANT, K_p , VOLTS PER METER OR $E_v(s) = K_p * E_x(s)$.

2) ACTUATOR MOTORS USED IN DISK DRIVES HAVE PERMANENT MAGNET FIELDS AND THEIR FORCE-CURRENT RELATION HAS THE FORM: $F_A = B * l * I_A(s)$ WHERE B IS THE MAGNETIC FLUX DENSITY IN THE WORKING AIR GAP (IN TESLA), l IS THE ACTIVE LENGTH OF CURRENT CONDUCTOR WHICH IS MUTUALLY ORTHOGONAL TO B AND THE DIRECTION OF MOTION (IN METERS), AND $I_A(s)$ IS THE CURRENT IN THE MOTOR (IN AMPERES). IN A GOOD DESIGN, THE PRODUCT $B * l$ IS A CONSTANT INDEPENDANT OF POSITION, TIME, AND TEMPERATURE (EVEN IF THE INDIVIDUAL COMPONENTS ARE NOT) AND IS USUALLY CALLED K_f , THE FORCE "CONSTANT," WITH UNITS OF NEWTONS PER AMPERE.

THIS IS NOT THE ONLY RELATION TO BE CONSIDERED IN MOTOR OPERATION HOWEVER. MOTION OF THE MOTOR CONDUCTORS IN THE MAGNETIC FIELD PRODUCES A TERMINAL VOLTAGE PROPORTIONAL TO VELOCITY (FARADAY'S LAW) $V_e(s) = B * l * \dot{x}(s) = K_e * \dot{x}(s)$ WITH

UNITS OF VOLTS PER METER PER SECOND. NOTE THAT THE PROPORTIONALITY FACTOR $B \cdot L$ IS THE SAME AS THAT FOR THE FORCE EQUATION; THUS $K_E \equiv K_F$ NUMERICALLY AS WELL AS IN FUNDAMENTAL UNITS WHEN SI ("MKS METRIC") IS USED.

WHEN ESTABLISHING THE CURRENT IN THE ACTUATOR, ITS ELECTRICAL IMPEDANCE R AND L MUST ALSO BE CONSIDERED IN ADDITION TO V_E . THUS COMPLETE RELATIONS FOR THE TERMINAL VOLTAGE V_T , CURRENT I_A , AND FORCE F_A OF THE ACTUATOR CAN BE SUMMARIZED AS:

$$\begin{cases} V_T(t) = K_F \cdot \dot{x}(t) + R \cdot I_A(t) + L \cdot \frac{d}{dt} [I_A(t)] \\ F_A(t) = K_F \cdot I_A(t) \end{cases}$$

SINCE THE COIL RESISTANCE R IS TEMPERATURE SENSITIVE AND VARIES FROM DUTY CYCLE DEPENDANT SELF HEATING AS WELL AS AMBIENT EFFECTS, AND THE INDUCTANCE L INCREASES THE ORDER OF THE SYSTEM, THE ACTUATOR IS ALMOST ALWAYS DRIVEN BY A TRANS CONDUCTANCE AMPLIFIER G_m WHOSE OUTPUT CURRENT I_A IS INDEPENDANT OF OUTPUT VOLTAGE V_T WITHIN A LARGE COMPLIANCE RANGE.

3) FOR PURPOSES OF CONTROL DESIGN THE MECHANICAL STRUCTURE, INCLUDING THE HEADS, CARRIAGE, ACTUATOR ARMATURE, ETC, IS CONSIDERED A RIGID BODY OF MASS M CONSTRAINED TO MOVE ONLY IN THE ACCESS COORDINATE DIRECTION, X . IN SI UNITS THE RELATIONSHIP BETWEEN ACTUATOR FORCE AND HEAD VELOCITY IS THEN GIVEN BY:

$$\dot{x}(t) = \frac{1}{M} \int F_A(t) dt \quad \text{WITH} \begin{cases} \dot{x} \text{ IN METER/SECOND} \\ M \text{ IN KILOGRAMS} \\ F_A \text{ IN NEWTONS} \end{cases}$$

4) NOW THAT ALL THE OTHER BLOCKS ARE DEFINED, THE MOST APPROPRIATE CONTROL STRATEGY AND THUS THE FUNCTIONS TO BE PLACED IN THE COMPENSATOR BLOCK CAN BE CHOSEN

REFERRING TO THE BLOCK DIAGRAM, IF THERE IS ANY STEADY STATE DISTURBANCE FORCE F_D , IT MUST BE OFFSET BY AN EQUAL AND OPPOSITE ACTUATOR FORCE F_A . SINCE IT IS DESIRED THAT E_V BE ZERO AND THE POSITION TRANSDUCER AND ACTUATOR MOTOR ARE ONLY PROPORTIONAL GAINS, IT IS THEREFORE NECESSARY THAT THE COMPENSATOR CONTAIN AT LEAST AN INTEGRATOR.

IN ORDER THAT THE CONVENIENT GRAPHICAL METHODS OF BODE AND NYQUIST MAY BE USED IN THE COMPENSATOR DESIGN, IT IS NECESSARY TO TAKE THE LAPLACE TRANSFORMS OF THE TRANSFER FUNCTION BLOCKS, WHICH IS EASILY DONE BY RECALLING THAT $\mathcal{L}[\text{CONSTANT}] = \text{CONSTANT}$, $\mathcal{L}[\frac{1}{s} f(t)] = s F(s)$, AND $\mathcal{L}[\int f(t) dt] = \frac{1}{s} F(s)$. THUS THE LAPLACE TRANSFORM OF THE FORWARD LOOP TRANSFER FUNCTION AS SO FAR DETERMINED CONSISTS OF:

$$K_P * \frac{1}{s} g(s) G_M * K_F * \frac{1}{MS} * \frac{1}{s}$$

WHERE $g(s)$ IS THE REMAINDER OF THE COMPENSATOR BLOCK (AFTER ACCOUNTING FOR THE INTEGRATOR) YET TO BE DETERMINED AND THE OTHER COMPONENTS ARE AS EARLIER DESCRIBED.

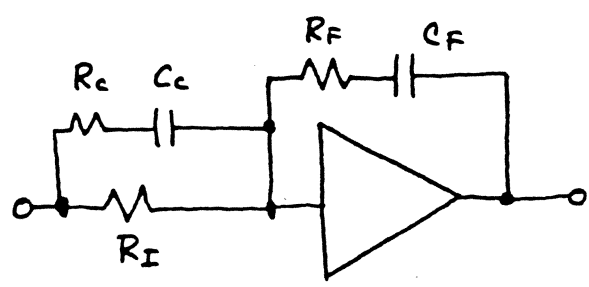
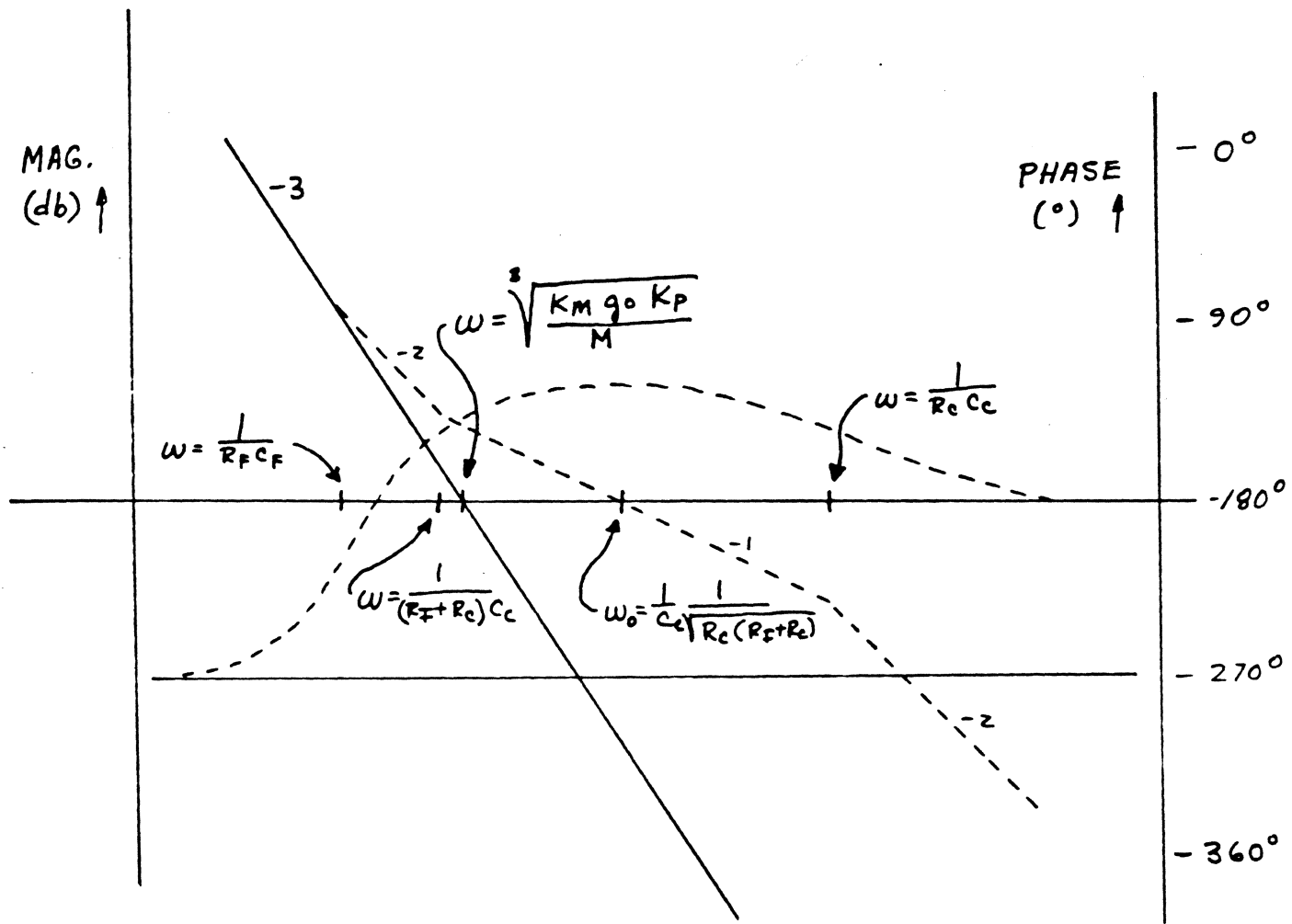
FOR THE SYSTEM TO BE CLOSED LOOP STABLE WITH AN ACCEPTABLE TRANSIENT RESPONSE, A PHASE MARGIN OF AT LEAST 45° TO 55° AND GAIN MARGIN OF 6 TO 10 db IS NECESSARY. SINCE THERE ARE THREE INTEGRATIONS IN THE LOOP, ITS LOW FREQUENCY RESPONSE STARTS OUT AT A LARGE GAIN AND -270° PHASE. BUT IT IS DESIRED THAT NEAR UNITY GAIN THE PHASE SHOULD BE -125° TO -135° AS SHOWN IN THE SKETCHES OF THE BODE AND NYQUIST DIAGRAMS. IF THE UNITY GAIN FREQUENCY IS SET AT f_0 , THEN ACHIEVING THIS SHAPE REQUIRES THE COMPENSATOR $g(s)$ TO PROVIDE TWO ZEROS AT ABOUT $\frac{f_0}{5\sqrt{12}}$ AND $f_0/\sqrt{12}$ AND A POLE AT $\sqrt{12} * f_0$.

THE CHOICE OF UNITY GAIN FREQUENCY f_0 MUST NOW BE MADE. AN IMPORTANT CONSIDERATION IS THE MECHANICAL

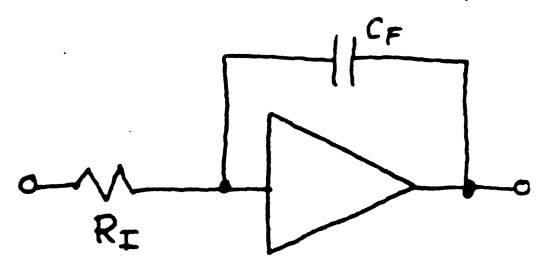
COMPENSATOR DESIGN ON THE BODE PLOT

SOLID = UNCOMPENSATED

DASHED = COMPENSATED

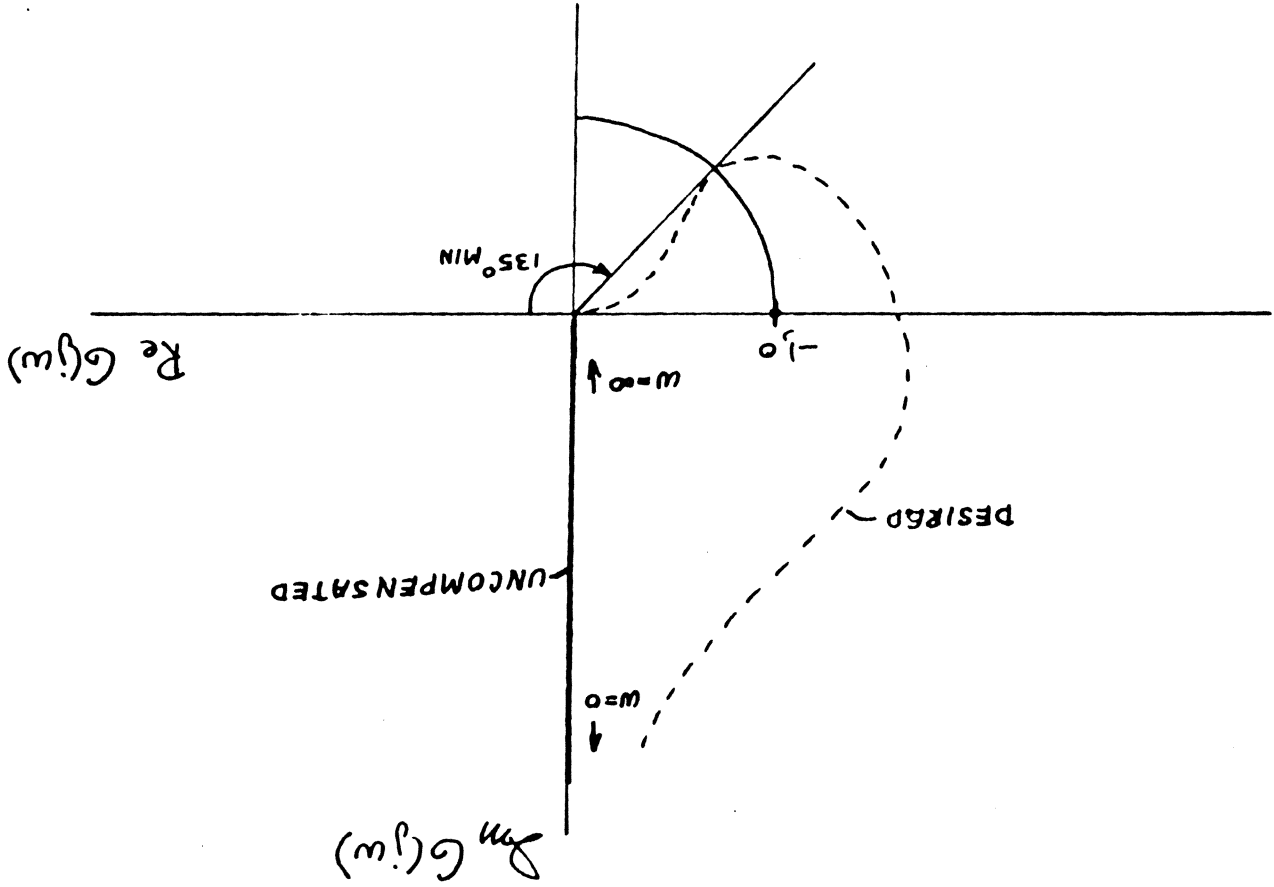


COMPENSATOR



UNCOMPENSATED INTEGRATOR

NYQUIST PLOT



MODES OF VIBRATION IN THE CARRIAGE AND RECORDING HEAD SUSPENSION STRUCTURE AT HIGH (OR NOT SO HIGH!) FREQUENCIES THAT ARE DEPARTURES THE RIGID BODY MODEL ASSUMED FOR STRUCTURE. THEY PRODUCE RESPONSE PEAKS AND PHASE SHIFTS IN THE OPEN LOOP TRANSFER FUNCTION AS SHOWN ON THE NYQUIST DIAGRAM. BECAUSE OF THESE DESTABILIZING EFFECTS A PRACTICALLY ACHIEVABLE VALUE FOR DISK DRIVES IS 450 Hz, WHICH REQUIRES ZEROS AT 26 Hz AND 130 Hz AND A POLE AT 1560 Hz. A NUMERICAL EVALUATION OF THE OPEN LOOP TRANSFER FUNCTION $G(s)$ FOR THESE VALUES INDICATES THAT:

$$G(s) = \frac{377 \times 10^6 \left(\frac{s}{2\pi \times 26} + 1 \right) \left(\frac{s}{2\pi \times 130} + 1 \right)}{s^3 \left(\frac{s}{2\pi \times 1560} + 1 \right)}$$

IT HAS A PHASE MARGIN OF 55° AND AT 60 Hz A MAGNITUDE OF $16.25 \angle -18^\circ$. THUS THE MAGNITUDE OF THE CLOSED LOOP TRANSFER FUNCTION $T(s) = \frac{G(s)}{1+G(s)}$ IS $1.0655 \angle 0^\circ$ WHEN EVALUATED AT 60 Hz, AND THE MAGNITUDE OF THE ERROR VOLTAGE $E_v(s)$ IS $-0.0655 \angle 0^\circ$ FOR AN INPUT OF $1 \angle 0^\circ$ OR AN ERROR OF 6.5% OF THE TRACK DISPLACEMENT WHEN FOLLOWING 60 Hz SINUSOIDAL RUN OUT.

THE TRANSIENT RESPONSE OF THE TRACK FOLLOWING CONTROL SYSTEM TO TRACK POSITION EXCITATION IS ALSO IMPORTANT, SINCE THE TRACK ACCESS SYSTEM CONTROLLER MAY NOT BE PERFECT AND LEAVE A RESIDUAL POSITION ERROR AT THE END OF A SEEK MOTION. WHEN THE TRACK FOLLOWING CONTROLLER IS THEN ENABLED AT THE END OF THE SEEK, IT SEES A STEP OF TRACK DISPLACEMENT INPUT. SINCE THIS TRACK FOLLOWING CONTROLLER IS A LINEAR SYSTEM ITS RESPONSE CAN BE CALCULATED WITH THE INVERSE LAPLACE TRANSFORMATION:

$$X_H(t) = \mathcal{L}^{-1} \left[\mathcal{L} \{u(t)\} * T(s) \right] = \mathcal{L}^{-1} \left[\frac{1}{s} * T(s) \right].$$

PROBABLY OF MORE INTEREST THAN THE ANALYTIC TIME FUNCTION $X_H(t)$ HOWEVER IS ITS GRAPH AND THIS IS SHOWN ON THE NEXT PAGE WHERE THE INPUT WAS A UNIT STEP AND THE CONTROLLER COEFFICIENTS HAVE THE VALUES CALCULATED PREVIOUSLY.

NOTICE THAT WHILE THE RESPONSE IS WELL DAMPED, BECAUSE THE SYSTEM IS OF FOURTH ORDER, THE PEAK OVERSHOOT IS ABOUT 28% AND SETTLING TIME TO 5% IS ABOUT 2.3MS EVEN THOUGH THE OPEN LOOP UNITY GAIN BANDWIDTH IS 450 Hz AND PHASE MARGIN IS 55°.

THE POSITION RESPONSE TO DISTURBANCE FORCES ACTING UPON THE CARRIAGE IS IMPORTANT TO CONSIDER BECAUSE, ESPECIALLY IN SMALL DISK DRIVES, THERE ARE MANY BOTH EXTERNAL AND INTERNAL DISTURBANCES, FOR EXAMPLE HOST SYSTEM FRAME SHOCK AND VIBRATION AND INTERNAL FLEX CIRCUIT BENDING AND AIR FLOW BIAS FORCES.

THE TRANSFER FUNCTION OF HEAD DISPLACEMENT AS A FUNCTION OF DISTURBANCE FORCE INPUT FOR THE EXAMPLE TRACK FOLLOWING CONTROL SYSTEM IS:

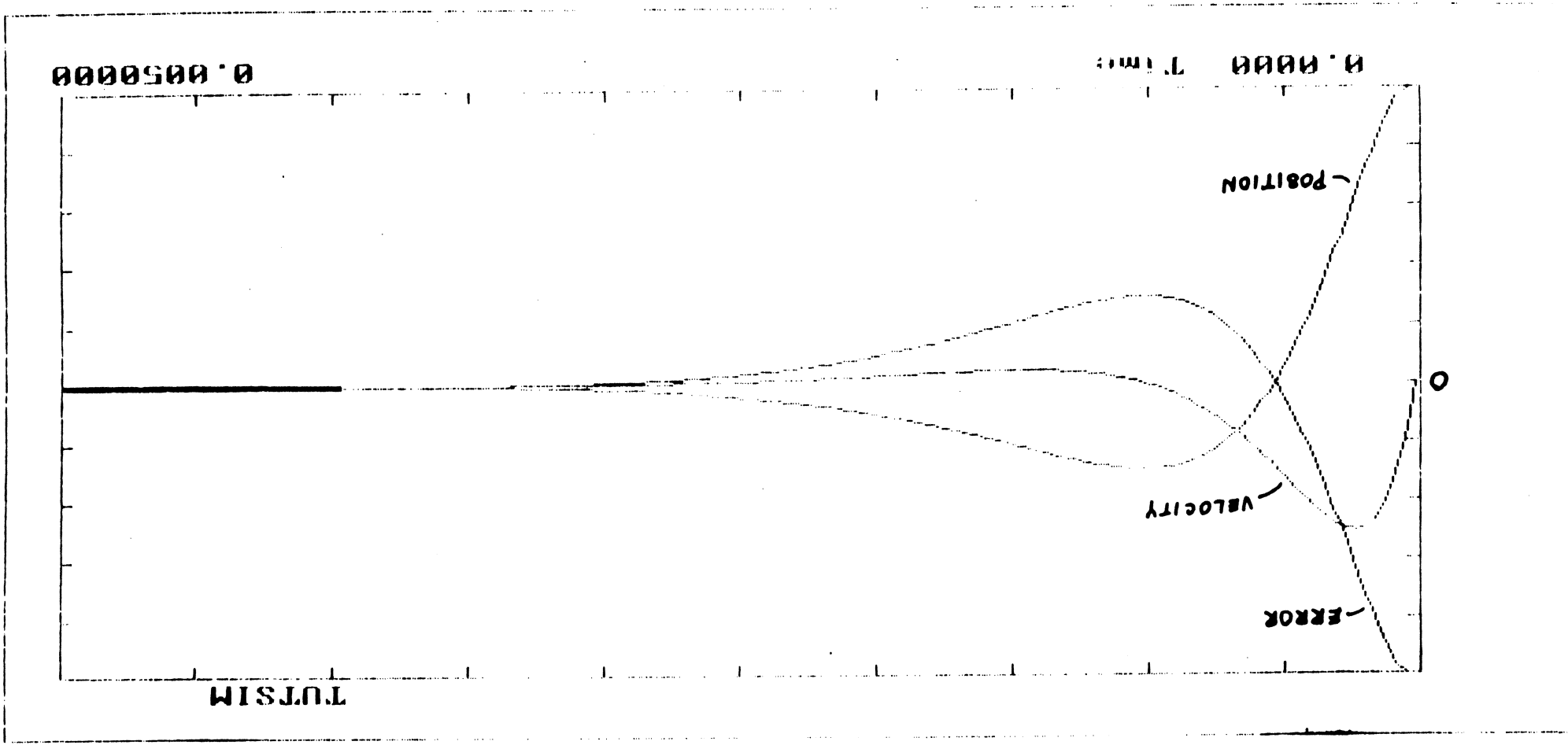
$$\frac{X_H}{F_D} = \frac{\frac{1}{MS^2}}{1 + K_P * \frac{g(s)}{s} * g_M * K_F * \frac{1}{MS^2}}$$

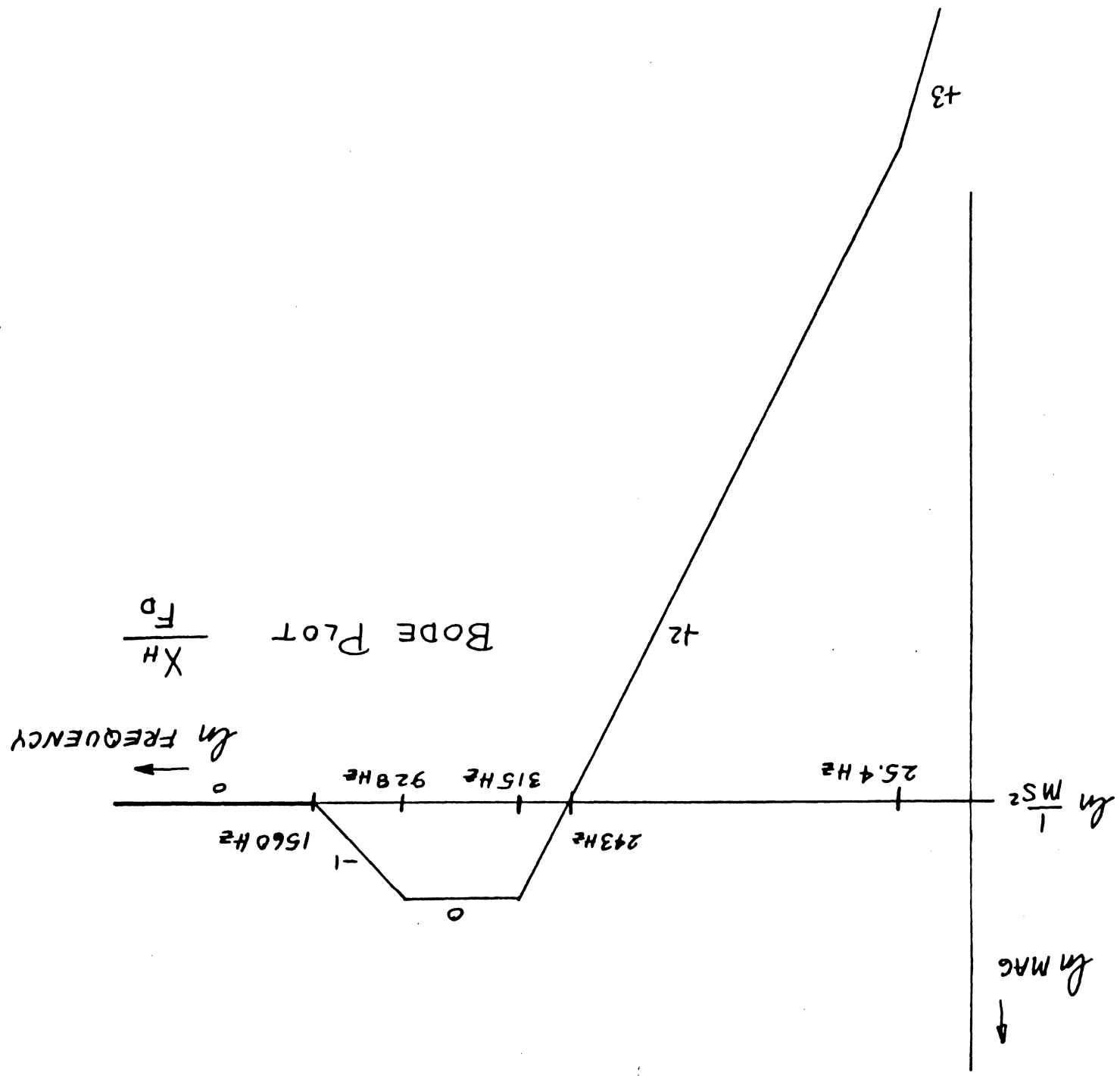
AND $g(s)$ IS THE COMPENSATOR DETERMINED PREVIOUSLY.

$$\therefore \frac{X_H}{F_D} = \frac{\frac{1}{MS^2}}{1 + \frac{377 * 10^6 \left(\frac{s}{2\pi * 26} + 1 \right) \left(\frac{s}{2\pi * 130} + 1 \right)}{s^3 \left(\frac{s}{2\pi * 1560} + 1 \right)}} \quad , \text{ AND BY FACTORING THE CHARACTERISTIC EQUATION:}$$

$$\frac{X_H}{F_D} = \frac{s^3 \left(\frac{s}{2\pi * 1560} + 1 \right)}{\left(\frac{s}{2\pi * 25.4} + 1 \right) \left(\left(\frac{s}{2\pi * 315} \right)^2 + \frac{2 * 962}{2\pi * 315} s + 1 \right) \left(\frac{s}{2\pi * 928} + 1 \right)} * \frac{1}{MS^2}$$

THE BODE PLOT FOR THE PORTION OF THIS TRANSFER FUNCTION REPRESENTING THE CLOSED LOOP TRACK FOLLOWING SYSTEM'S MODIFICATION OF THE OPEN LOOP FREE INERTIAL BODY RESPONSE OF THE SYSTEM: $\frac{1}{MS^2}$, IS SHOWN ON THE NEXT PAGE.





NOTICE THAT WHILE THE CONTROL SYSTEM MAKES THE APPARENT MASS MUCH LARGER AT LOW FREQUENCIES, BETWEEN 243 AND 1560 Hz THE APPARENT MASS IS SMALLER, IN FACT AT ABOUT 540 Hz IT IS 68% SMALLER. THUS THE NEED FOR A PASSIVE ISOLATION SYSTEM BETWEEN THE DISK DRIVE HEAD-DISK ASSEMBLY AND THE MOUNTING FRAME THAT CAN ATTENUATE EXTERNAL SHOCK AND VIBRATION COMPONENTS IN THIS FREQUENCY RANGE IS VERY EVIDENT.

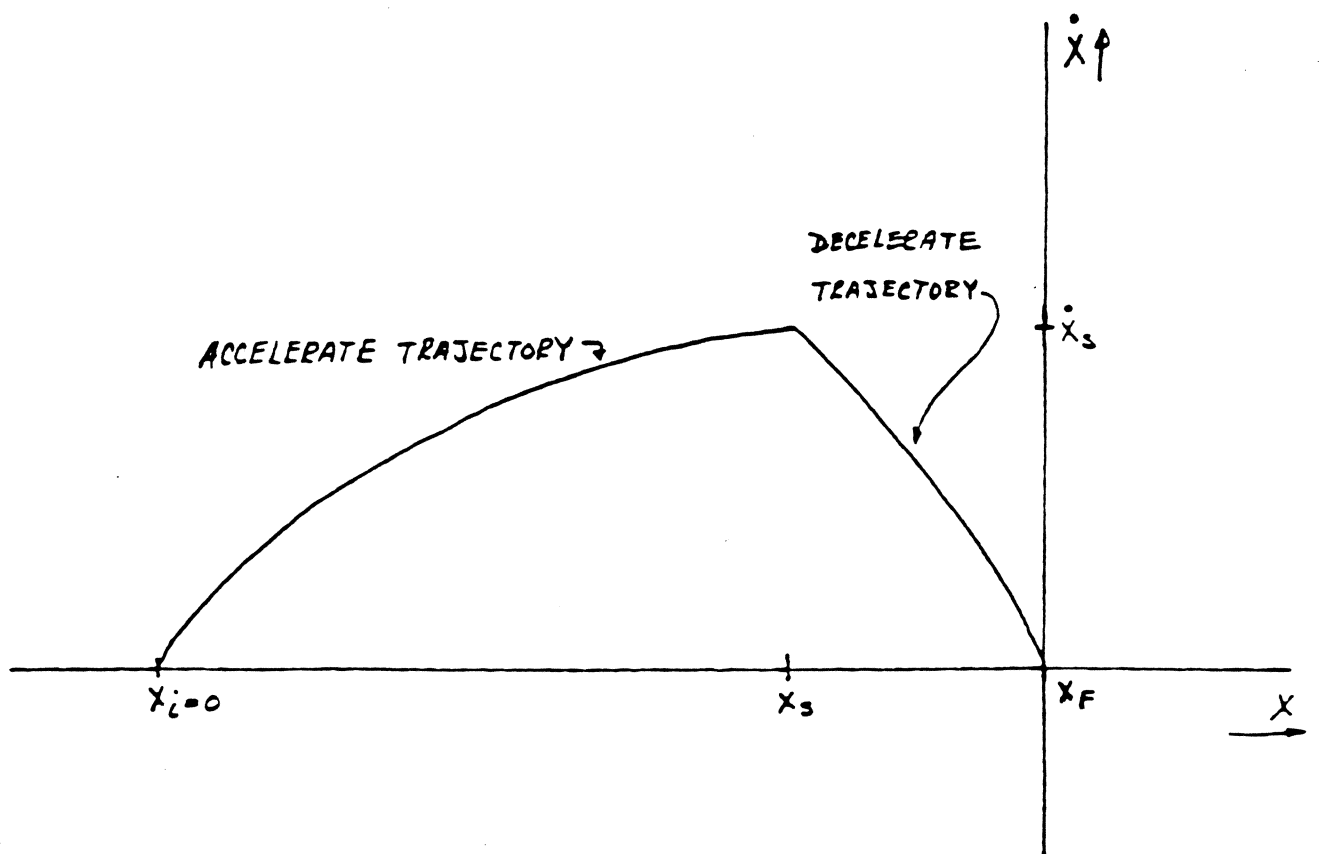
B) THE TRACK ACCESS CONTROLLER

THE OBJECTIVE OF THE ACCESS CONTROL SYSTEM IS TO MOVE THE ACTUATOR FROM THE INITIAL TRACK POSITION X_i TO THE FINAL TRACK POSITION X_f IN MINIMUM TIME AND WITH NO RESIDUAL SETTLING TRANSIENT (I.E. WITH $\dot{X}_f = \ddot{X}_f = 0$). SIMPLE REASONING SHOWS THAT A NECESSARY CONDITION FOR THE CONTROL STRATEGY TO BE MINIMUM TIME AND THUS TIME OPTIMAL IS THAT IT BE AN EXTREMAL CONTROL WHICH APPLIES THE MAXIMUM AVAILABLE POWER SUPPLY VOLTAGE TO THE ACTUATOR THROUGHOUT THE MOTION TIME. IF A SMALLER VOLTAGE WERE TO BE APPLIED THEN THE INCREMENTAL TIME TO MOVE COULD CONTINUE TO BE REDUCED BY INCREASING THE APPLIED VOLTAGE UNTIL THE MAXIMUM VOLTAGE IS USED. THUS ANY TIME OPTIMAL CONTROL MUST ALSO BE AN EXTREMAL CONTROL BUT NOT ALL EXTREMAL CONTROLS ARE OPTIMAL. WITH EXTREMAL CONTROL THE ONLY CHOICE TO BE MADE BY THE CONTROLLER IS THE POINTS AT WHICH TO REVERSE THE APPLIED VOLTAGE FROM ACCELERATE TO DECELERATE POLARITY.

IT CAN BE SHOWN THAT FOR AN N^{th} ORDER SYSTEM THE TIME OPTIMAL CONTROL HAS AT MOST $N-1$ POLARITY REVERSALS. THUS THE SIMPLEST CONTROL CASE WILL BE FOR A SECOND ORDER SYSTEM WHICH REQUIRES ONLY $N-1 = 2-1 = 1$ POLARITY REVERSAL. THE ACTUATOR AND MECHANICAL SYSTEM DESCRIBED IN THE PREVIOUS PART FOR TRACK FOLLOWING IS SECOND ORDER IF ACTUATOR COIL INDUCTANCE IS NEGLECTED, BUT

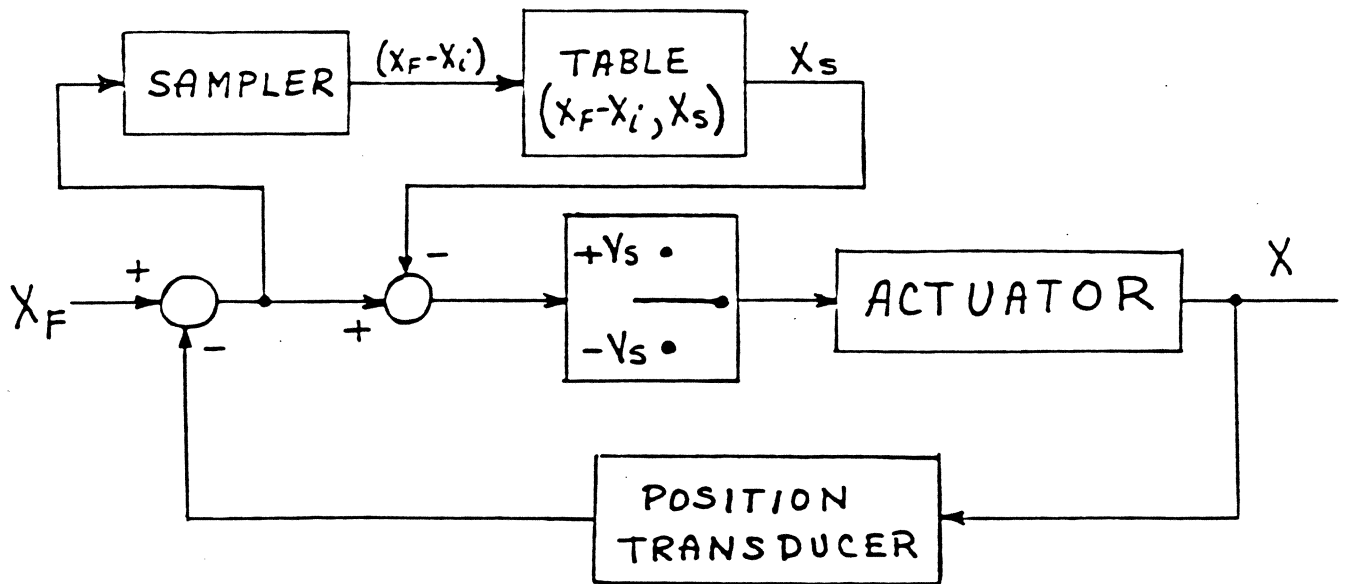
GENERATED BACK VOLTAGE IS STILL INCLUDED. ITS OPERATION CAN BE DESCRIBED BY A STATE SPACE WHICH IS A PHASE PLANE WITH COORDINATES OF VELOCITY AND POSITION, AS SHOWN BELOW.

OPERATION AS VIEWED ON THE PHASE PLANE



THE SIMPLEST WAY TO DEFINE THE POLARITY OR SWITCH POINT X_s IS IN TERMS OF ITS POSITION COORDINATE, $(X_s - X_F)$ SINCE IN THAT CASE ONLY A POSITION TRANSDUCER WHICH IS ALREADY PRESENT FOR TRACK FOLLOWING CONTROL WILL BE REQUIRED. THE ADDITIONAL HARDWARE NEEDED FOR CONTROLLER IMPLEMENTATION CONSISTS OF A LOOK UP TABLE FOR THE FUNCTION $X_s = f(X_F - X_i)$, A COMPARATOR, AND A POWER DRIVER THAT OPERATES AS AN IDEAL RELAY. IT IS SHOWN BELOW.

TIME OPTIMAL CONTROLLER FOR A SECOND ORDER, CONSTANT COEFFICIENT SYSTEM



THE SYSTEM DIFFERENTIAL EQUATION FOR THIS CASE OF EXTREMAL CONTROL, NEGLIGIBLE INDUCTANCE, AND NO FRICTION OR MECHANICAL BIAS FORCE DERIVES FROM:

$$\left. \begin{array}{l} 1. M \ddot{X} = F \\ 2. F = KI \\ 3. I = \frac{\pm V_s - K\dot{X}}{R} \end{array} \right\}$$

WHERE: F = FORCE IN NEWTONS
 M = MASS IN KILOGRAMS
 X = DISPLACEMENT IN METERS
 V_s = NET SUPPLY VOLTAGE
 K = ACTUATOR FACTOR, $\frac{\text{NEWTON}}{\text{AMP}}$

$$\therefore \ddot{X} + \frac{K^2}{MR} \dot{X} = \pm \frac{K}{MR} V_s \quad [1]$$

AND BY DEFINING $\tau = \frac{MR}{K^2}$ AND $A = \frac{KV_s}{MR}$,
 THE SYSTEM EQUATION BECOMES:

$$\ddot{X} + \frac{1}{\tau} \dot{X} = \pm A \quad [2]$$

SOLVING FOR ACCELERATE WITH THE $+$ SIGN FOR $X_i < X < X_s$

$$(X_s - X_i) = -\tau \dot{X}_s - A \tau^2 \ln \left(1 - \frac{\dot{X}_s}{A\tau} \right) \quad [3]$$

SOLVING FOR DECELERATE WITH THE $-$ SIGN FOR $X_s < X < X_f$:

$$(X_f - X_s) = \tau \dot{X}_s - A \tau^2 \ln \left(1 + \frac{\dot{X}_s}{A\tau} \right) \quad [4]$$

SIMULTANEOUS EQUATIONS [3] AND [4] ARE TRANSCENDENTAL BECAUSE OF THE $\ln(\cdot)$ FUNCTION, BUT HAVE ONLY TWO UNKNOWN, X_s AND \dot{X}_s SO THEY MAY BE NUMERICALLY SOLVED TO OBTAIN THE TABLE OF VALUES $(X_F - X_i), (X_s)$.

A BETTER UNDERSTANDING OF THE RELATIONSHIP OF THE TRAJECTORIES TO ACTUATOR PARAMETERS IS OBTAINED IF THE POWER SERIES EXPANSION OF THE $\ln(\cdot)$ IS USED.

$$\ln(1-z) = z - \frac{1}{2}z^2 + \frac{1}{3}z^3 - \frac{1}{4}z^4 - \dots \quad -1 \leq z \leq +1$$

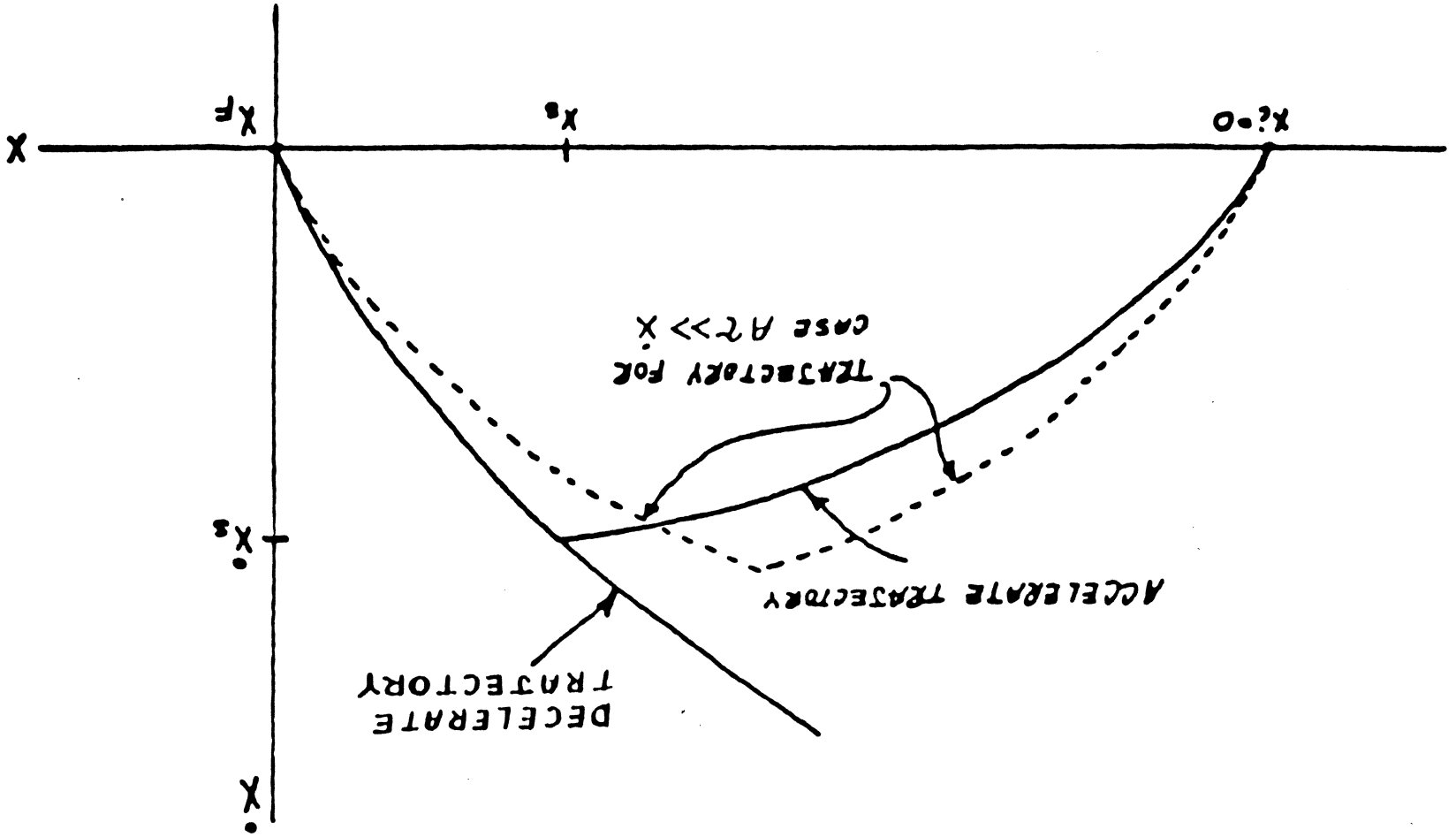
THE EQUATIONS [3] AND [4] BECOME:

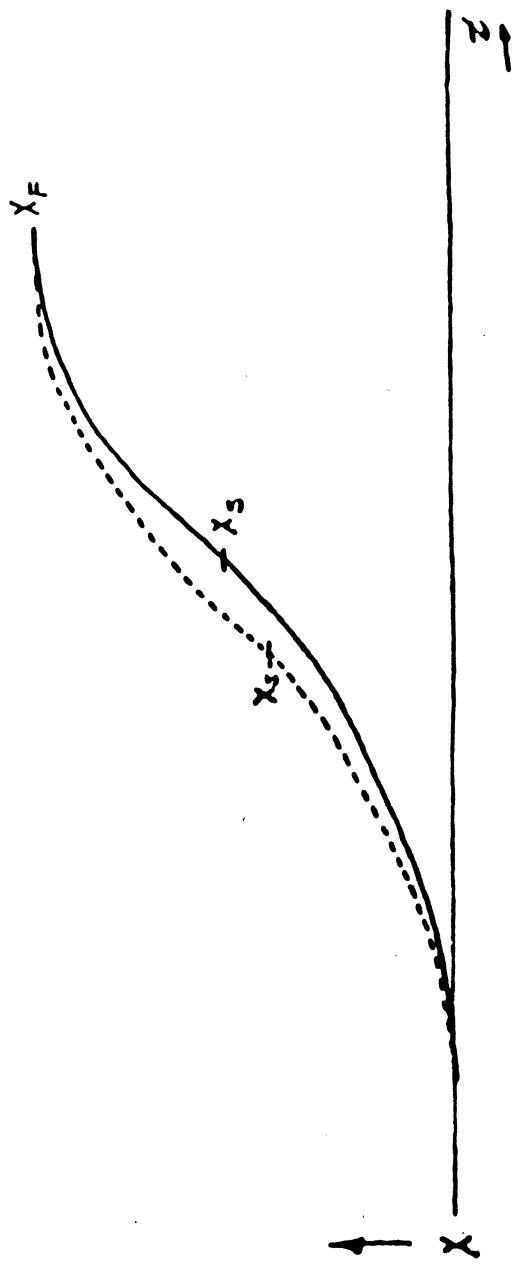
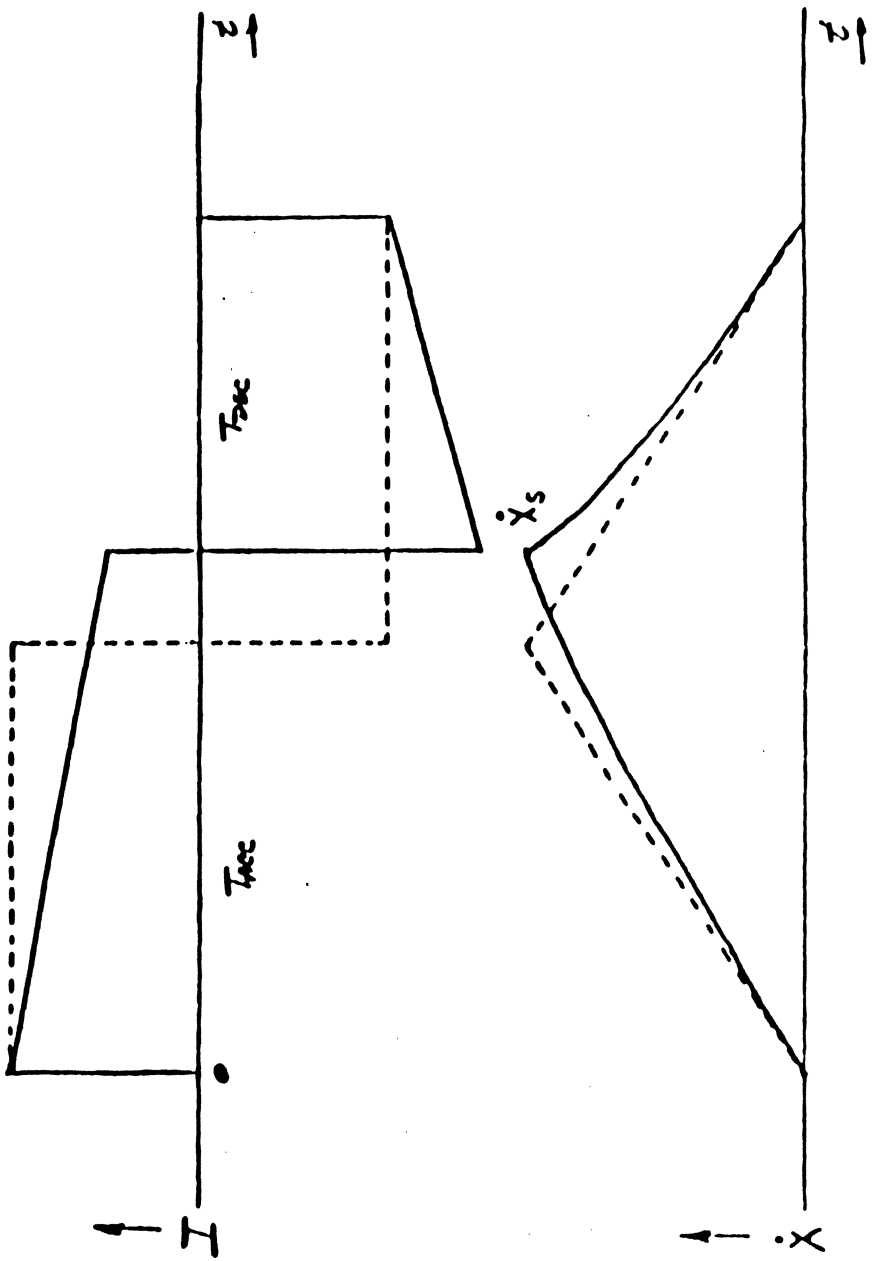
$$(X_s - X_i) = \frac{\dot{X}_s^2}{2A} + \left(\frac{\dot{X}_s^3}{3A^2\tau} + \frac{\dot{X}_s^4}{4A^3\tau^2} + \frac{\dot{X}_s^5}{5A^4\tau^3} - \dots \right)$$

$$(X_F - X_s) = \frac{\dot{X}_s^2}{2A} - \left(\frac{\dot{X}_s^3}{3A^2\tau} - \frac{\dot{X}_s^4}{4A^3\tau^2} + \frac{\dot{X}_s^5}{5A^4\tau^3} - \dots \right)$$

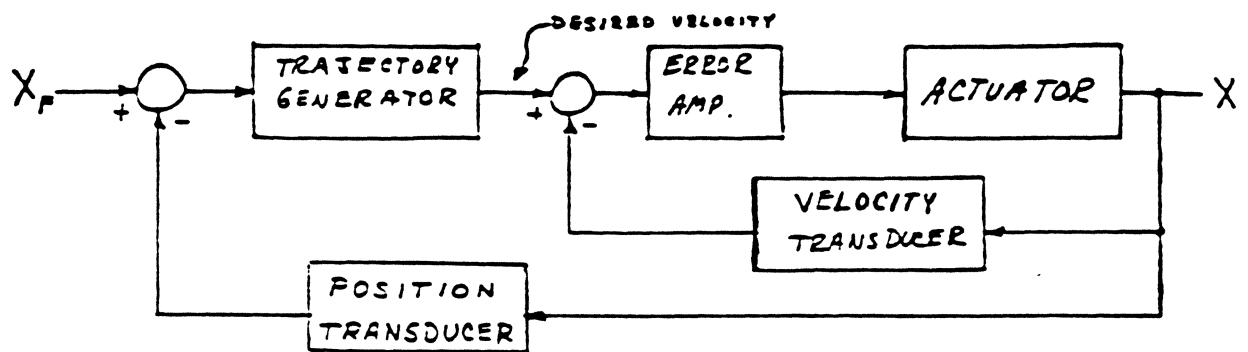
THE PRODUCT $A\tau$ IN FUNDAMENTAL UNITS IS $\frac{V_s}{K}$ (THE POWER SUPPLY LIMITING VELOCITY), AND IF $A\tau \gg \dot{X}$ THEN ONLY THE FIRST TERMS ARE OF SIGNIFICANCE AND IN THE LIMIT:

$$X = \frac{\dot{X}^2}{2A} \quad \text{OR} \quad \dot{X} = 2A\sqrt{X}, \text{ THE "SQUARE ROOT" TRAJECTORY}$$

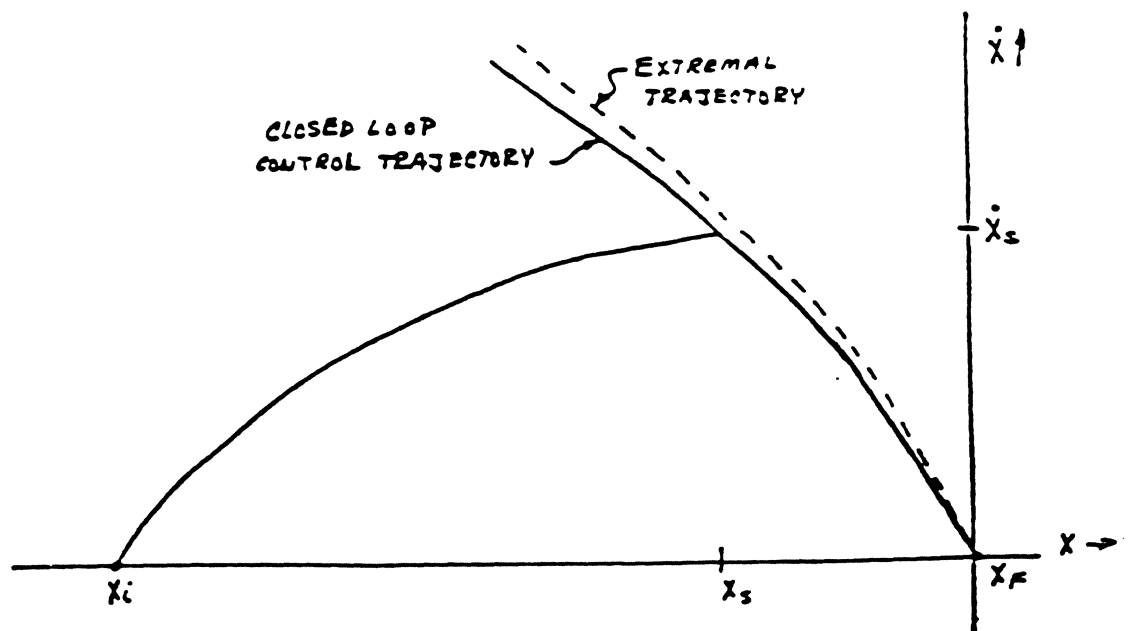




THE SWITCH POINT TABLE FOR EXTREMAL CONTROL IS UNIQUE FOR EACH SET OF SYSTEM PARAMETERS. IN PRACTICE, PARAMETER TOLERANCES AND VARIATIONS ARE LARGE (ESPECIALLY K AND R), PURE EXTREMAL CONTROL DOES NOT GIVE SATISFACTORY ARRIVAL ACCURACY, AND CLOSED LOOP DECELERATE CONTROL WITH A VELOCITY TRANSDUCER IS USED.



CLOSED LOOP DECELERATE TRAJECTORY CONTROL



OPERATION AS VIEWED ON THE PHASE PLANE

THUS FAR THE ASSUMPTION HAS BEEN MADE THAT THE ACTUATOR INDUCTANCE IS NEGLIGIBLE AND CAN BE IGNORED. IN PRACTICE, INDUCTANCE HAS SIGNIFICANT EFFECT ON THE TRANSIENT RESPONSE, ESPECIALLY IN FAST ACCESS TIME SYSTEMS. WITH INDUCTANCE INCLUDED BUT FRICTION AND MECHANICAL BIAS FORCE IGNORED THE SYSTEM DIFFERENTIAL EQUATION DERIVES FROM:

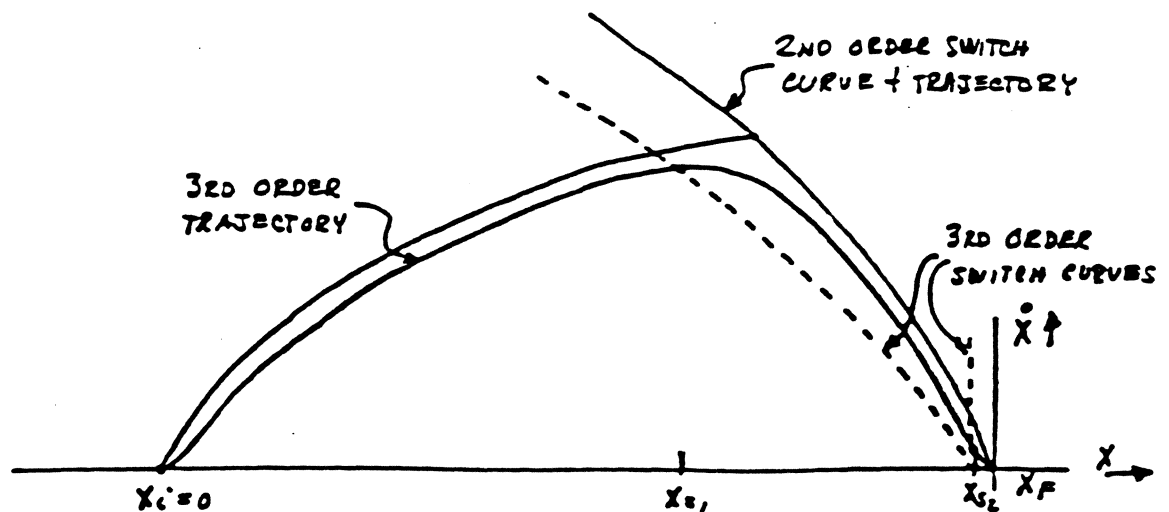
$$1. M\ddot{x} = F \quad 2. F = KI \quad 3. L \frac{dI}{dt} + RI + K\dot{x} = \pm V_s$$

$$\therefore \ddot{\ddot{x}} + \frac{R}{L} \ddot{x} + \frac{K^2}{ML} \dot{x} = \pm \frac{K}{ML} V_s$$

$$\text{LET: } \frac{L}{R} = \tau_e, \quad \frac{MR}{K^2} = \tau, \quad \frac{KV_s}{MR} = A \quad \text{THEN:}$$

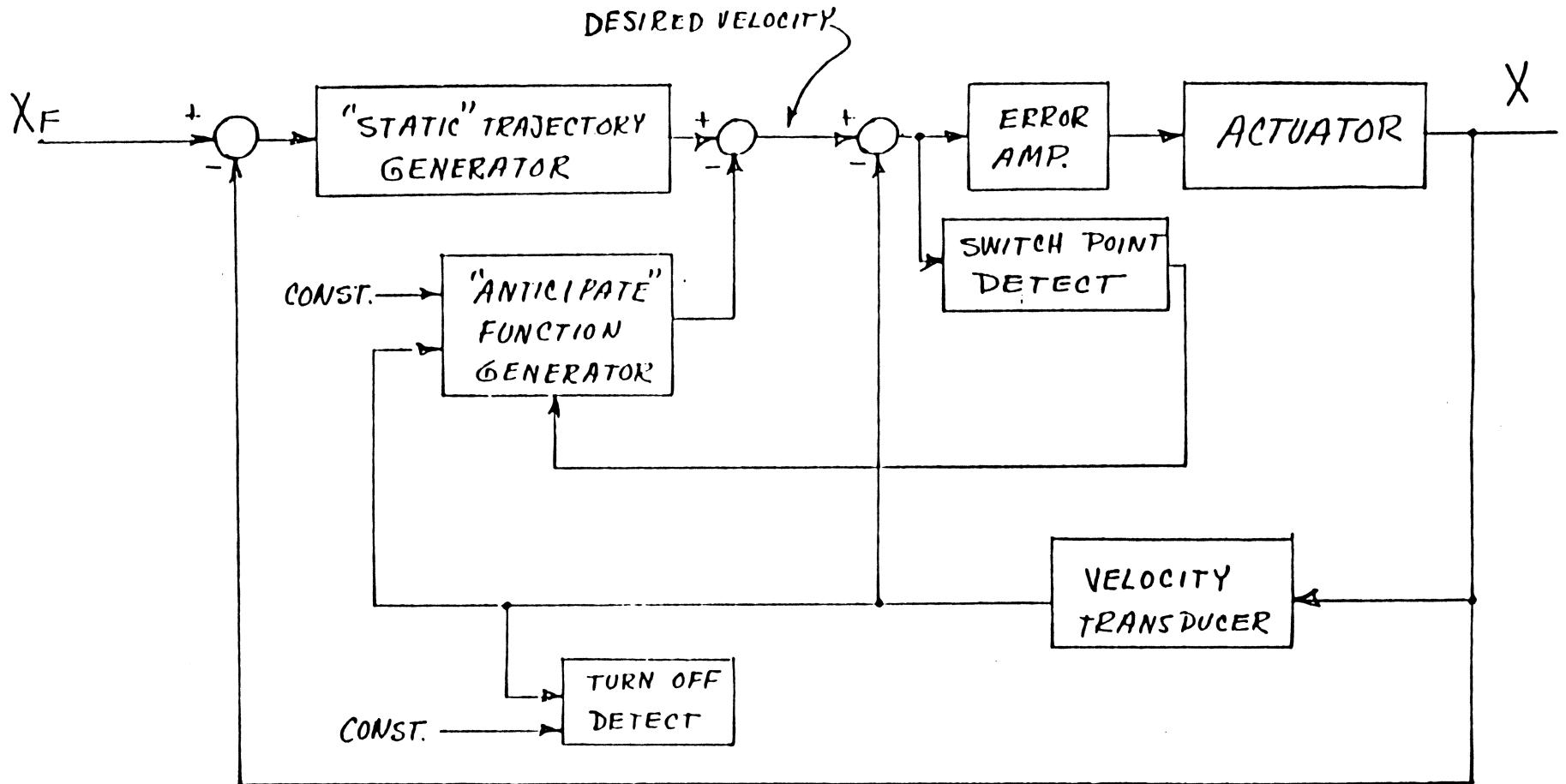
$$\ddot{\ddot{x}} + \frac{1}{\tau_e} \ddot{x} + \frac{1}{\tau_e \tau} \dot{x} = \pm \frac{1}{\tau_e} A$$

AN EXAMPLE PHASE PLANE TRAJECTORY FOR A SYSTEM WITH AND WITHOUT INDUCTANCE IS SHOWN BELOW.



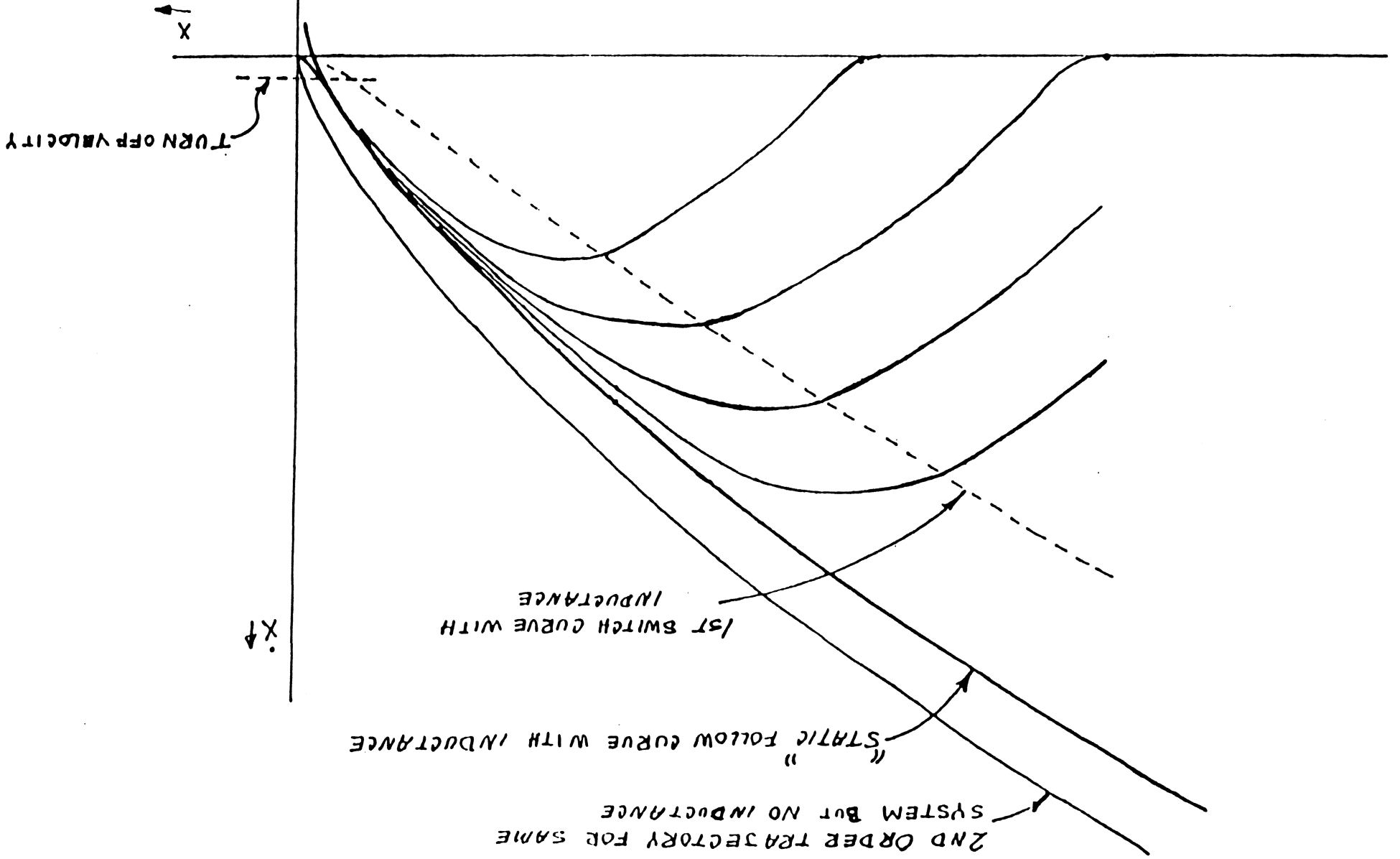
NOTE THAT NOW WITH A THIRD ORDER SYSTEM THE PHASE PLANE IS NO LONGER A STATE SPACE SINCE THAT WOULD REQUIRE THREE STATE VARIABLE COORDINATES. THUS THE SWITCH CURVES ARE REALLY TWO DIMENSIONAL PROJECTIONS OF THE ACTUAL THREE DIMENSIONAL SURFACES WHICH WOULD BE PROHIBITIVELY COMPLEX AND EXPENSIVE TO IMPLEMENT IN A DISK DRIVE. AS A RESULT, OVER THE YEARS THE PRACTICAL CONTROLLER DESCRIBED BY THE FOLLOWING BLOCK DIAGRAM HAS EVOLVED MOSTLY BY EMPIRICAL DESIGN PROCEDURES AND HAS BECOME THE STANDARD CONFIGURATION USED IN HIGH PERFORMANCE DISK DRIVES.

BOTH A SWITCHING CURVE AND A FOLLOWING CURVE ARE NEEDED SO THAT VOLTAGE REVERSAL CAN OCCUR EARLY ENOUGH BEFORE ENCOUNTERING THE FOLLOWING TRAJECTORY THAT THERE WILL BE NO OVERSHOOT PAST IT AND YET STILL NEARLY EXTREMAL CONTROL FOR TIME OPTIMALITY. FOR MINIMIZING COST ONLY A "STATIC" TRAJECTORY USED DURING CLOSED LOOP DECELERATE IS IMPLEMENTED WITH GOOD PRECISION. THE SWITCHING TRAJECTORY NEEDED ONLY DURING OPEN LOOP ACCELERATE IS CONSTRUCTED BY SUBTRACTING AN "ANTICIPATE" FUNCTION, WHICH INCLUDES BOTH STATIC AND DYNAMIC COMPONENTS, FROM THE STATIC TRAJECTORY. THE CONFIGURATION OF THE ANTICIPATE FUNCTION IS HIGHLY DEPENDANT UPON HOW MUCH THE THIRD ORDER SYSTEM WITH INDUCTANCE DIFFERS FROM SECOND ORDER BEHAVIOR WHEN VIEWED IN PHASE PLANE COORDINATES.



TRAJECTORY CONTROL FOR 3RD ORDER SYSTEM

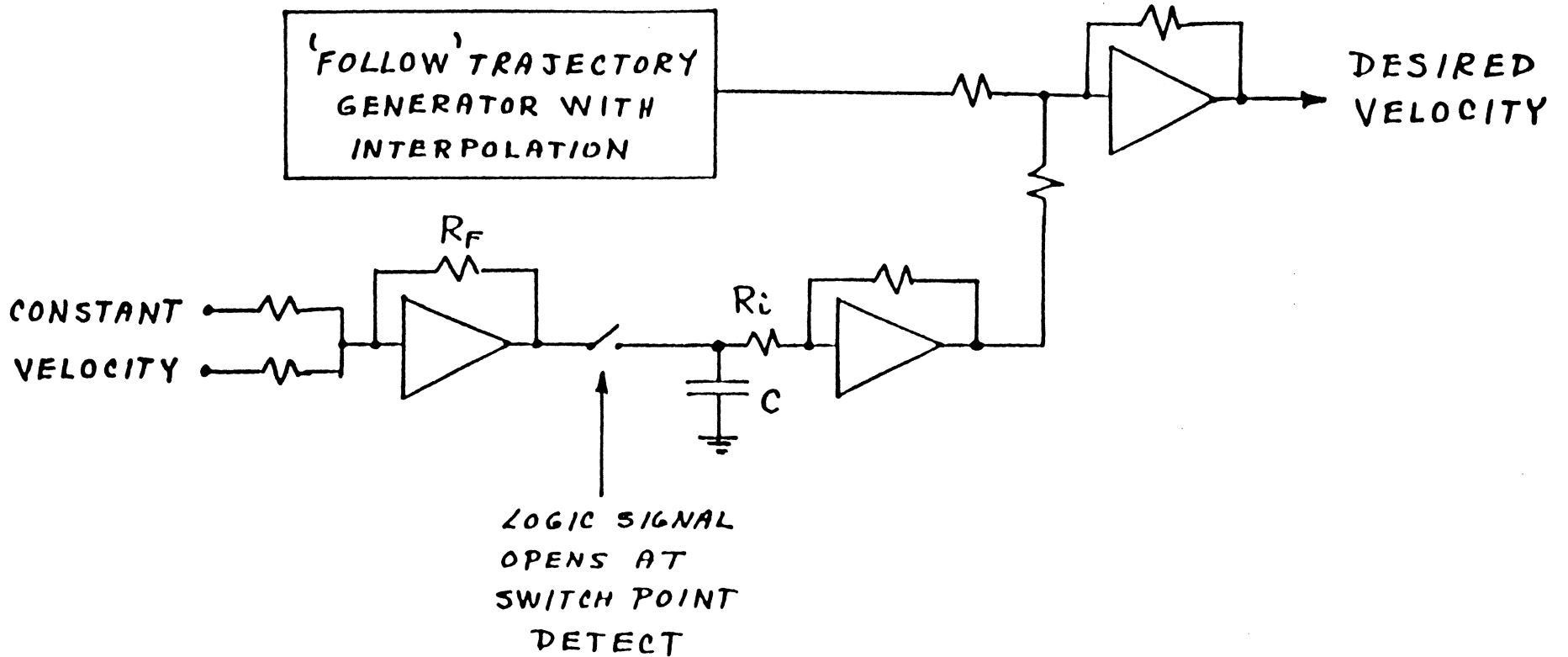
PHASE PLANE, 3RD ORDER SYSTEM



THE FOLLOWING SCHEMATIC IS AN EXAMPLE IMPLEMENTATION OF AN ANTICIPATE FUNCTION FOR USE TOGETHER WITH A CONTINUOUS STATIC FOLLOWING TRAJECTORY GENERATOR.

IN OPERATION, THE SWITCH IS CLOSED AT THE START OF MOTION. THE FIXED CONSTANT VOLTAGE INPUT SUMMED WITH A FRACTION OF THE MEASURED VELOCITY MAKE UP THE MAGNITUDE BY WHICH THE FIRST SWITCH CURVE IS TRANSLATED VERTICALLY DOWNWARD FROM THE FOLLOW CURVE ON THE PHASE PLANE. THE VOLTAGE REPRESENTING THIS VALUE IS FORCED TO APPEAR ON CAPACITOR C BY THE LOW OUTPUT IMPEDANCE OF THE FIRST OPERATIONAL AMPLIFIER. WHEN THE ACCELERATION PHASE OF MOTION HAS REACHED THE POINT OF INTERSECTION WITH THE FIRST SWITCH CURVE, A CONTROL SIGNAL FROM THE SWITCH POINT DETECTOR OPENS THE SWITCH AND THE TRANSLATION VOLTAGE PRESENT ON THE CAPACITOR DECAYS TO ZERO AT AN EXPONENTIAL TIME RATE DETERMINED BY TIME CONSTANT $R_i C$. THIS TIME CONSTANT IS CHOSEN TO MATCH THE TIME RESPONSE OF THE ACTUATOR CURRENT IN CHANGING FROM $\frac{V_s - V_e}{R_T}$ TO $\frac{-V_s - V_e}{R_T}$ (WHICH IS RELATED PRIMARILY TO τ_c) AND THUS CREATES THE TRANSITION REGION OF PHASE PLANE TRAJECTORY LYING BETWEEN THE FIRST SWITCHING CURVE AND THE FOLLOWING CURVE.

A GOOD TRAJECTORY FIT FOR AN ACTUATOR HAVING SHORT-LEAD-TIME INDUCTANCE COMPENSATION MAY REQUIRE TWO TIME CONSTANTS AND/OR A NONLINEAR BREAK POINT IN THE FEEDBACK IMPEDANCE R_f . IF FEEDFORWARD CURRENT CONTROL IS USED AS WILL BE DESCRIBED LATER, AND ITS TIME RESPONSE IS ALSO MATCHED TO THAT OF THE ACTUATOR CURRENT, TRAJECTORY GENERATOR ACCURACY IS MUCH LESS CRITICAL AND TIME OPTIMAL PERFORMANCE EASIER TO OBTAIN IN THE TRANSITION REGIONS BETWEEN THE FIRST SWITCH AND FOLLOW, AND FROM THE SECOND SWITCH TO FINAL POSITION IN THE PHASE PLANE.

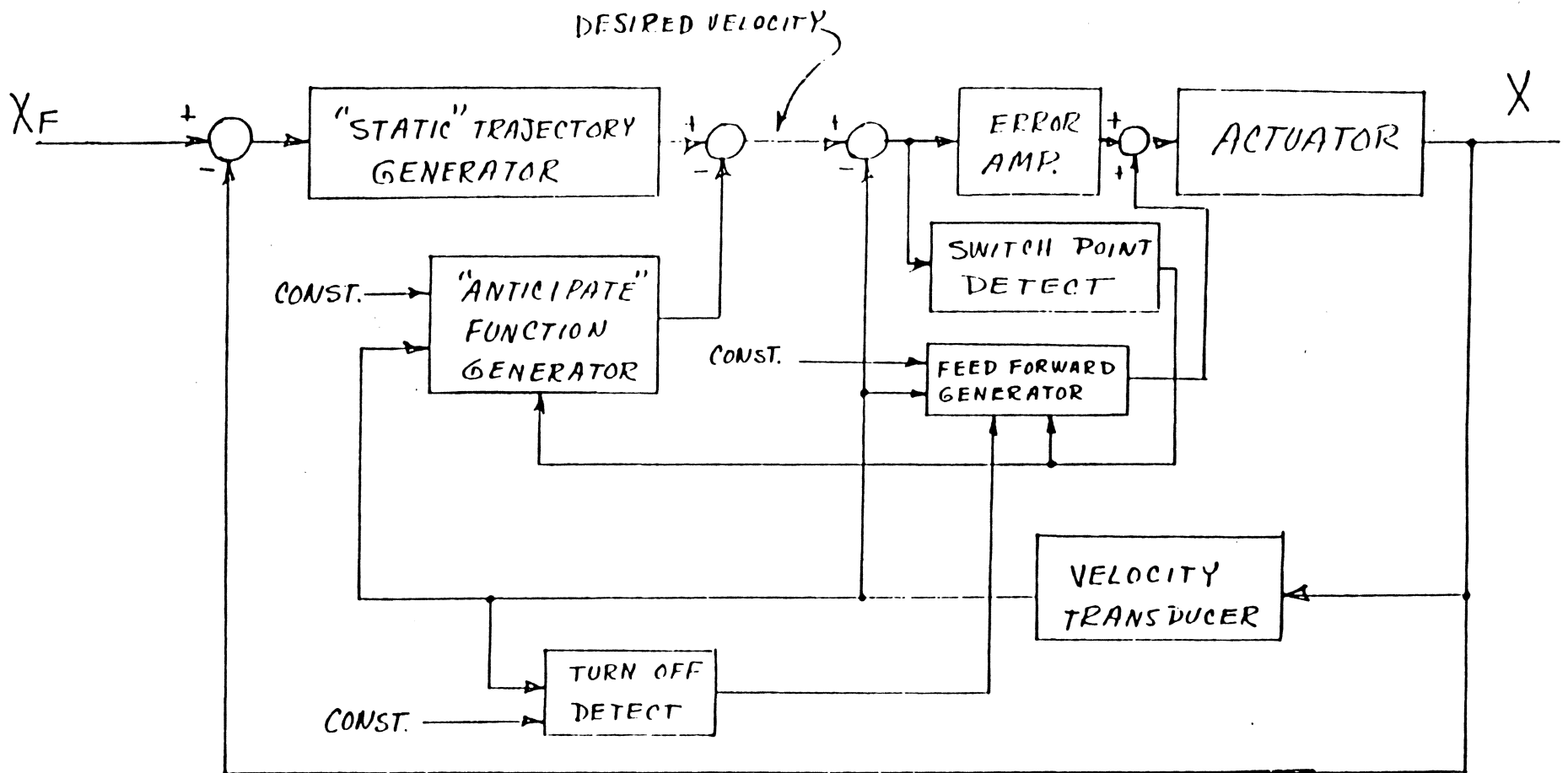


EXAMPLE IMPLEMENTATION OF ANTICIPATE

A KEY FACTOR FOR GOOD PERFORMANCE OF THE ACCESS CONTROLLER IS SUFFICIENT GAIN IN THE ERROR AMPLIFIER SO THAT THE DIFFERENCE BETWEEN THE DESIRED TRAJECTORY VELOCITY AND THE ACTUAL MEASURED VELOCITY IS KEPT SMALL. WITH THE TYPICAL MECHANICAL RESONANCES PRESENT IN THE ACTUATOR AND CARRIAGE, HOWEVER, THE MAXIMUM GAIN THAT CAN BE USED WITHOUT CAUSING INSTABILITY IS OFTEN TOO LOW. COMPENSATION FILTERS THAT MIGHT ALLOW HIGHER GAIN WITHOUT INSTABILITY CAN GENERALLY NOT BE USED SINCE THEY RAISE THE ORDER OF THE SYSTEM AND CAUSE SETTLING TRANSIENTS UPON ARRIVAL AT THE DESTINATION TRACK.

HOWEVER IT SHOULD BE NOTED THAT THE ACTUATOR CURRENT WHICH IS FORMED BY AMPLIFYING THE ERROR SIGNAL IS NOT UNKNOWN, BUT IS A WELL DEFINED FUNCTION OF TIME THAT WAS CALCULATED IN DETERMINING THE DESIGN OF THE TRAJECTORY. THUS IF THE REQUIRED ACTUATOR CURRENT WAVEFORM WERE SYNTHESIZED AND SUMMED DIRECTLY INTO THE ACTUATOR POWER AMPLIFIER THEN THE ERROR AMPLIFIER WOULD ONLY NEED TO FURNISH THE DEVIATIONS BETWEEN THE DESIGN NOMINAL CURRENT AND THE ACTUAL REQUIRED CURRENT DUE TO SYSTEM PARAMETER VARIATIONS.

THIS IS THE CONCEPT OF FEEDFORWARD CONTROL AND IT CAN SIGNIFICANTLY REDUCE THE MAGNITUDE OF THE ERROR WITHOUT REQUIRING HIGH ERROR AMPLIFIER GAIN THAT CAUSES STABILITY PROBLEMS.



TRAJECTORY CONTROL FOR 3RD ORDER SYSTEM
(INCLUDING FEEDFORWARD)

AS AN EXAMPLE OF WHAT THIS APPROACH CAN ACCOMPLISH, ASSUME THE DIFFERENCE BETWEEN THE ACTUALLY REQUIRED SIGNAL AND THE FEEDFORWARD SIGNAL IS $\pm 10\%$; THEN THE ERROR SIGNAL WILL NEED SUPPLY ONLY 10% OF THE ACTUATOR CURRENT RATHER THAN 100% WITHOUT FEEDFORWARD, AND THE REMAINING TRAJECTORY TRACKING ERROR WILL BE REDUCED BY ROUGHLY A FACTOR OF 10 FROM THAT PRESENT IN THE SAME SYSTEM WITHOUT FEEDFORWARD.

THE DESIGN OF THE FEEDFORWARD FUNCTIONAL BLOCK FOLLOWS DIRECTLY FROM THE TIME EQUATIONS FOR CURRENT AND VELOCITY DURING DECELERATE (FOR THE SYSTEM IGNORING INDUCTANCE) GIVEN PREVIOUSLY.

$$I(t) = -\frac{M}{k} \left(\frac{\dot{X}_s}{\tau} + A \right) e^{-\frac{t}{\tau}}$$

$$\dot{X}(t) = \left(\dot{X}_s + \tau A \right) e^{-\frac{t}{\tau}} - \tau A$$

$$\therefore I(t) = -\frac{M}{k\tau} \dot{X}(t) - \frac{AM}{k} = -\frac{1}{R_T} (k \dot{X}(t) + V_s)$$

THUS THE FEEDFORWARD CURRENT SIGNAL IS JUST THE SUM OF A GAIN FACTOR TIMES VELOCITY AND A CONSTANT, AS WAS SHOWN ON THE PREVIOUS BLOCK DIAGRAMS

PART II C) CONSIDERATIONS WHEN SAMPLED DATA ARE USED

IN THE CONVENTIONAL MULTI-DISK DRIVE CONFIGURATION, BY FAR THE DOMINANT FACTOR LIMITING THE ACHIEVABLE TRACK DENSITY IS THE DIMENSIONAL STABILITY OF THE MECHANICAL STRUCTURE. MAINTAINING THE SERVO HEAD ALIGNED ON THE SERVO SURFACE DOES NOT ASSURE THAT EACH OF THE DATA HEADS IS ALIGNED WITH ITS DATA TRACK. THE TOTAL MISPOSITION ERROR CAN BE BROKEN OUT INTO THE SUM OF A FEW BROAD CATEGORIES OF COMPONENTS WITH DISTINCT CHARACTERISTICS;

1. "STATIC" ERROR THAT IS INDEPENDANT OF RADIAL AND CIRCUMFERENTIAL HEAD LOCATION AND CHANGES ONLY VERY SLOWLY; EXAMPLES ARE UNEQUAL THERMAL EXPANSIONS FROM THERMAL GRADIENTS AND CREEP AT BOLTED JOINTS DUE TO THERMAL CYCLING OR MECHANICAL SHOCK.

2. "STATIC" ERROR THAT IS INDEPENDANT OF CIRCUMFERENTIAL LOCATION BUT VARIES WITH RADIAL LOCATION; A TYPICAL CAUSE IS CARRIAGE BEARING PRECESSION.

3. DYNAMIC ERROR THAT VARIES AT OR MORE SLOWLY THE DISK SPINDLE ROTATION RATE; THE USUAL CAUSE IS SPINDLE BEARING REPEATABLE AND NON-REPEATABLE RUNOUT.

4. DYNAMIC ERROR THAT CONTAINS COMPONENTS AT HIGHER FREQUENCIES THAN THE DISK ROTATION; USUAL SOURCES ARE VIBRATION OF THE DRIVE STRUCTURE AND/OR HOST SYSTEM, HEAD FLUTTER, SUSPENSION VIBRATION, HIGHER HARMONICS OF SPINDLE BEARING IMPERFECTIONS, ETC

SINCE THESE EFFECTS MAY BE DIFFERENT ON EACH DATA HEAD, THEIR CORRECTION REQUIRES MEASUREMENT OF THE OFFTRACK POSITION OF EACH DATA HEAD WITH RESPECT TO ITS RECORDING TRACK. THEREFORE SOME MEANS OF MULTIPLEXING BETWEEN THE DATA RECORDING AND POSITION MEASURING FUNCTIONS OF THE HEAD AND POSSIBLY ITS CHANNEL ELECTRONICS MUST BE ACCOMPLISHED.

MULTIPLEXING CAN BE IMPLEMENTED WITH EITHER: A) SPATIAL DIVISION, B) FREQUENCY DIVISION, OR C) TIME DIVISION METHODS.

A) SPATIAL DIVISION INVOLVES THE USE OF AN ADDITIONAL PARALLEL MEASUREMENT CHANNEL IN CLOSE PROXIMITY TO THE REGULAR RECORDING TRANSDUCER. AN EXAMPLE IMPLEMENTATION USES AN OPTICAL TRANSDUCER MOUNTED ON THE SLIDER AND READING CONCENTRIC LIGHT AND DARK BANDS ON THE DATA DISK THROUGH SEPARATE ELECTRONICS. THESE METHODS ARE FEASIBLE BUT GENERALLY ECONOMICALLY IMPRACTICAL AND TO MY KNOWLEDGE HAVE NOT BEEN USED IN MASS PRODUCED PRODUCTS.

B) FREQUENCY DIVISION UTILIZES A RECORDING MEDIUM THAT IS THICKER THAN THAT REQUIRED FOR DATA RECORDING ALONE AND A RECORDING CODE THAT RESERVES A BAND OF FREQUENCIES BELOW THOSE USED FOR DATA RECORDING FOR PRERECORDED POSITION INFORMATION SIMILAR TO THAT USED ON A REGULAR SERVO SURFACE. FREQUENCY DIVISION FILTERS SEPARATE POSITION AND CUSTOMER DATA SIGNALS IN THE RECORDING CHANNEL TO PERMIT READING OF POSITION WHILE BOTH READING AND WRITING DATA

C) TIME DIVISION TIME SHARES A SINGLE RECORDING CHANNEL BETWEEN POSITION INFORMATION AND CUSTOMER DATA AT RATES RANGING FROM A WHOLE TRACK AT A FEW PLACES ON THE DISK TO A FEW PERCENT OF EVERY TRACK IN MANY SEGMENTS LOCATED BETWEEN THE DATA SECTORS.

TIME DIVISION AND FREQUENCY DIVISION METHODS ARE SCHEMATICALLY SHOWN ON THE FOLLOWING FIGURE. THEIR APPLICABILITY TO THE FOUR PREVIOUSLY LISTED ERROR CATEGORIES DEPENDS PRIMARILY UPON THE CHANNEL CAPACITY DEVOTED TO POSITION MEASUREMENT. THE FOUR ERROR CATEGORIES ARE IN ASCENDING ORDER OF BANDWIDTH REQUIREMENT.

FLEXIBLE DISK DRIVES

Brier Technology fields a first: a 20M-byte, 3½-inch flexible drive

Mike Seither, Senior Editor

San Jose start-up Brier Technology Inc. hopes to turn a few heads at the COMDEX/Fall show in Las Vegas next month when it introduces a 20M-byte, 3½-inch flexible disk drive. That's more than double the storage of the newest breed of high-capacity 5¼-inch flexible disk drives.

With an average access time of 35 msec, Brier's BT 3020 high-capacity product also rivals the performance of comparable-size Winchester disks and offers a removable media to boot. This is something that is attractive to OEMs and system integrators working in the engineering, scientific and military segments, where workstations are shared and the best way to protect one's data is to remove it.

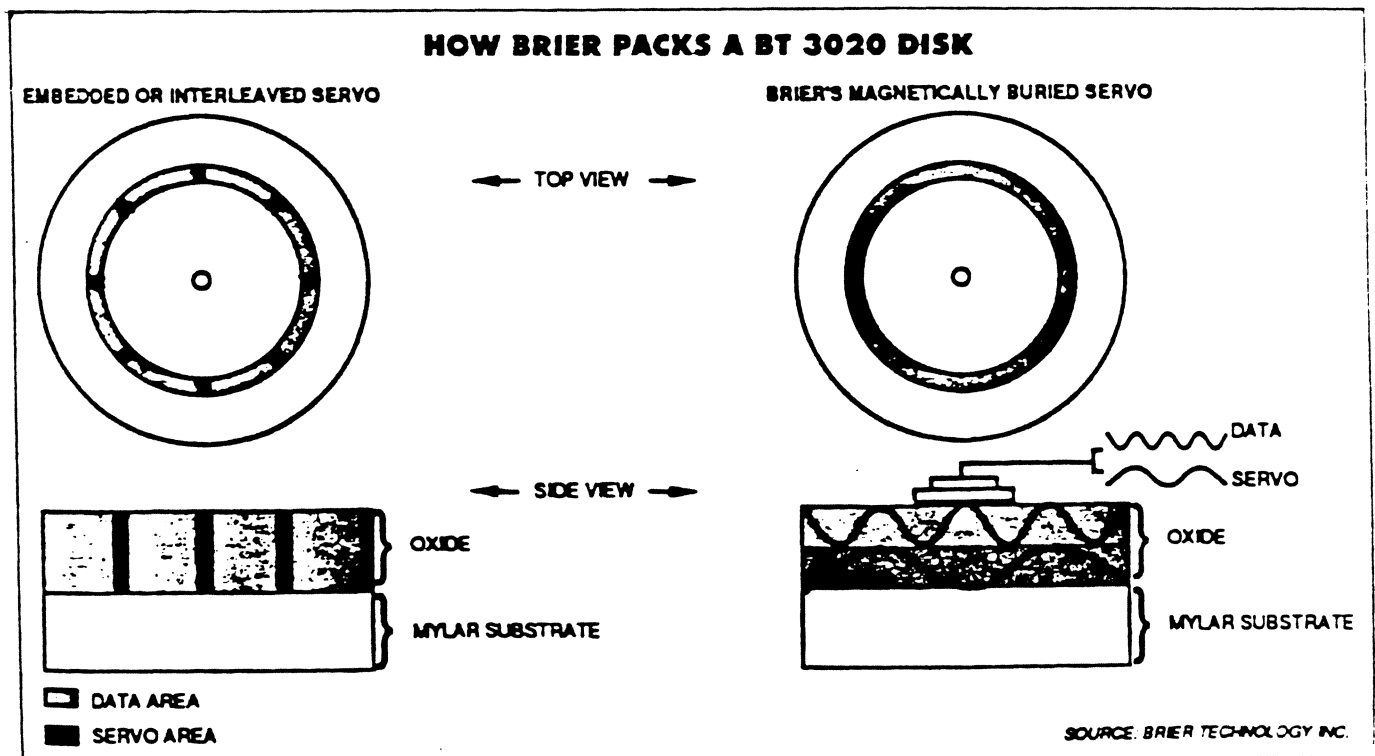
Brier's first product uses a proprietary system that embeds continuous servo information into the magnetic oxide coating of a standard 3½-inch high-density disk. The company claims that it has been able to divide the disk's oxide media into two logical layers. Servo information in the deeper layer, recorded at a very low frequency, is used to keep the read/write head on track. The upper layer is dedicated solely to user data and is written at a much higher frequency than the servo information.

By comparison, most vendors selling 5¼-inch disk drives in the range of 4M bytes to 10M bytes embed servo information directly on the data surface. As a result, up to half the total data area is given up to servo.

Thanks to this buried-servo system,

Brier has been able to overcome the biggest technical hurdle—track density. The BT 3020 has 777 tracks per inch, compared with the 96 tpi on a regular 5¼-inch disk. By increasing the bit density and using advanced

Embedded servos (left) typically use part of the data surface to the entire depth of the oxide media to store read/write-head tracking information. Brier horizontally divides the oxide into two logical layers (right). Prerecorded, continuous servo information is written at a low frequency onto the lower. Data is written over the entire upper layer at a high frequency. Brier's drive electronics sends data one way and head tracking information another.



CATEGORY 1 STATIC ERRORS CAN BE CORRECTED BY ALLOCATING ONLY ONE TRACK PER DATA SURFACE TO POSITION AND READING IT ONLY INFREQUENTLY, STORING THE MEASUREMENT RESULT AND THEN USING IT AS AN OFFSET CORRECTION TO THE SERVO SURFACE DATA FOR THAT HEAD UNTIL THE NEXT TIME THE POSITION INFORMATION TRACK IS READ, MANY SECONDS OR MINUTES LATER. THIS OF COURSE IS THE SIMPLEST, LOW COST IMPLEMENTATION. IT CAN USE VERY SLOW AND INEXPENSIVE MEASUREMENT HARDWARE.

CATEGORY 2 ERRORS ARE IN GENERAL DIFFERENT AND CHANGING ON EVERY TRACK BUT NOT CHANGING AROUND THE CIRCUMFERENCE. THEY MAY BE CORRECTED BY STORED OFFSET VALUES PROVIDED FOR EACH HEAD AT EACH TRACK LOCATION, WHICH ARE OBTAINED BY A ONCE PER REVOLUTION TIME DIVISION SAMPLE OR A VERY LOW BANDWIDTH FREQUENCY DIVISION CHANNEL.

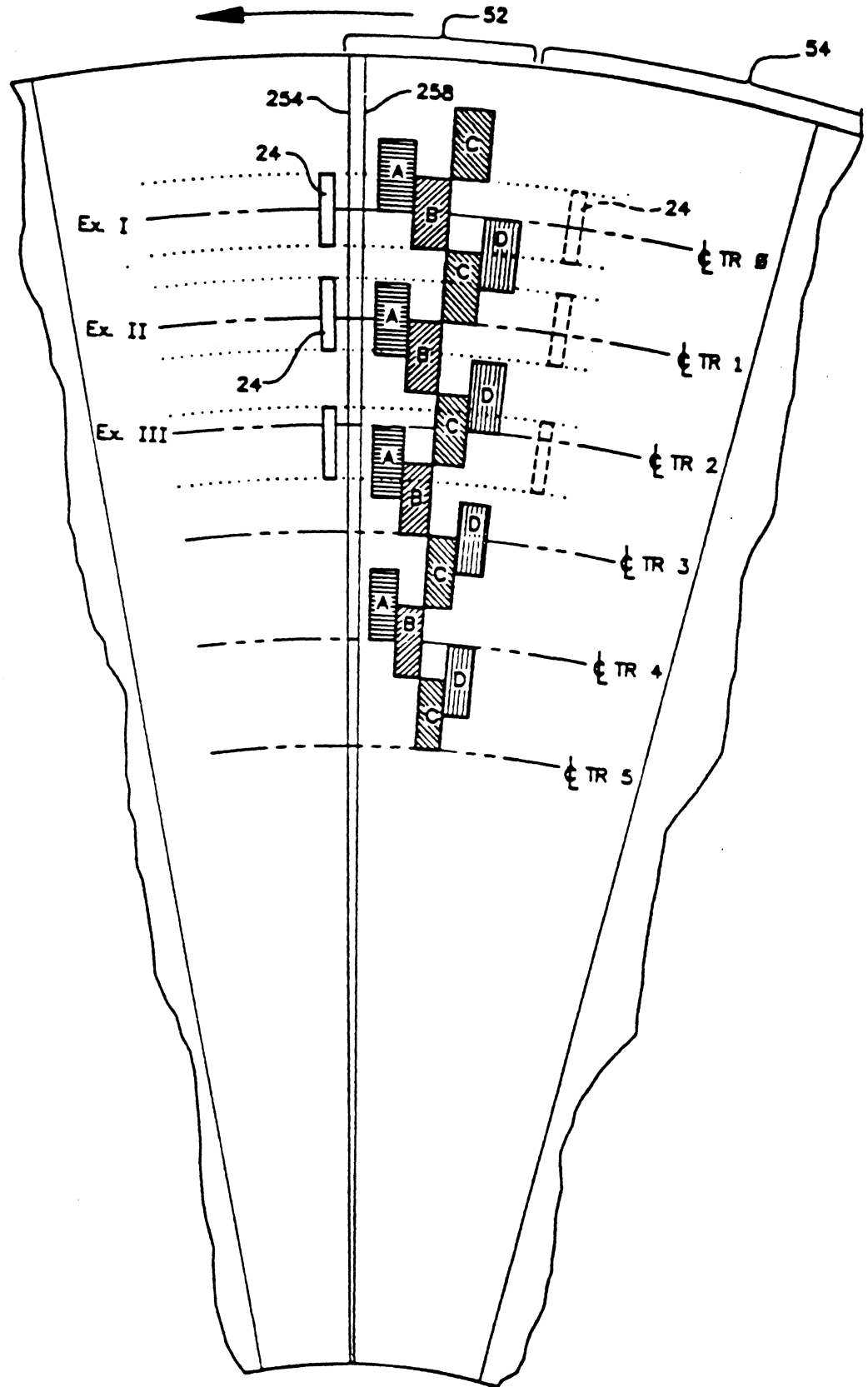
CATEGORY 3 ERRORS ARE DYNAMIC AND REQUIRE CONTINUOUS, REAL TIME CORRECTION, NOT JUST A STORED OFFSET REFERENCED TO THE SERVO SURFACE. THIS CORRECTION CAN BE ACCOMPLISHED WITH A TIME DIVISION SYSTEM HAVING 8 TO 30 SAMPLES PER REVOLUTION OR A FREQUENCY DIVISION SYSTEM WITH SEVERAL KILOHERTZ POSITION CHANNEL BANDWIDTH.

CATEGORY 4 ERRORS ARE DYNAMIC AND REQUIRE FULL BANDWIDTH POSITIONING SYSTEMS EQUIVALENT IN PERFORMANCE TO A CONTINUOUS SERVO SURFACE SYSTEM, THUS ELIMINATING THE NEED FOR IT. THIS IS QUITE EASILY DONE WITH FREQUENCY DIVISION SYSTEMS HAVING WELL OPTIMIZED SEPARATION FILTERS BUT IN TIME DIVISION SYSTEMS IT IS VERY DIFFICULT TO ACHIEVE. SAMPLE RATES OF 30 TO 80 OR MORE PER REVOLUTION ARE NEEDED TOGETHER WITH MULTI-PHASE POSITION ENCODING AND VERY FAST AND SOPHISTICATED ADAPTIVE SIGNAL PROCESSING. THIS TYPE OF DRIVE IS TECHNICALLY FEASIBLE BUT NOT ECONOMICALLY VIABLE AT THIS TIME, EXCEPT FOR LARGE MAINFRAME OR PERHAPS OPTICAL RECORDING APPLICATIONS.

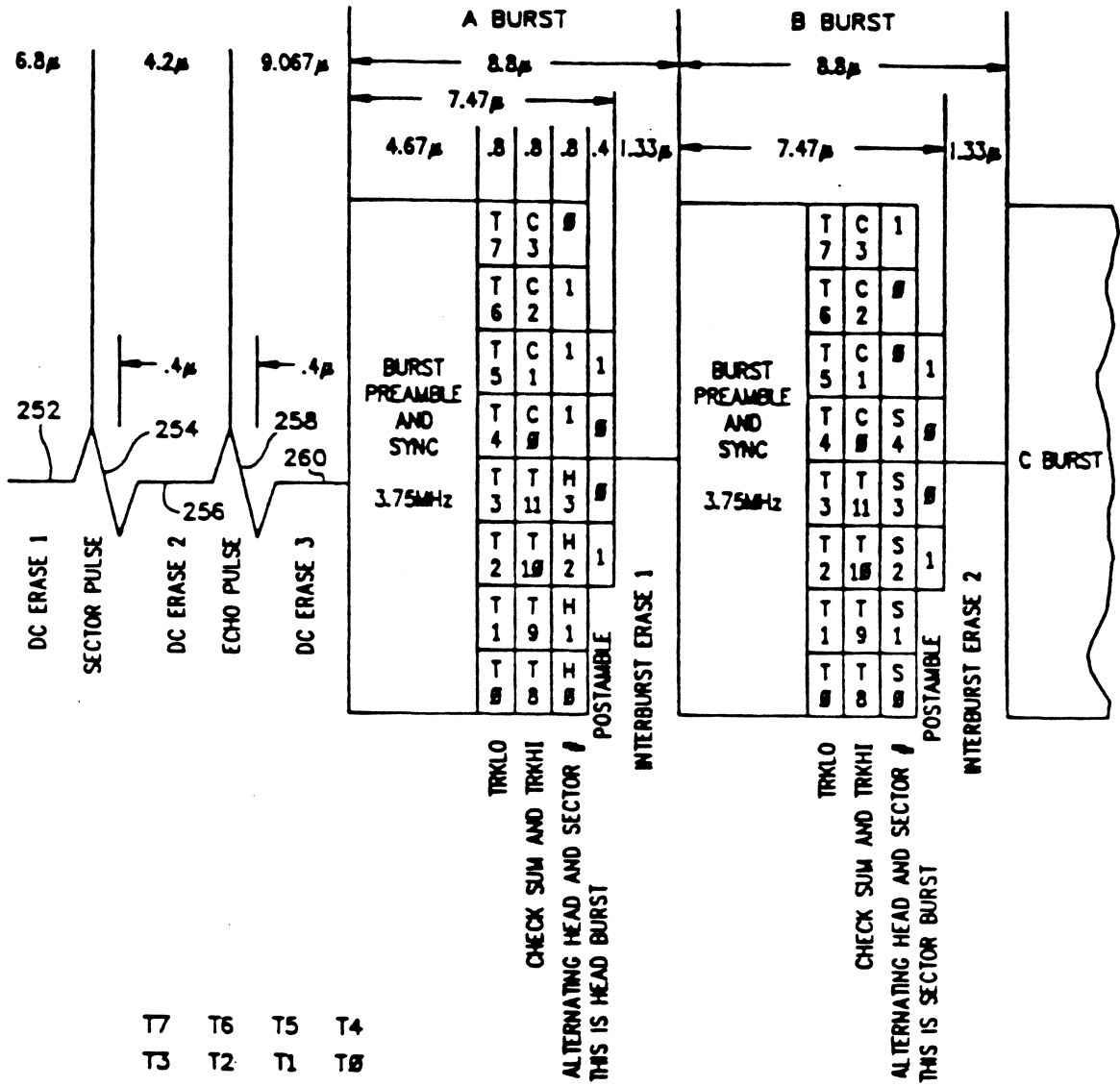
SINCE THERE IS A LOT OF CURRENT INTEREST IN SMALL DRIVES USING ONLY TIME DIVISION MULTIPLEXING IN THE FORM OF : POSITION INFORMATION BETWEEN DATA SECTORS, A GENERAL PURPOSE MICROPROCESSOR WITH BUILT IN A/D CONVERTER, MICRO CODED DIGITAL FILTER CONTROLLER, AND NO CONTINUOUS POSITION INFORMATION SOURCE, WE SHALL EXAMINE A FEW IMPORTANT CONSIDERATIONS FOR THIS TYPE OF SYSTEM.

SMALL DRIVES OF THIS TYPE GENERALLY HAVE SPINDLE ROTATION RATES OF 3600 RPM AND, DEPENDING UPON BIT DENSITY, 24 TO 48 SECTORS OF 512 DATA BYTES PLUS HEADER AND POSITION INFORMATION PER REVOLUTION. AN EXAMPLE POSITION ENCODING SYSTEM USED IN A DRIVE OF THIS TYPE IS SHOWN ON THE FOLLOWING PAGES. IT CAN PROVIDE ADEQUATE POSITION INFORMATION FOR BOTH ACCESS AND TRACK FOLLOWING.

IN ADDITION TO THE POSITION TRANSDUCER SAMPLE RATE, HOWEVER, THE COMPUTATIONAL SPEED AND OUTPUT SAMPLE RATE HAVE VERY SIGNIFICANT EFFECTS ON THE PERFORMANCE OF DRIVES OF THIS TYPE. THE SPINDLE ROTATION FREQUENCY IS USUALLY 60 Hz GIVING A SAMPLE RATE OF 1.5 TO 3.0 K SAMPLES PER SECOND. CLASSICAL SAMPLE DATA THEORY ASSUMES THAT EACH NEWLY ACQUIRED INPUT INFORMATION SAMPLE IS IMMEDIATELY USED TO OUTPUT A NEW CONTROL VALUE. SUCH A SYSTEM CAN YIELD ACCEPTABLE TRANSIENT RESPONSE WITH AN OPEN LOOP UNITY GAIN-BANDWIDTH OF $\frac{1}{10}$ TO $\frac{1}{12}$ OF THE SAMPLE RATE. HOWEVER THIS IS NOT REPRESENTATIVE OF THE USUAL LOW COST IMPLEMENTATION WHERE THERE IS AN APPRECIABLE TIME DELAY BETWEEN THE INPUT SAMPLE AND THE OUTPUT TO ALLOW FOR ANALOG TO DIGITAL CONVERSION, COMPUTATION OF THE NEW OUTPUT, AND DIGITAL TO ANALOG CONVERSION. WITH PRESENT GENERAL PURPOSE MOS MICROPROCESSORS THIS TIME IS AT LEAST 50 μ SEC AND OFTEN MUCH LONGER. THIS TIME DELAY IS VERY DETRIMENTAL TO PERFORMANCE AS CAN BE SEEN FROM THE FOLLOWING TIME RESPONSE CURVES FOR A



BURST TIMING



OR

T7	T6	T5	T4
T3	T2	T1	T0
C3	C2	C1	C0
T11	T10	T9	T8
1	0	0	S4
0	1	1	1
H/S3	H/S2	H/S1	H/S0
1	1	1	1

SECTOR BURST ONLY
 HEAD BURST ONLY

BURST	SECTOR	
	ODD	EVEN
A	S	H
B	H	S
C	H	S
D	S	H

CONTINUOUS SIGNAL PROCESSING TRACK FOLLOWING SYSTEM WITH OPEN LOOP UNITY GAIN BANDWIDTH OF 450 HZ, THE ADDED DELAYS CORRESPOND TO $0, \frac{1}{4}, \frac{1}{2}$, AND 1 TIMES THE PERIOD OF A SAMPLER THAT IS 11 TIMES HIGHER RATE THAN THE UNITY GAIN FREQUENCY.

ANOTHER PERFORMANCE LIMITATION OCCURS IN THE ACCESS CONTROL ALGORITHM NORMALLY IMPLEMENTED IN THESE SYSTEMS. AS WAS SEEN EARLIER, A TIME EFFICIENT CONTROL STRATEGY ACCELERATES FOR ABOUT HALF THE TIME OR DISTANCE AND DECELERATES FOR THE REMAINING HALF. AN AVERAGE MOVE TIME OF 15 MILLISECONDS FOR A 1 INCH STROKE ACTUATOR REQUIRES ABOUT 15 G ACCELERATION RATE WITH AN EXTREMAL, TIME OPTIMAL CONTROLLER. MOVING ONE TRACK AT 1500 TRACKS PER INCH REQUIRES ACCELERATE AND DECELERATE TIMES OF $\frac{1}{48}$ REVOLUTION AT 15 G. THE FOLLOWING TABLE TABULATES THE SWITCHING POINT FOR OTHER LENGTH MOVES FOR SUCH A SYSTEM:

ACCESS LENGTH AT 1500 TPI	SWITCH TIME AT 3600 RPM
1	$\frac{1}{48}$ REV.
2	$\frac{1}{34}$ "
3	$\frac{1}{28}$ "
4	$\frac{1}{24}$ "

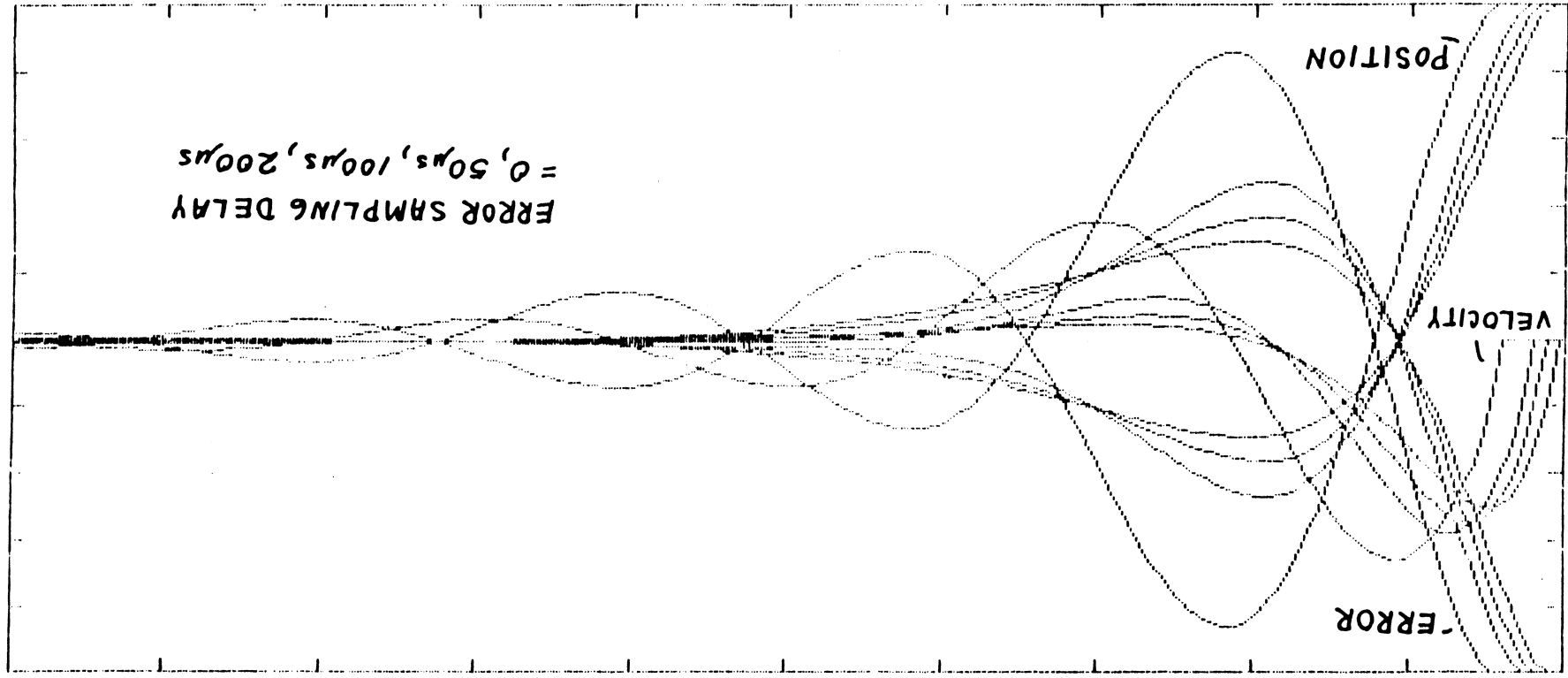
IF THE SYSTEM HAS THE USUAL 32 SECTORS PER REVOLUTION AND ONE OUTPUT SAMPLE PER INPUT SAMPLE IT IS APPARENT THAT THE TIME QUANTIZATION OF THE OUTPUT IS FAR TOO COARSE TO HAVE ANYWHERE NEAR TIME OPTIMAL RESPONSE.

THE EFFECTIVE SOLUTION TO THIS PROBLEM IS A MULTI-RATE SAMPLING SYSTEM WHICH OUTPUTS AT A MUCH HIGHER AND/OR VARIABLE SAMPLE RATE AS COMPARED TO THE INPUT. IT IS ALSO VERY USEFUL FOR IMPROVING TRACK FOLLOWING ACCURACY SYSTEMS WITH A SMALL AMOUNT OF STICKING FRICTION AND RELATIVELY LOW INPUT INFORMATION SAMPLING RATES. THE QUICKEST WAY TO CORRECT AN OFF TRACK POSITION ERROR APPLIES ACCELERATE THEN

0.0050000

0.0000 Time

ERROR SAMPLING DELAY
= 0, 50 μ s, 100 μ s, 200 μ s



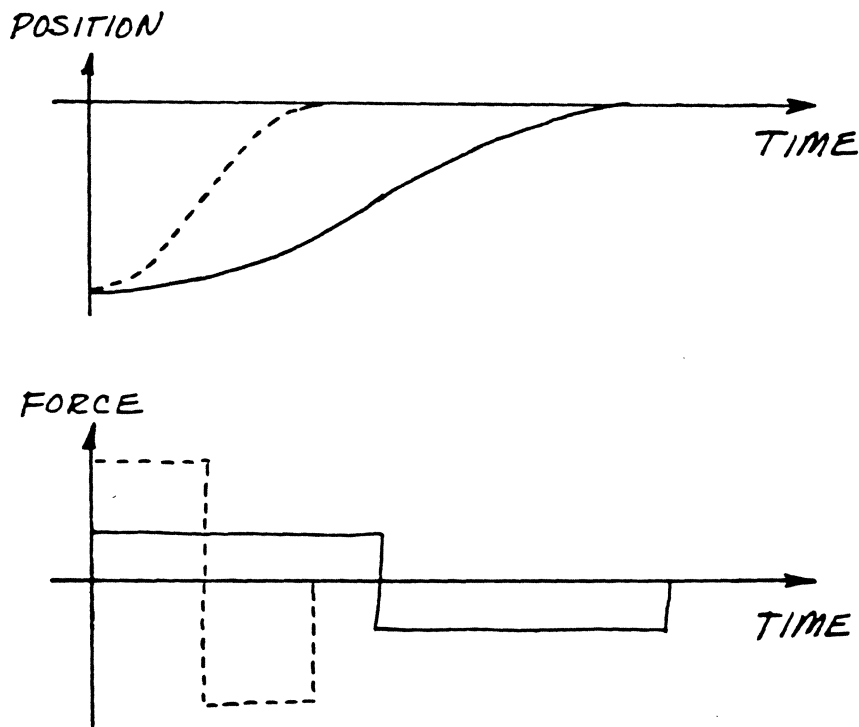
POSITION

VELOCITY

ERROR

0

DECELERATE OUTPUTS, SIMILAR TO AN ACCESS CONTROLLER. HOWEVER WHEN THE DISTANCES TO MOVE ARE SMALL AND THE OUTPUT SAMPLE INTERVALS ARE LONG, THE APPLIED FORCES BECOME VERY SMALL AND CANNOT OVERCOME CARRIAGE BEARING STICKING FRICTION CAUSING A LIMIT CYCLE AND POOR ACCURACY. A VARIABLE OUTPUT SAMPLE RATE CAN ALLOW LARGER FORCES FOR SHORTER TIMES AND PROVIDE IMPROVED ACCURACY OVER WHAT CAN BE DONE EVEN WITH CONTINUOUS LINEAR SYSTEMS HAVING HIGHER BANDWIDTHS.



IT IS A PROGRAMMING CHALLENGE TO IMPLEMENT A MULTI-RATE SAMPLING SYSTEM WITH MICROCODE IN A GENERAL PURPOSE MICROPROCESSOR HOWEVER. THUS IT IS SELDOM USED AT PRESENT.

MUCH HIGHER PERFORMANCE SIGNAL PROCESSING INTEGRATED CIRCUITS THAN GENERAL PURPOSE MICROPROCESSORS ARE NOW BECOMING AVAILABLE AT COSTS THAT MAKE THEIR USE IN DISK DRIVES FEASIBLE. EXAMPLES INCLUDE: HALF-FLASH 8 BIT 8 CHANNEL A TO D CONVERTERS WITH ACQUISITION

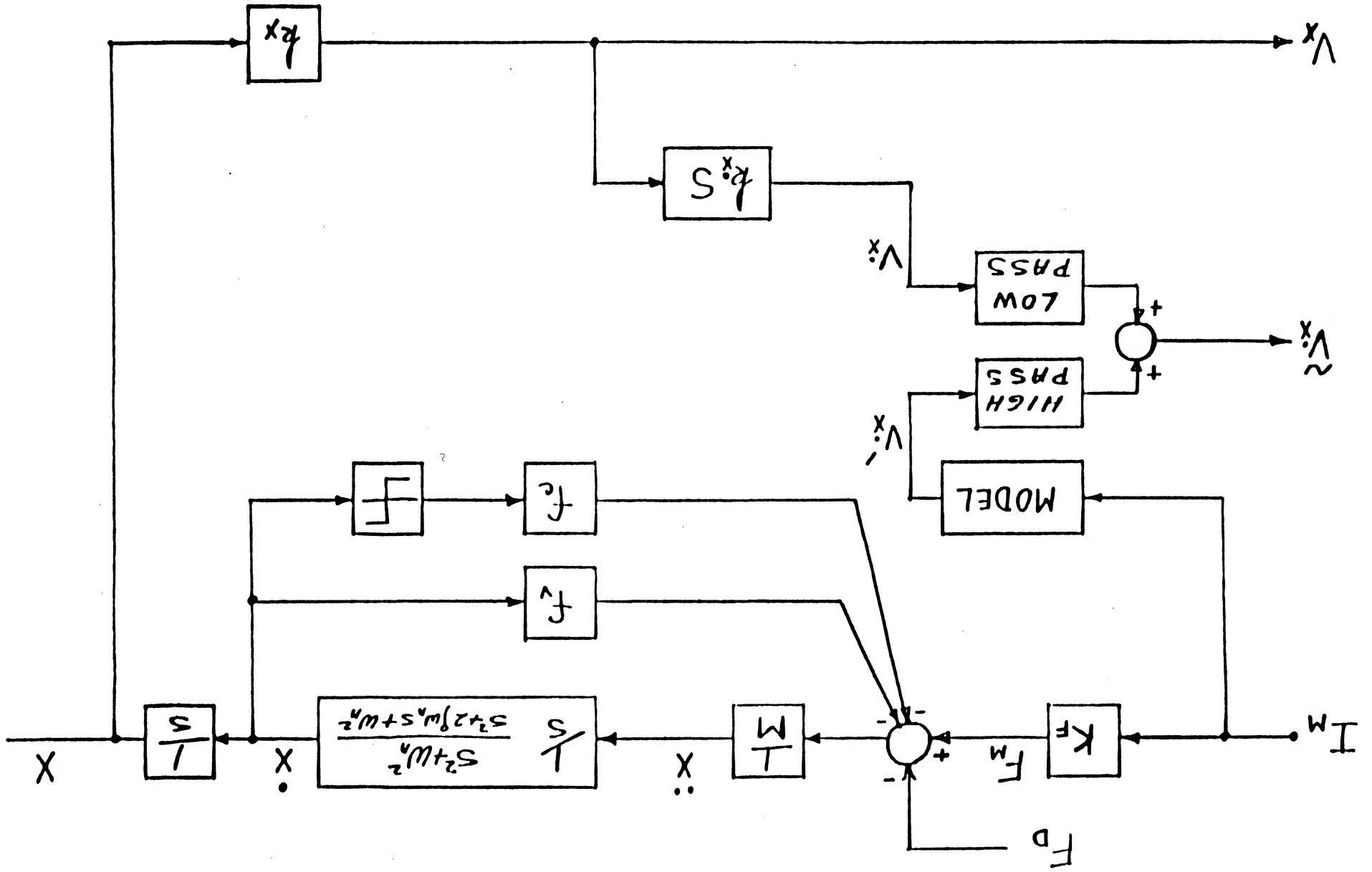
TIMES OF LESS THAN 2μ SECONDS, SPECIAL PURPOSE MICRO PROCESSERS OPTIMIZED FOR DIGITAL SIGNAL PROCESSING THAT HAVE HIGH SPEED 32 BIT ARITHMETIC CAPABILITIES SUCH AS A MULTIPLY AND ADD IN 200 N SECONDS, AND SINGLE SUPPLY, VOLTAGE OUTPUT 12 BIT D TO A CONVERTERS WITH SLEW AND SETTLE TIMES OF LESS THAN 2μ SECONDS. WHEN IMPLEMENTED WITH THESE DIGITAL SIGNAL PROCESSING COMPONENTS, CONSTANT COEFFICIENT CONTROL ALGORITHMS HAVE NEARLY AS GOOD PERFORMANCE AS CONTINUOUS UNQUANTIZED IMPLEMENTATIONS. BUT IN ADDITION MUCH MORE POWER FULL NONLINEAR AND ADAPTIVE CONTROL ALGORITHMS CAN BE USED WHICH ARE COMPLETELY IMPRACTICAL TO IMPLEMENT BY OTHER MEANS. AN EXAMPLE IS A VELOCITY ESTIMATOR FOR USE IN A TIME OPTIMAL CONTROLLER.

AS WAS DISCUSSED EARLIER, A TIME OPTIMAL ACCESS CONTROLLER REQUIRES VELOCITY AS WELL AS POSITION INFORMATION FROM THE PLANT AS SHOWN IN PART I. BUT COST, SPACE AND PERFORMANCE ISSUES PREVENT THE USE OF A VELOCITY TRANSDUCER IN DISK DRIVES. THEREFORE FOR MANY YEARS VELOCITY ESTIMATORS AS SHOWN ON THE NEXT PAGE HAVE BEEN USED.

SINCE THE MECHANICAL VELOCITY IS NOT ACCESSIBLE FOR DIRECT MEASUREMENT WITH OUT A VELOCITY TRANSDUCER, THE EASILY MEASURED CURRENT I IS APPLIED TO AN ELECTRONIC MODEL OF THE ACTUATOR WHICH SHOULD HAVE THE SAME RESPONSE FROM CURRENT TO VELOCITY AS THE REAL PHYSICAL SYSTEM. THE OUTPUT OF THE ELECTRONICALLY IMPLEMENTED MODEL IS AN ESTIMATE OF TRUE VELOCITY THAT CAN BE USED IN THE CONTROL SYSTEM.

THE PREDOMINANT SOURCES OF ERROR IN THE ESTIMATED VELOCITY ARE THE LACK OF KNOWLEDGE OF THE BIAS FORCE F_D AND D.C. DRIFT IN THE INTEGRATION. THUS THE D.C. AND LOW FREQUENCY INFORMATION IN THE MODEL OUTPUT IS INACCURATE AND MUST BE REJECTED

VELOCITY ESTIMATION



BY A HIGH PASS FILTER. THIS MISSING LOW FREQUENCY DATA MAY BE RESTORED BY TAKING THE TIME DERIVATIVE OF THE MEASURED POSITION SIGNAL, BAND LIMITING IT AT THE SAME FREQUENCY AS THE HIGH PASS FILTER CUTOFF AND SUMMING THE TWO FILTER OUTPUTS.

A VERY USEFUL PROPERTY OF THIS METHOD OF OBTAINING VELOCITY INFORMATION IS THE ATTENUATION OF THE DESTABILIZING INFLUENCE OF THE MECHANICAL RESONANCE. THE MODEL OUTPUT IS NOT CONTAMINATED BY THE RESONANCE AND ITS COMPONENTS IN THE MEASURED POSITION CAN BE SIGNIFICANTLY ATTENUATED BY THE LOW PASS FILTER. THUS THE STABLE BANDWIDTH OF THE ACCESS CONTROL SYSTEM USING AN ESTIMATED VELOCITY CAN BE CONSIDERABLY LARGER THAN IF A VELOCITY TRANSDUCER WERE USED.

THE IMPLEMENTATION OF VELOCITY ESTIMATORS WITH CONVENTIONAL HARDWARE HAS SEVERAL LIMITATIONS: THE MODEL REQUIRES THAT THE VALUE OF K_f AS WELL AS F_d BE KNOWN, AND ACCURACY OF K_f IS ESPECIALLY IMPORTANT SINCE IT IS A MULTIPLICATIVE FACTOR FOR THE ENTIRE SPECTRUM OF THE MODEL OUTPUT, NOT JUST AN ADDITIVE D.C. OFFSET THAT IS MORE EASILY REJECTED. UNFORTUNATELY, FOR MANY LOW COST DISK DRIVE ACTUATORS, K_f IS NOT CONSTANT BUT IN ADDITION TO INITIAL TOLERANCES, VARIES WITH TEMPERATURE, MAGNITUDE AND DIRECTION OF CURRENT, AND POSITION IN THE STROKE. THUS A SIMPLE MODEL THAT ASSUMES K_f TO BE A FIXED CONSTANT MAY HAVE LARGE INACCURACY, AND MAKING THE MODEL HAVE THE CAPABILITY TO TRACK VARIATIONS IN K_f ADDS COMPLEXITY THAT IS VERY EXPENSIVE TO IMPLEMENT IN CONTINUOUS SYSTEMS. HOWEVER WITH A POWERFUL DIGITAL SIGNAL PROCESSOR IMPLEMENTATION OF THE MODEL, A-PRIORI DESIGN KNOWLEDGE OF K_f VARIATION AS WELL AS OF F_d MAY BE INCORPORATED AT NO HARDWARE COST, AND ADAPTIVE LEARNING TECHNIQUES USED TO TRACK OTHER VARIATIONS.

AN ADDITIONAL CONSEQUENCE OF THE USE OF DIGITAL SIGNAL PROCESSING WHICH QUANTIZES THE ACTUATOR CURRENT IN BOTH AMPLITUDE AND TIME IS THE GENERATION OF ACOUSTIC NOISE. THE FREQUENCY SPECTRUM OF THE ENERGY CONTAINED IN THE STEP CHANGES OF MAGNITUDE AT THE OUTPUT SAMPLE INSTANTS IS VERY BROAD. WHILE IT MAY BE ABOVE THE BANDWIDTH OF SERVO RESPONSE IT STILL CAN EXCITE THE MECHANICAL STRUCTURAL RESONANCES INCLUDING THOSE IN DIRECTIONS OTHER THAN THE ACCESS COORDINATE. DESIGNERS MUST REMEMBER THAT THERE HAS BEEN GOOD REASON FOR CALLING ACTUATORS "VOICE COIL MOTORS" AND CAREFULLY CONSIDERING ACOUSTIC NOISE GENERATION FROM THIS AS WELL AS OTHER SOURCES, SINCE SUCH NOISE IS VERY OBJECTIONABLE IN DESK TOP EQUIPMENT IN CLOSE PROXIMITY TO AN OPERATOR.